HYDRODYNAMIC LUBRICATION OF DEEP DRAWING

by

Zhi - Min Shao

1990

HYDRODYNAMIC LUBRICATION OF DEEP DRAWING

A thesis submitted in accordance with the regulations

of the degree of

Master of Engineering

by

Zhi-Min Shao

Department of Manufacturing and Process Engineering

Manufacturing Systems Engineering

Royal Melbourne Institute of Technology

Victoria, Australia

1990

DECLARATION

I, Zhi - Min Shao, hereby declare that this thesis is my own work, except where duly acknowledged to others, and has not submitted previously in whole or in part, in respect of any other academic award.

The work presented in thesis has been carried out since the official date of commencement of the research programme.

ABSTRACT

An isoviscous steady hydrodynamic lubrication model for a deep drawing process is developed. Equations to calculate lubricant film thickness, radial, and drawing stresses are presented. The die inlet film thickness is related to the properties of the lubricant and the sheet metal, the tooling geometry and the operating conditions.

A series of experiments with low carbon steel sheet blanks and different types of lubricant was conducted. The formation of a thick hydrodynamic lubricant film associated with a matt surface finish was observed for using certain lubricants. In each experiment, the thickness of the lubricant film was estimated from the difference in diameter between the lubricated and unlubricated drawn cups.

The experimental measurements of lubricant film thickness and drawing force were compared with values calculated from the theoretical model. There is some degree of agreement between these results.

ACKNOWLEDGMENTS

I wish to express my sincere thanks with a deep sense of gratitude to Dr. Mahdi Mahdavian, principle academic supervisor, for his inspiring guidance, enlightening discussions and indispensable personal favour, throughout the course of the research programme.

I am highly grateful to Mr. Brian Thorpe, second supervisor, for the helpful correcting during the preparation of the thesis.

My gratitude is also due to Mr. Roger La Brooy, Head of the Manufacturing Systems Engineering, for providing the necessary departmental facilities and financial assistance.

I am greatly indebted to Mr. Ron Fraser and Mr. Geoff Collins, for many hours spent on creative discussion for setting up the experimental rig and taking measurement during the work of experimental investigation.

I extend my gratitude to Steel Improvement Pty. Ltd. and Nulon products (Australia) Pty. Ltd., for supplying lubricant samples.

I should express my deep appreciation and gratitude to my wife who was very patient and supportive during my course of study.

TABLE OF CONTENTS

LIST OF FIGURES

LIST OF TABLES

CHAPTER I

INTRODUCTION

1.1 Introduction to Deep Drawing Process

The deep drawing operation, as a type of deformation in sheet metal forming process, first developed in the 1700s, has been studied extensively and has become an important metal working process. In this operation, as shown in FIG. <1>, a flat circular sheet metal " blank " is positioned over a radiused die opening. The blank is held, with a controlled force, over the die by a blank-holder, or hold-down ring. A flat-bottomed punch then descends, pushing the blank through the die cavity and converting the flat blank to a cylindrical cup.

If the difference between the punch diameter and the die opening is less than the thickness of the blank being drawn, the cup wall is simultaneously thinned and elongated. This process is often called ironing or wall ironing. In contrast, when the clearance between the die and punch is greater than the blank thickness, the cup wall is bent plastically and its thickness changes very little or not at all. The process is then known as deep drawing.

To draw a cup-shaped part without wrinkling, tearing, necking, or undesirable variation in thickness, the following parameters must be controlled:

a. Properties of sheet metal blank.

   1. Yield stress of sheet metal blank. (σ_y)
   2. The strain rate sensitivity index (m) of the sheet metal. (the higherthe (m) value, the more defects are caused)

b. The ratio of the blank diameter (D_o) to the punch diameter (D_p).

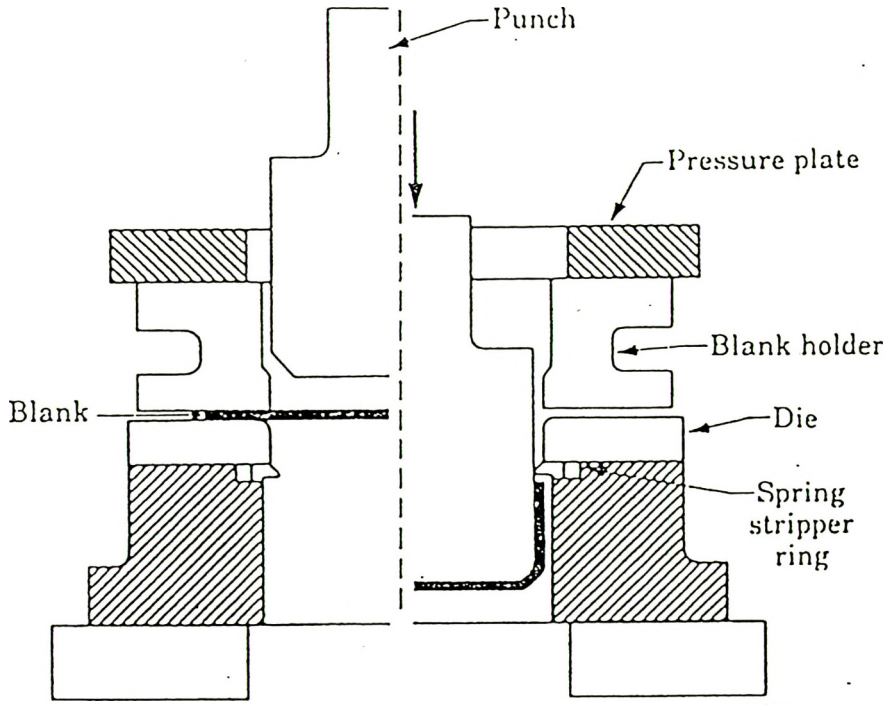

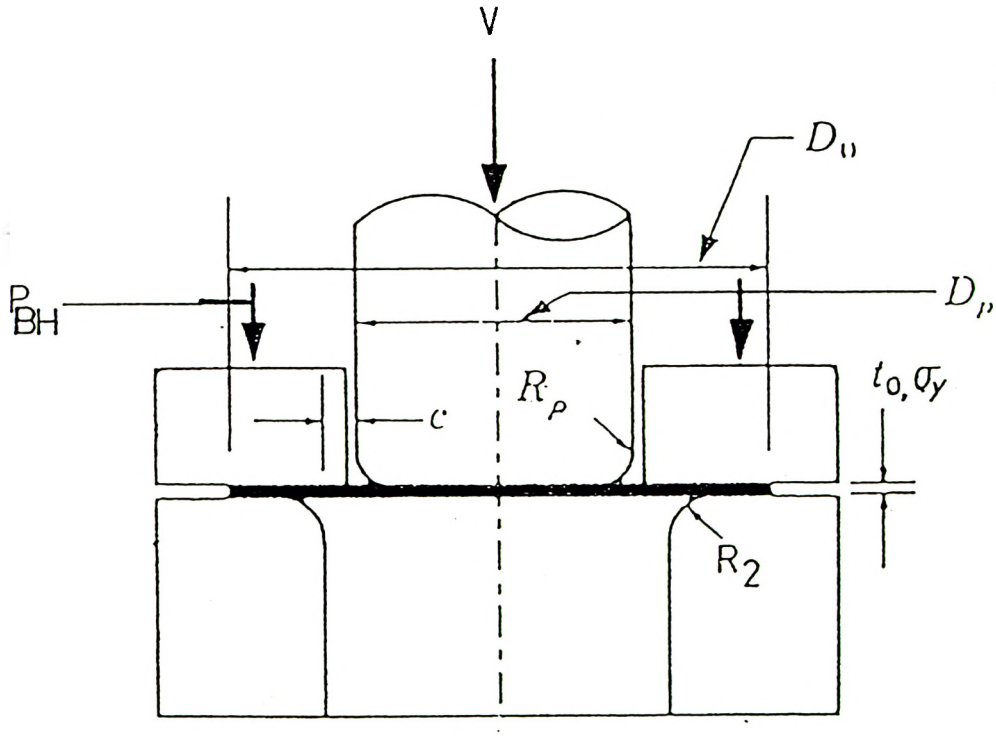

FIG. 1 DEEP DRAWING PROCESS

c. The clearance (c) between the punch and die.

d. Punch and die corner radii.(r_p and r_2)

e. Blank holder pressure.(p_{BH})

f. Speed of punch.(V)

g. Friction between punch, die and blank interfaces.

h. Lubrication. (formation of a thick lubricant film between the interface of the punch, die and blank in deep drawing process)

The tools for drawing operations are made of special tool steel. They are generally quite expensive. Consequently, it is essential to improve the life of tooling in order to reduce the manufacturing cost.

The deformation of the sheet metal takes place mainly over the die and the blank begins to stretch and bend to the required shape by the pounch. During bending, the surface of the die and punch are subjected to drawing force, and metallic contact with the blank. If the metallic contact would not be prevented, the gradual wear of tooling will shorten the life span of drawing tools.

1.2 Significance and Function of Lubrication for Deep Drawing process

In the deep drawing operation, as in most metal forming operations, lubrication and friction are of great importance. The friction force between the blank and the tooling may cause defects in drawn products in form of tearing, necking and wrinkling.

An effective lubrication regime can prevent direct metal to metal contact. With an appropriate operating conditions, the formation of a thick lubricant film between the surfaces of the tooling and blank can be achieved, leading to reductions in:

a. Friction.

b. Tool wear.

c. Drawing force.

d. Production costs.

And leading to increase drawability of product and improve product surface quality.

An effective lubricant may also provide an insulating film between the tool and the blank interface which in turn allows the use of a higher drawing speed and reduces the surface metallurgical damage on the product caused by adhesive material transfer from the blank to tooling.

Computer techniques have done much to assist in the development of complex-shaped drawn products, but their success is still variable. Successful deep drawing is still a combination of science, experience, empirical data, and experimentation. The body of existing knowledge is insufficient for an adequate understanding the mechanism of lubrication in deep drawing process.

A review of deep drawing lubrication research is given in Chapter II. It indicates that there are several unanswered questions, such as " Under what conditions is a hydrodynamic lubricant film established? " " Is there a theoretical model to estimate the lubricant film thickness and drawing force under hydrodynamic lubrication ?". This work is aimed to answer above questions.

The present work seeks to develop a mathematical model of hydrodynamic thick film lubrication for the deep drawing (cupping) process. A complete analysis for each of the stages and zones in the process is presented.

The conditions that enhance the formation of a hydrodynamic lubricant film and pressure are investigated. A theoretical model is introduced for estimating the drawing force and lubrication efficiency in the presence of a hydrodynamic lubricant film. Results from experiments and their comparison with the theoretical model are presented.

CHAPTER II

LITERATURE SURVEY

2.1 Historical Background of Hydrodynamic Lubrication in Metal Forming Processes

The basic mechanisms of metal forming lubrication such as wire drawing, forging, cold extrusion, rolling and hydrostatic extrusion have already been extensively studied by many researchers as given in REF.[1 - 62]. Different theoretical models and theoretical analysis for these processes have been developed that range from the application of simple isothermal hydrodynamic lubrication to thermal plastohydrodynamic lubrication on steady or unsteady states.

Plasohydrodynamic lubrication has been received considerable interest in recent years. Detailed plastohydrodynamic analyses of a number of metal forming operations such as wire and tube drawing, cold strip rolling and hydrostatic extrusion are now available. These analyses are useful in estimating the magnitude of lubricant film thickness, identifying the parameters affecting the film thickness and modeling of entrapment and entrainment of liquid and solid film and their subsequent transport and breakdown in various processes. The variation of lubricant viscosity and film thickness as a result of high pressures involved in metal forming operations and due to thermal effects has also been investigated.

2.1.1 Lubrication in Hydrostatic Extrusion

In the hydrostatic extrusion, a hydrodynamic lubrication region between the billet and die interface is established when the operating conditions are appropriate. It is

recognised that the formation of a hydrodynamic lubricant film is influenced by following various factors:

a. Viscosity of lubricant.

b. Geometry of the die and punch.

c. Yield strength of the metal.

d. Extrusion speed.

e. Extrusion force (pressure).

Numerous theoretical models have been developed to estimate the thickness of the hydrodynamic lubricant film and extrusion pressure related to these factors.

Hiller [1] has used an energy method to calculate the film thickness in the work zone. He has neglected hydrodynamic effects in the inlet zone of the die.

Studies by Wilson and Walowite [2], and by Snide, Dowson and Parson [3] have show that the inlet zone plays a dominant role in fixing the lubricant film in the work zone and therefore in estimating the extrusion pressure.

Wilson and Mahdavian [4] have carried out thermal inlet and work zone analysis for hydrostatic extrusion. Their results reveal that neglecting thermal effects in the inlet and work zone results in overestimating of both film thickness and extrusion pressure. Their analysis is limited to extrusion metals with constant yield strength. Obviously, no real metal actually behaves in this way when formed cold, and a constant yield strength assumption underestimates the extrusion pressure.

Nevertheless, Snidle, Parson and Dowson [5] in their analysis include the strain hardening of metal and both viscous shear heating and plastic deformation heat in the

work zone, but their theory predicts infinite pressure for some values of non-dimensional pressure viscosity coefficient which is in contradiction with experimental evidence.

In a later analysis Snide et al [6] presented a closed-form equation to calculate the hydrostatic extrusion pressure for strain hardening metal. They have considered an isothermal inlet zone film and neglected the viscous shearing heat effect in the work zone. This analysis is only useful for low strength metal and low speed extrusion where thermal viscous shearing heat in the inlet and work zone is minimal.

A thermal hydrodynamic lubrication analysis for hydrostatic extrusion of a work hardening metal has been developed by Mahdavian [7]. The analysis covers the hydrostatic extrusion of a wide range of metals and over a wide range of operating conditions. It indicates that thermal strain hardening effects play an important role in determining extrusion pressure for high reduction of area and high strength metals. It shows that the strain hardening and thermal effects inverse effects on extrusion pressure. The thermal effect tends to reduce the extrusion pressure particularly for high reduction of area and non-dimensional pressure viscosity coefficient. The extrusion pressure will be underestimated if the strain hardening of the metal is neglected.

Extrusion experiments using aluminium billets lubricated with castor oil were conducted by Wilson and Mahdavain [4]. Estimates of the inlet film thickness in these experiments based on measurements of the product diameter show good agreement with the theoretical model over a wide range of conditions. Experimental measurements of extrusion pressure were also in agreement with the theoretical model.

In an earlier experimental investigation of lubrication in hydrodynamic extrusion by Wuerscher [8]. Paraffin wax was extruded, to test the validity of a theory proposed by Iyengar and Rice concerning the conditions necessary for hydrodynamic lubrication.

However, there is not enough information about the type of lubricant used nor are there any measurements that can be employed to estimate the film thickness.

2.1.2 Lubrication in Cold Extrusion

In cold extrusion, Thompson and Symmons [9] have investigated the effect of viscosity of trapped lubricant film in the extrusion of lead billets. They have presented a plastohydrodynamic lubrication analysis for inlet upsetting of a billet. Their analysis is limited to calculation of trapped lubricant film thickness between the billet and the container.

A refined analytical model for hydrodynamic lubrication in cold extrusion has been developed by Mahdavian [10]. This analysis is concerned with presenting a refined model for the lubrication process which includes thermal effects in the inlet and work zone of a cold extrusion process. A thermal transient hydrodynamic lubrication theory has been extended to the cold extrusion process to calculate the lubricant film thickness and unsteady extrusion process.

2.1.3 Lubrication in Forging

Kalpakjian [11] gives a useful review of lubrication in the forging operation. Oyane and Osakda [12 - 13] hydrodynamically modelled the formation of the lubricant film been upsetting between flat dies. Wilson [14] extended this work to include the subsequent transport and thinning of the lubricant film. This revealed that the lubrication breakdown can be explained by the inability of the lubricant to keep up with the outward motion of the workpiece surface.

Wilson and Carpenter [15] and Wilson and Delmolino [16] have shown the importance of thermal effects on the lubricant transport process. The most important thermal effect during the film formation process is due to shear heating within the lubricant film.

2.1.4 Lubrication in Wire Drawing

One of the factors limiting the rate at which wire can be drawn through tungsten carbide or diamond dies is the severe die wear which may occur at high speed of drawing. If effective lubrication can be provided in the die the die wear can be reduced considerably. It is suggested by Christopherson and Naylor [17] that this can be achieved by supplying lubricating oil to the entry of the die at a pressure comparable with the yield stress of the wire. The necessary pressure can be conveniently generated by causing the wire to approach the die through a tube of diameter slightly larger than the wire diameter (termed a Christopherson tube), sealed on the inlet side of the die. Experimental work by these authors showed a reduction in drawing force and die wear.

The theoretical analysis of the inlet tube configuration suggested by the above workers has been extended together with considerations of the lubricating conditions in the deformation zone by Tattersall [18] and Osterle and Dixon [19].

Based on the principle of minimum energy dissipation rate, Bedi [20] developed a hydrodynamic model of wire drawing and calculated the lubricant film thickness and viscous friction coefficient. The effect of die geometry and speed was also investigated, however the analysis did not incorporate the effect of pressure and temperature variation on the lubricant viscosity and film thickness.

Dowson, Parsons and Lidgitt [21] have further analysed the performance of the Christopherson tube by considering the effect of temperature on lubricant viscosity.

The study of lubrication in steel wire drawing using a Christopherson tube and a polymer melt as a lubricant has been carried out by Thompson and Symmons [22] to determine the coating thickness and the variables affecting it. They concluded that the thickness of the polymer melt depends on the Sommerfeld number, which is a function of lubricant viscosity, speed of wire drawing, yield stress of material and tube geometry.

The analysis of Thompson and Symmons was modified by Hashmi, Crampton and Symmons [23] to account for the strain hardening and strain rate sensitivity. It assumed non-newtonian behaviour for the polymer melt by utilizing an empirical expression relating shear stress and rate of shear together with an experimentally derived pressure coefficient of viscosity.

Based on his experimental and theoretical study of lubricant film thickness in wet wire drawing by using a very viscous lubricant (chlorinated paraffin oil), Felder [24] reported a complete separation of the die and wire at high speed (.5 to 4m/sec). The theoretical analysis of Felder incorporated thermal effects by making use of Brinman's number. During the discussion on his paper Felder suggested that the plastohydrodynamic theory may be exploited by manufacturing industry for finding solutions for actual problems such as diminishing the cost of metal working by elimination of surface coatings (for example phosphating) or substitution of liquid lubricants(oil or emulsions) for soaps in wire drawing.

2.1.5 Lubrication in Tube Drawing

Friction increases the drawing force in tube drawing, causes inhomogeneity of deformation and is contributory to the development of residual stresses in the drawn

product [Avitzur, 25]. Friction also limits the maximum reduction that may be taken in a single draw and adversely affects the die life. Reduced friction is therefore desirable in tube drawing. This can be achieved by some form of lubrication between the die-tube interface in tube sinking and die-tube and plug-tube interfaces in plug drawing.

For increasing the lubricant film thickness, a tandem die arrangement has been used industrially since about 1955 [Schey, 26]. In this arrangement two dies are used, the first taking a small sizing reduction and the second around 40%, while the region between the dies is enclosed so that the lubricant can build up a high pressure, thus promoting thick film lubrication at the second die. This technique works well at 30 m/min, with the tubes coated with sodium-based soap.

Matsuura [27] proposed a method of tube drawing with two plugs and a mandrel in which lubricant is supplied under pressure to both the internal surface, through the mandrel, and the external surface. In addition, hollow plug bars with chlorinated oil pumped to the working interface can be used to ensure adequate supply of lubricant [Schey, 25].

A plastohydrodynamic analysis of tube sinking [Nauhria and Bedi, 28], [Nauhria, 29] provides for the calculation of lubricant film thickness in addition to identifying the process parameters which affect the film thickness. The analysis is based on the principle of minimum energy dissipation rate and is capable of explaining the thickening and thinning of tube wall during the sinking process.

The lubricant film thickness was found to depend on the modified Sommerfeld number, which is a function of lubricant viscosity, speed of drawing, yield stress of the tube material and initial tube diameter.

It has been suggested [Nauhria and Bedi 30] that the hydrodynamic lubrication in tube sinking breaks down when the lubricant film thickness falls below some critical value, which is consistent with the concept of a critical value of the modified Sommerfeld number for the sinking process. The analysis accounts for the strain hardening of the tube material and thermal effects on lubricant viscosity and film thickness. It can be used to determine a suitable combination of sinking parameters along with a critical Sommerfeld number, so as to achieve a full fluid film lubrication in the deformation zone, together with acceptable surface finish of the drawn product.

The plastohydrodynamic analysis of plug drawing [Nauhria and Bedi, 31] has been used to calculate the lubricant film thickness at the die-tube and plug-tube interfaces. The analysis reveals that the lubricant film thickness in plug drawing depends on the modified Sommerfeld number or critical modified Sommerfeld number to ensure conditions of full fluid film lubrication.

2.1.6 Lubrication in Cold Strip Rolling

Hydrodynamic lubrication of cold rolling processes has advantages in the production of sheet and strip products. A thick lubricant film would prevent contact and excessive friction between the roll and strip. If too much surface contact is allowed, metal pick-up and transfer can destroy the product and prohibitive maintenance costs can result from excessive roll wear.

If the friction is too high, heating can exceed material limits and reduce production speeds, workability of difficult material can be limited and equipment capacity can be exceeded [Dow, Kannel and Bupara, 32]. At the same time the friction between the strip and rolls must be sufficient to draw the strip through the rolls.

As the demand for sheet and strip products increases, higher production speeds are proposed for rolling mills. Since the thickness of the hydrodynamic film generated increases with rolling speed, future high-speed mills will operate in a regime conducive to hydrodynamic lubrication. Under current conditions, thick films are sometimes achieved in production operations, but they are usually associated with an unstable or not easily controlled rolling situation. This may be caused by inadvertently operating with a lubricant which exhibits excellent boundary lubricating characteristics under conditions which produce a thick hydrodynamic film. The bulk properties of the lubricant may be inappropriate for the thick-film regime and the resulting friction too low for proper mill control.

Most rolling theories have been based on the assumption of a constant friction coefficient between strip and roll. This coefficient has been derived using empirical data taken from production and laboratory rolling mills and other related reduction processes. However, the fact that the assumption of a constant friction coefficient is not valid for conditions of hydrodynamic lubrication, in addition to the question of validity of the empirical coefficient of friction for particular conditions, has led to more specific theories for hydrodynamically lubricated strip rolling.

A number of investigators have studied the hydrodynamic lubrication in cold strip rolling. Chen [33] used the elastohydrodynamic theory to estimate the entrained film thickness in cold rolling of strips. Bedi and Hillier [34] and Avitzur and Grosman [35] applied a minimum energy method within the work zone to calculate the film thickness, but did not include the thermal effects on lubricant viscosity and film thickness.

Wilson and Walowit [36] developed an isothermal model for the lubrication of rolling which used an inlet zone analysis to calculate the entrained film thickness. They defined a non-dimensional pressure coefficient of viscosity, G as the product of

lubricant pressure coefficient of viscosity and the workpiece flow strength, which must be controlled within narrow limits. If G is too large, very high friction and excessive roll separating forces will result, while if G is too low, skidding will occur. The ideal value of G decreases with increasing reduction and the usable range can be extended by the use of controlled front and back tension.

Dow, Kannel and Bupara [32] developed a thermal Newtonian model of lubricant behaviour in cold strip rolling. They found that thermal effects could result in substantial reductions in the entrained film thickness. The analysis reveals that the pressure distribution for the case of hydrodynamic lubrication is more uniform than that where metal to metal contact take place. Using this theory a good approximation of the performance of a hydrodynamic rolling lubricant can be calculated. The effect on film thickness and pressure distribution of lubricants with different properties can also be evaluated.

Wilson and Murch [37] developed an analytical model for the hydrodynamic lubrication of high speed strip rolling. They proposed a semi-empirical equation for the reduction of entrained film thickness due to thermal effects in the inlet zone. They found that apart from the non-dimensional pressure coefficient G proposed by Wilson and Walowit [35], there are two additional parameters namely, the plastic thermal parameter K and the viscous thermal parameter L, which are important in deciding friction in the roll bite. The parameter K is a function of the temperature coefficient of viscosity, workpiece flow strength and workpiece volumetric specific heat. The parameter L is defined in terms of lubricant base viscosity, inlet strip speed, roll speed, temperature coefficient of viscosity and lubricant thermal conductivity. Increasing either K or L tends to reduce friction and may induce skidding. As L increases with rolling speed, skidding can be a problem at high speeds.

Tsao and Sargent [38 - 39] developed mixed lubrication models for strip rolling. They used conventional isothermal and thermal inlet analyses to calculate the entrained film thickness. Using information on the roll and workpiece surface topography they estimated the amount of boundary contact and its contribution to the overall friction level. The results reflect the reduction in friction which occurs as the system undergoes a transition from boundary to thick film lubrication.

Reid and Schey [40] published the results of a series of experiments on rolling aluminium alloys with a variety of well characterized mineral oils. Many of their experiments were conducted in the thick film regime and their results are helpful in modelling the hydrodynamic lubrication process in rolling.

Aggarwal and Wilson [41] developed an analytical model for hydrodynamically lubricated strip rolling which allows for different types of roll heating. They calculated the entrained film thickness with different inlet strip and roll temperatures by making use of an effective mean speed. Theoretical predictions of entrained film thickness were found to be lower than the published experimental results of Reid and Schey [40]. Ref.[41] suggested that if an empirical correction is made for the rounding-in effect a good agreement can be achieved between theoretical and experimental results.

2.2 Lubrication in Sheet Metal Forming Processes

As discussed by Wilson [42] four different regimes of lubrication are possible in sheet metal forming. Of these, the full film regime in which the surfaces are completely separated by a lubricant film with a thickness much larger than the molecular size, will displace the boundary and mixed regimes if conditions are favourable. The hydrodynamic analysis of sheet metal forming will be useful in improving lubrication.

2.2.1 Lubrication in Stretch Forming

Wilson and Wang [43] developed theoretical model of hydrodynamic thick film lubrication in stretch forming processes. The lubricant is treated as an isoviscous Newtonian liquid. The model indicates that a hydrodynamic film can be entrained by a wedge shaped inlet zone formed at the outer edge of the contact between punch and sheet as the sheet wraps around the punch.

The film is thickest near the punch centre and decreases near the edge of the contact zone, consequently as the process proceeds breakdown of the hydrodynamic film may occur in this outer region in the later stages of the process. The initial central film thickness in a plane strain process depends on the lubricant viscosity, the punch velocity, the punch radius, the sheet flow stress, the initial sheet half width and the initial sheet thickness.

The film thickness in an axisymmetric process is substantially less than that in the equivalent plain strain process due to the higher interface pressures and less favourable inlet geometry in the axisymmetric case. Plastic heating of the sheet tends to increase the lubricant film thickness and to decrease friction.

Hydrodynamic friction levels are so low as to be generally negligible. Thus the main frictional effects in practical processes will be due to asperity inter action in the mixed and boundary regimes.

2.2.2 Lubrication in Deep Drawing

Newnham [44] has indicated that there are two regions of the hydrodynamic lubrication are possible in deep drawing operation:

a. Around the radius of die.

b. Along the punch.

However, from most investigators point of views Ref.[45-49], lubricating along the punch would be a disadvantage to the drawability of sheet metal. Conversely, lubricating along the radius of the die (interface between the die and sheet) while the punch is unlubricated, will produce a similar increase in the limit of drawing ratio (LDR).

Due to the high friction between surfaces of the die and the blank sheet metal, the deep drawing load is borne only by the blank sheet metal. With a well-lubricated between die and blank sheet metal provided, the some extent of deep drawing load is transmitted to the punch. As a result of the reduced load on the blank sheet metal, the greater total loads can be accommodated, and hence deeper draws can be obtained before failure.

In many pressing operations there will be regions where sheet metal is pushed downward by the punch surface and other regions where metal is drawn over a flat region of a die or around a die corner. In this latter instance, a hydrodynamic wedge can form provided that the processing speed and lubricant viscosity are high enough.

Such a lubrication mechanism would be welcome, since the die corner is the area where metal pick up and lubricant breakdown most frequently occur. Pure hydrodynamic lubrication would guarantee that this is prevented. But in practice speed and viscosities are high enough only to give fluid-film condition.

Lubricant will initially be squeezed from the blank/die and blank/hold-down ring interfaces as the tooling starts to close. This process has already been analyzed in another context and Moore [50] gives the following equation for the time t after the

application of a load w required to reduce the film thickness from a initial value h_0 to a value h

$$t=[3\pi\mu(d_2^4-2d_1d_2^3+2d_1^3d_2-d_1^4)(1/h^2-1/h_0^2)]/64w$$

where μ is the lubricant viscosity and d_1 and d_2 are the inner and outer diameters of the interface respectively.

Wilson [42] has also indicated that when deep drawing starts, the residual film at the blank/die and blank/hold-down ring will be wiped inwards by motion of the blank. During this phase there will be some redistribution of load within the annular interface due to the fact that it is drawn inwards. This will tend to thin out the film near the inner diameter. However, it seems likely that a relatively thick film can be maintained. Lubrication at the blank/die radius is particularly crucial in deep drawing.

It is unfortunate that little analytical work has been done on this area. However, the geometry is almost identical to the foil bearing analyzed by Blok [51].

He gives the film thickness h_1 over the radius as

$$h_1/r_D=1.405(\mu v/T)^2$$

where r_D is the radius of the die corner, μ is the lubricant viscosity, v is the surface velocity of the blank, and T is the tension in the strip per unit width.

2.3 Deformation in Deep Drawing and Ironing Processes

Most of the research into the deep drawing process deals with the deformation of a metal blank without lubrication. The coefficient of friction between the die, punch

and blank holder is assumed to be the result of surface to surface contact and considered to be constant (coulomb friction).

Theoretical models based on the application of upper-bound, lower-bound and finite element methods have been developed to predict drawing load, defects and other aspects of drawing that is related to the plastic deformation of a blank. An upper-bound approach to the analysis of axisymmetric deep drawing was introduced by Hasek and Kramer [52]. For this purpose the part being drawn is subdivided into critical regions, each one of which is analyzed. The results of the analysis are compared with those of a different analytical approach, and with experimental results.

Forming-limit curves are useful for assessing the formability of sheet metal. The results of an investigation of the forming limit diagram are presented by Hasek [53]. Forming-limit curves were obtained with a specially designed drawing tool set-up and the effects of isotropy, sheet metal thickness, lubrication, strain history, and grid element diameter were observed. A mathematical description of the forming limit diagram accounting for localized and diffuse necking is provided by Hasek. Limited agreement between theory and experiment was achieved. The analytical approach is claimed to be useful for determining the effect of parameters, such as an isotropy and the strain hardening coefficient, on the location of the curves.

Forming-limit curves were established by Muschenborn and Sonne [54] for fully killed titanium stabilized deep drawing steel sheet, without prior deformation and with different prestrains. Equations were derived from the experimental results which estimate the influence of the deformation path. The effects of prior deformation upon forming limits are presented.

The influence of the R-value (the parameter characterizing the anisotropic behaviour of material), upon strength and formability of Tia15Sn2.5 sheet was investigated by Mae [55] Formability was tested using the Erichsen and Fukui cup tests and strength values were obtained from a three point bending test using 90-deg. v-notches. In all three different R-values were examined.

Hasek [56] presents a mathematical description of the effect of plastic anisotropy in the drawing of large sheet metal parts.

Based on a study of the properties of the alloy AlMg2, drawing and bulge behaviour were studied by Neubauer et al. [57] using correlation analysis. Economic and production advantages in replacing commercial-purity aluminium with this alloy are discussed.

Tangermann [58] presents a state-of-the-art review of deep drawing technology with particular emphasis on production of aluminium beverage cans by ironing.

Neubauer et al.[57] showed the results of an experimental investigation of drawing axisymmetric and rectangular plastic-coated steel parts. Drawing ratios, maximum drawing force and hold-down force were the main variables under study. Single and multiple draws were investigated.

Starting with a fundamental consideration of the limiting drawing ratio for the first and subsequent draws, Osterburg [59] reviewed the five-stage reduction sequences for drawing three different materials. Calculations of reductions with and without intermediate annealing were developed and compared with existing guide values.

An investigation into the use of square blank for drawing cylindrical cups was conducted by Galinowski [60]. Differences in stress-strain behaviour as well as in

power and amount of work required for square and circular blanks were analyzed, and guide lines for the use of square blanks recommended.

The results of an investigation of the material behaviour and force requirements in free reverse second drawing of cups are presented by Radtke and Dirke [61] as a function of drawing path for different reverse drawing punch diameters. An isotropy effects were included in the study.

2.4 Objectives

The survey of previous work indicates that the available theoretical analyses are not directed towards an understanding of the mechanism of hydrodynamic lubrication in the deep drawing process. Also, the available experimental results are not sufficient to check any developed or adapted theoretical models to the deep drawing process. Therefore, there is a need to develop a theoretical model for the deep drawing process, which can be compared with experiment.

The development of a new theoretical model to estimate the hydrodynamic lubricant film thickness, and drawing force is one objective of the present work. The model covers the deformation stages from sheet metal blank to the drawn cup-shaped product. The drawing process is divided into approaching, yielding, and steady deformation phases. The analysis is carried out for each phase. The model considers only for the drawing case where there is only pure plastic bending deformation and the thickness of the drawn blank remains unchanged. Conditions that lead to the establishment of a thick hydrodynamic lubricant film will be investigated.

The other objective is to develop an experimental deep drawing system and make measurements of the drawing force and the lubricant film thickness so that these can be compared with the theoretical values. Changes in cup diameter due to presence

of the thick hydrodynamic lubricant film will be used as a method of estimating the lubricant film thickness.

CHAPTER III

THEORETICAL ANALYSIS

3.1 Process to be Analyzed

Detailed analyses will be restricted to the conventional pure deep-drawing (so called cupping) operation, in which the clearance between die and punch is slightly larger than, or just equal to the material thickness t_o. The punch is flat bottomed, and deformation of the blank is under condition of plane-strain state.

The main action of the clamping flange is to improve stability of the blank as well as to prevent the blank wrinkling when it is being drawn through the die. The blank-holder force is small relative to yield stress of the blank, so that the tooling and the blank are rigid. The lubricant film thickness does not vary with position and interfaces are completely separated by the local lubricant film thickness h.

The process may be divided into three phases (stages):

1. The approaching phase (early stage).

2. The yielding phase (intermediate stage).

3. The steady deformation phase (late stage).

Figures 2, 3 and 4 respectively show these three phases, during hydrodynamically lubricated deep drawing.

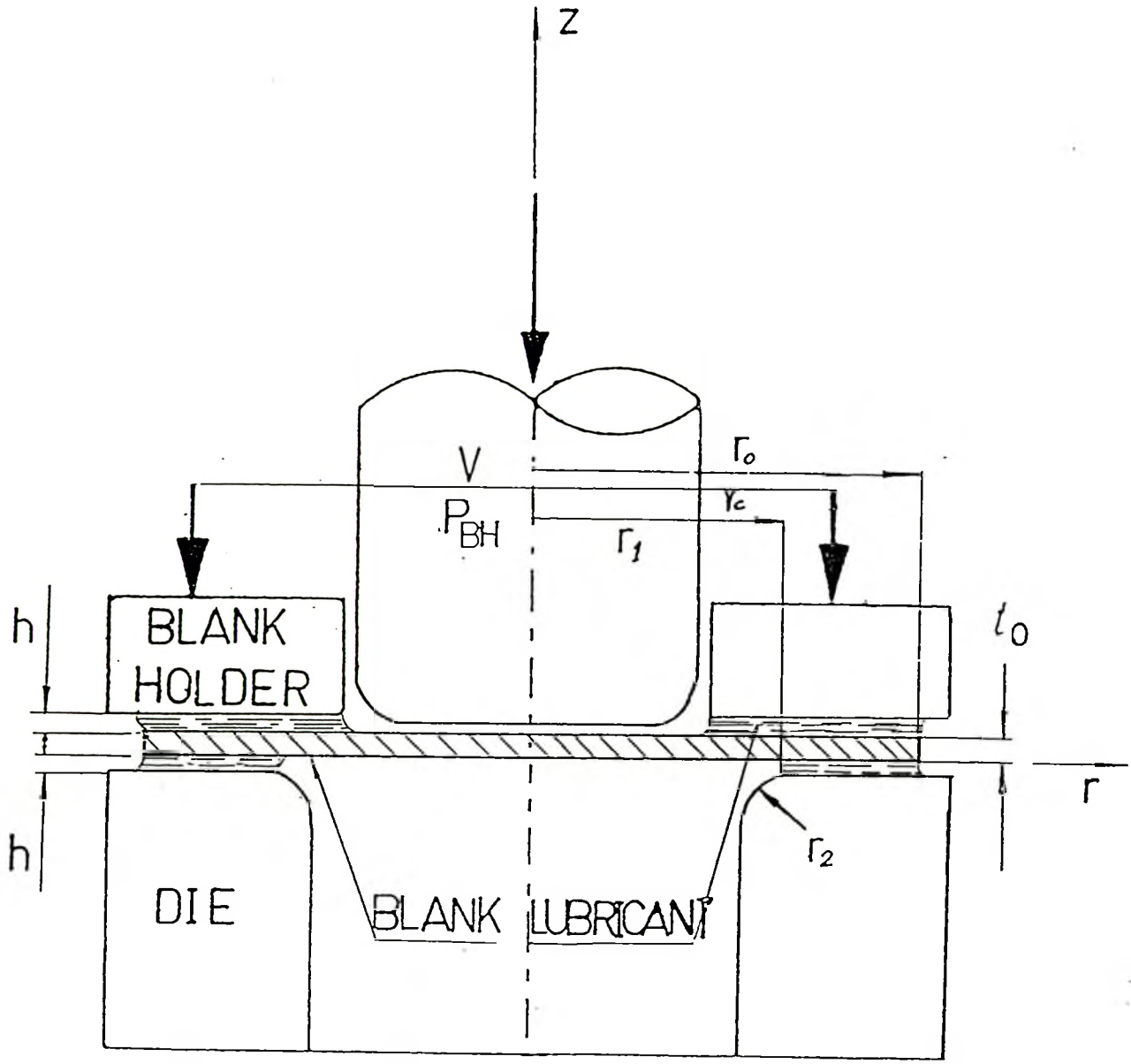

FIG. 2 THE APPROACHING PHASE (EARLY STAGE)

3.1.1 Approach Phase

At this stage, both the upper and lower surfaces of the blank separated from the die and blank holder surfaces by a viscous lubricant film due to squeeze action.

As shown in FIG.<2>, the blank holder approaches the die surface with a constant velocity V, to clamp down the blank to the die surface. This causes the lubricant film between both surface of the blank and surfaces of the die and blank-holder to be squeezed outwards and support the load.

3.1.2 Yielding Phase

At this stage, the process is being characterized as following:

1. The blank, as shown in FIG.<3>, is pushed by the bottom surface of the moving punch into the die cavity.

2. As the blank is bent at the corner of the die, a converging wedge space with an angle Θ is formed between the surfaces of blank flange and die.

3. The viscous fluid over the surface of the flange is transported in the wedged space by two simultaneous actions. The first one is the squeezing action by the blank-holder with the vertically approaching velocity V and the other action is sliding of the blank flange towards the centre of the die. The later action drags the lubricant film from the compression zone into the die zone. At this stage, a steady hydrodynamic lubrication regime is established between the blank and die until the drawing process is completed.

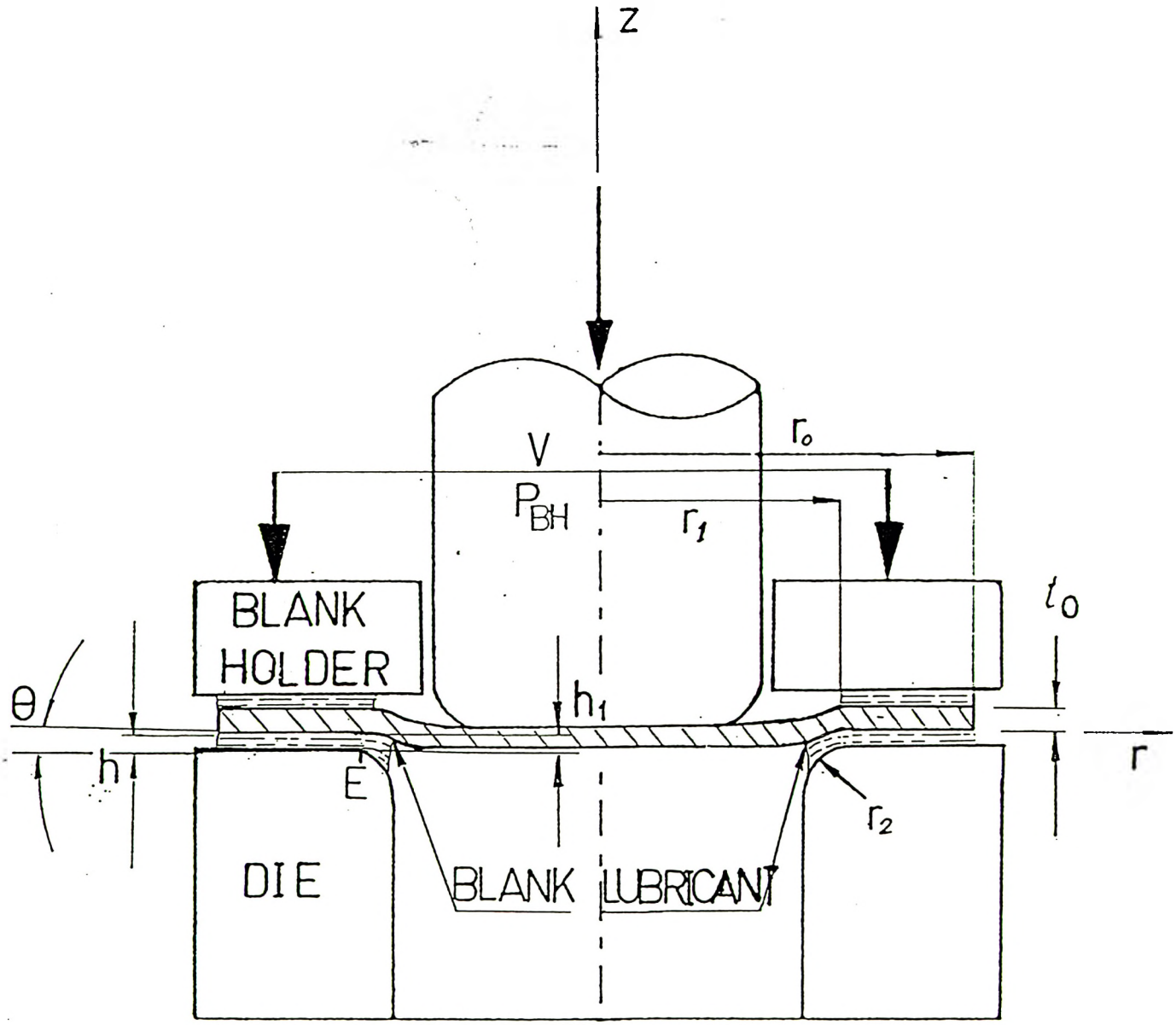

FIG. 3 THE YIELDING PHASE (INTERMEDIATE STAGE)

4. The lubricant film pressure p, is being increased up to the yielding stress of the blank material σ_y, at the corner of the die at location E, as shown in FIG.<3>. It is evident that the pressure profile of the lubricant film is different from the approaching stage.

5. The lubricant film thickness is being reduced down to a value h_1 at the corner of the die at location E. The film thickness h_1 remains unchanged during the transition from the yielding to steady states.

The yielding phase duration is a quite short period. This phase is terminated once the blank starts to conform to the shape of the die as shown in FIG.<4>.

3.1.3 Steady Deformation Phase

After the period of approaching and yielding phases, the blank-holder clamps down the blank firmly to the die plate. This action prevents any defects in the cup from wrinkling during subsequent drawing in steady deformation phase.

In the steady deformation phase, the punch continues to move down. Simultaneously, the lubricated flange part of the blank slides between the die and blank-holder as its width decreases progressively and enters into the die cavity. Finally, as the blank is drawn and bent over the curved shoulder of the die, the cup-shaped product emerges from the die at this stage, the pressure generated in the lubricant film enables it to withstand applied blank-holder pressure. The blank-holder will not move further down, and the phenomenon of lubricant squeezing is stopped. This sliding motion of the blank establishes a steady hydrodynamic lubrication regime that separates the blank by a lubricant film. The blank sliding velocity is equally to the punch velocity V.

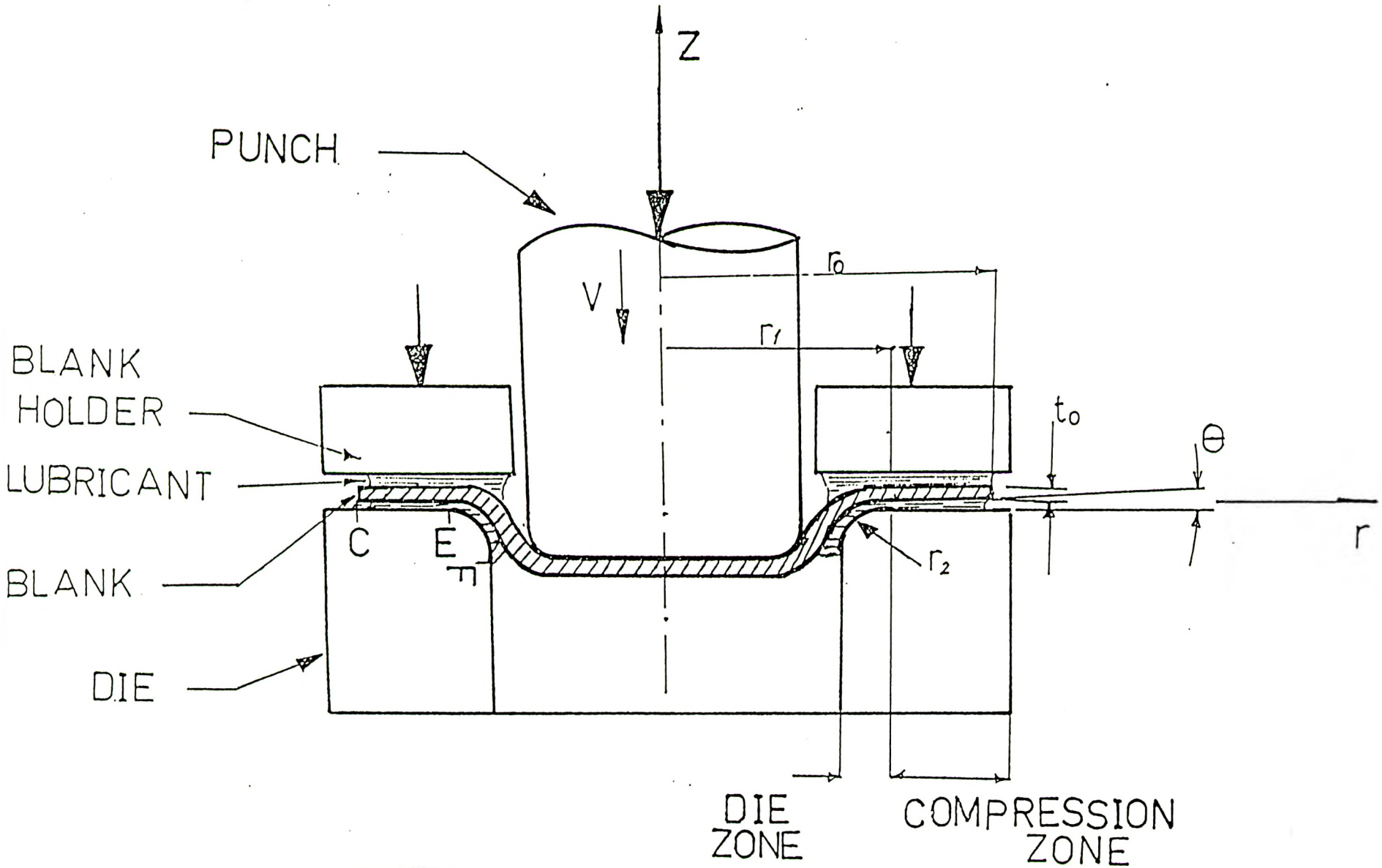

FIG. 4 THE STEADY DEFORMATION PHASE (LATE STAGE)

Through out the deformation phase, the geometry of the hydrodynamically lubricated blank and its deformation does not remain uniform. In order to model the lubrication process, the deformation phase region is divided into zones as follows.

1. Compression zone. (flange zone)

2. Die zone. (curved zone)

3.1.3.1. Compression Zone

The compression zone is the flat part of the drawing tool as shown in FIG.<4>. The boundaries of this region is limited between points C and E which are located at distance of r_0 and r_1 respectively. Once a thick hydrodynamic lubricant film is created, the interfaces between the die and the flange of the blank are completely separated. The lubricant film thickness h linearly varies with the position r, and is proportional to the value of h_1 (the lubricant film thickness at the boundary location of compression and die zones). The film thickness h_1 is referred as to the inlet film thickness of the compression zone. As shown in FIG.<10>, the stresses acting in the compression zone are tangential compression stress σ_t, radial tension stress σ_r, lubricant pressure p and lubricant friction shearing stress τ_0.

3.1.3.2. Die Zone

FIG.<4> depicts the die zone boundaries between locations E and F. The bending of the blank is started and completed in this zone. The local lubricant film thickness remains constant and equal to inlet film thickness h_1 with insignificant lubricant pressure gradient.

Stresses acting on the blank in the die zone are tensile stress σ_z, lubricant frictional shearing stress τ_d and lubricant compression pressure p.

3.2 Assumptions Used in the Analysis

3.2.1 General Assumptions Related to Hydrodynamic Lubrication Analysis

1. The fluid lubricant is incompressible.
2. The fluid lubricant is Newtonian.
3. The fluid flow is to be laminar.
4. The fluid flow is steady.
5. The flow is taken one-dimensional fluid flow into account.
6. The pressure across the thickness of the fluid film is constant.
7. The lubricant viscosity is independent of pressure and temperature.
8. Effects due to the inertia of the fluid are neglected.

3.2.2 Additional Assumptions for Plastic Deformation Analysis

9. The interfaces between contacts of the tooling are smooth and parallel.
10. The tools are rigid. Punch and blank-holder descend with a constant normal speed V.

11. The surface velocity of the blank U is constant during deformation process, and equal to normal speed of the punch V.

12. The material of the blank behaves as a rigid-plastic solid. Yield and subsequent plastic deformation are governed by Tresca or Maxwell-Mises law. The resistance to deformation is characterized by a constant plane-strain yielding stress σ_y.

13. The deformation process is one of homogeneous deformation under conditions of plane-strain.

14. The pressure generated in the region of compression zone does not deform the blank.

15. The pressure gradient in the region of plastic deformation is insignificant so that its effect on lubricant flow may be neglected.

16. The lubricant film thickness h is small compared with the thickness of the blank t_o.

17. The thickness of the blank t_o is small compared with the radius of the punch r_p, the curvature radius of die r_2, and the position r_1.

General assumptions (1-8) are used in the development of steady one-dimensional incompressible Reynold's equations.

Assumption (3) makes the analysis of hydrodynamic lubrication to be isoviscous fluid flow model. Thermal and pressure effect variations of viscosity are neglected in fluid flow.

Additional assumptions (9-17) are made to simplify the plasticity and mathematical problems.

Assumption (9) eliminates the influence of surface roughness on lubricant transport which has been investigated by Wilson and Delmolino [16].

Assumptions (11,16) based on the insignificant of strain in the radial direction of the blank during deformation process. This is justified because the thickness and velocity of the blank are constant during steady deformation phase.

Assumption (12) neglects the effects of elastic deformation of the blank on the lubricant flow film value.

Assumptions (14,15) are all valid and have been used in previous analytical models of hydrodynamic lubrication of metal forming processes.

3.4 Development of Mathematical Models

3.4.1 Approaching Phase

FIG.<2> shows the case of approaching phase. Since the die, workpiece, and blank-holder are rigid and parallel according to assumptions (9-10) and (14), the lubricant film thickness h does not vary with radial position r and thus, is given by

$$dh/dt = -V \qquad (1)$$

where V is the velocity with which the blank-holder approachs to the blank and die surfaces.

Assumptions (1-8) yield the Reynolds equation

$$d[(h^3/12\mu)(dp/dr)]/dr = dh/dt \qquad (2)$$

where r is the local radial distance from the vertical axis of the centre line, μ is the lubricant viscosity, p is the local pressure of the lubricant, h is the local lubricant film thickness and t is the approaching time.

Substituting for dh/dt from equation (1) into equation (2) and reranging, gives

$$d(dp/dr)/dr = -12\mu V/h^3 \qquad (3)$$

Then integrating equation (3)

$$dp/dr = -12\mu Vr/h^3 + C_0 \qquad (4)$$

where C_0 is a constant of integration.

From symmetrical geometry of the tooling, the maximum pressure of the lubricant film is at the centre of blank-holder, located at

$$r = r_c \qquad (5)$$

$$dp/dr = 0 \qquad (6)$$

Using this boundary condition and substituting into equation (4), yields

$$C_0 = 12\mu Vr_c/h^3 \qquad (7)$$

Substituting for C_0 from equation (7) into equation (4) it becomes

$$dp/dr = 12\mu V(r_c-r)/h^3 \qquad (8)$$

From FIG.<2> r_c is given by

$$r_c = (r_o-r_1)/2 + r_1 \qquad (9)$$

where r_o is the initial outer radius of the blank, r_1 is the distance along die radius from origin to the location E.

Substituting for r_c from equation (9) into equation (8), it yields

$$dp/dr = -6\mu V(r_o+r_1-2r)/h^3 \quad (10)$$

Integrating equation (10)

$$p = -3\mu V(r_o+r_1-2r)^2/2h^3 + C_1 \quad (11)$$

where C_1 is a constant of integration.

At the edge of the contact where

$$r = r_o, \text{ and } r = r_1 \quad (12)$$

$$p = 0 \quad (13)$$

Using this boundary condition and substituting for p and r into equation (11) yields

$$C_{11} = 3\mu V(r_1-r_o)^2/2h^3 \quad (14)$$

$$C_{12} = 3\mu V(r_o-r_1)^2/2h^3 \quad (15)$$

Since $(r_1-r_o)^2$ and $(r_o-r_1)^2 > 0$, thus

$$C_{11} = c_{12} \quad (16)$$

Substituting for C_{12} from equation (15) into equation (11) and reranging it yields

$$p = 6\mu V(r-r_1)(r_o-r)/h^3 \quad (17)$$

The analysis for the approaching phase is similar to Wilson (14)'s method that used to model forging process. Equation (17) reveals that the lubricant film pressure

profile during the approach phase is a parabolic. The maximum pressure in the lubricant film occurs at the centre of the blank-holder pressure P_{BH} where $r = r_c$, substituting for r_c from equation (9) into equation (17) yields

$$p_m = 3\mu V(r_0-r_1)^2/2h^3 \qquad (18)$$

In the approaching phase, as the lubricant film thickness h decreases, the central maximum pressure p_m rises until it reaches to a limiting value p_{BH}. This blank-holder pressure limit is given by Lange [62] as follows

$$p_{BH} = 10^{-3}D[(1/B'-1)^3 + 0.005d_0/t_0]\sigma_y \qquad (19)$$

where B' is the drawing ratio r_3/r_0, r_3 is the radius of the die, t_0 is the thickness of blank, σ_y is the yield stress of material, D is a factor of 2 - 3. This pressure p_{BH} is sufficient to prevent any wrinklings when the drawing process proceeds to the deformation phase.

The lubricant film thickness h_{BH} at this limit is given by

$$h_{BH} = [3\mu V(r_0-r_1)^2/(2p_{BH})]^{1/3} \qquad (20)$$

Substituting for p_{BH} from equation (19) into equation (20) yields

$$h_{BH} = \{3\mu V(r_0-r_1)^2/[2*10^{-3}D[(1/B'-1)^3 + 0.005d_0/t_0]\sigma_y]\}^{1/3} \qquad (21)$$

In order to facilitate the plotting of pressure distribution and film thickness variation with different parameters, equation (17) is written in nondimensional form as

$$P' = H'^{-3}(R-B)(1-R) \qquad (22)$$

where the nondimensional parameters are defined by

$$P' = pr_0^2/(6\mu V) \quad (23)$$

$$H' = h/r_0 \quad (24)$$

$$R = r/r_0 \quad (25)$$

$$B = r_1/r_0 \quad (26)$$

Also, equation (21) can be written in nondimensional form as

$$H_{BH} = B/(10^{-1})[K/(1-B)]^{1/3} \quad (27)$$

the nondimensional parameters are defined by

$$H_{BH} = h_{BH}/r_0 \quad (28)$$

$$K = \mu V/(2\sigma_y r_0) \quad (29)$$

$$D = 3 \quad (30)$$

neglecting $0.005d_0/t_0$ in equation (19) and simplifying

$$B' = B - (r_2/r_0) = B \quad (31)$$

where r_2 is the radius curvature of the die.

3.4.1.1 Discussion of Results

The variation of nondimensional pressure P' with respect to nondimensional radius R for various values of nondimensional film thickness H' is shown in FIG.<5>. The nondimensional lubricant pressure P' increases with nondimensional film thickness H' from zero pressure at the outer edge to a maximum pressure p_m at the blank-holder

centre and then decreases to the zero pressure at the outer edge in compression zone. The p_m raised up to blank-holder pressure p_{BH} at its centre during the approaching phase.

The graphs for the nondimensional pressure P' with respect to nondimensional film thickness H' for various values of nondimensional radius R is also shown in FIG.<6>. The lubricant pressure P' decreases nonlinearly with film thickness H' as it increases for various values of radius R. Location of R = 0.75 shows a variation of pressure change with film thickness at the centre of blank-holder. It also shows that geometry parameter B of width in compression zone has a significant influence on changing pressure.

FIG.<7> shows the variation of nondimensional film thickness H_{BH} with respect to nondimensional hydrodynamic parameter K for a value of B = 0.5. It indicates that the establishment of film thickness H_{BH} depends on the lubricant viscosity, velocity and clamping pressure of the blank.

3.4.2 Steady Deformation Phase [1]

FIG.<4> shows the deformation phase. Two approaches are introduced to model this phase. The first approach is based the on introduction of the following assumptions:

1. A hydrodynamic film between both the top and lower sides of the metal sheet blank and the blank holder and the die surfaces are formed due to the wedge action.

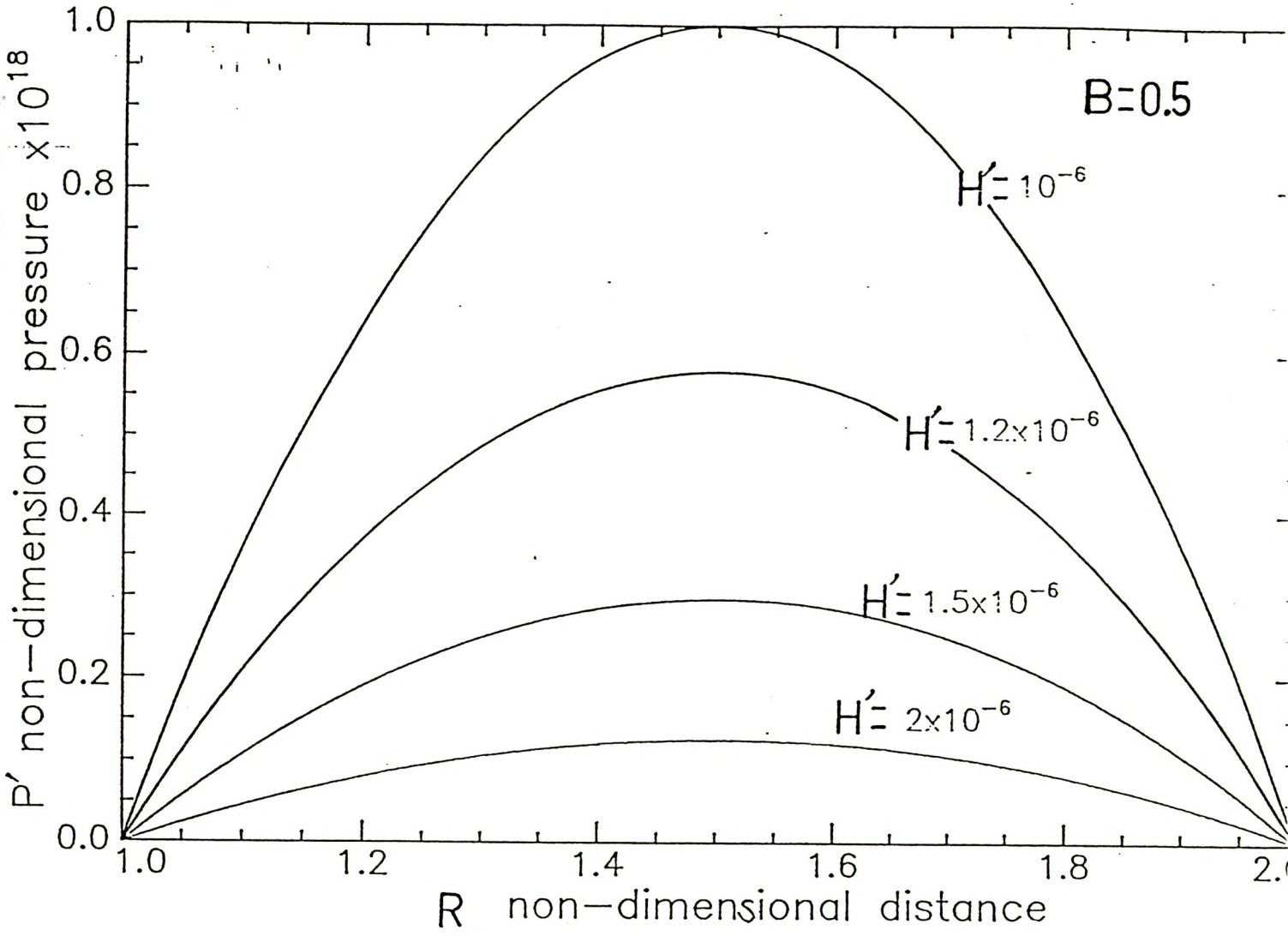

FIG. 5 VARIATION OF NONDIMENSIONAL PRESSURE P' WITH NONDIMENSIONAL RADIUS R FOR NONDIMENSIONAL FILM THICKNESS H'

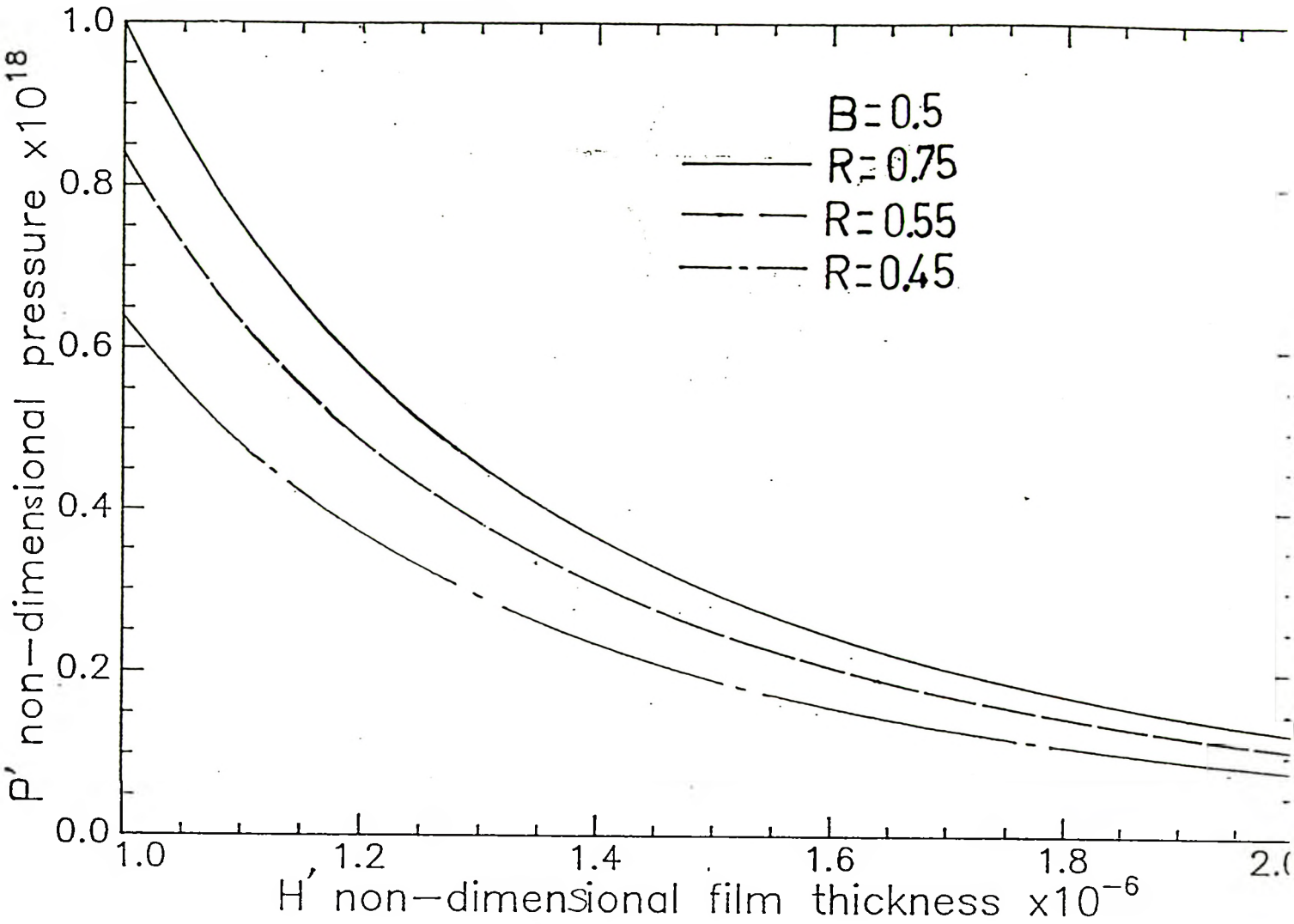

FIG. 6 VARIATION OF NONDIMENSIONAL PRESSURE P' WITH NONDIMENSIONAL FILM THICKNESS H' FOR NONDIMENSIONAL RADIUS R

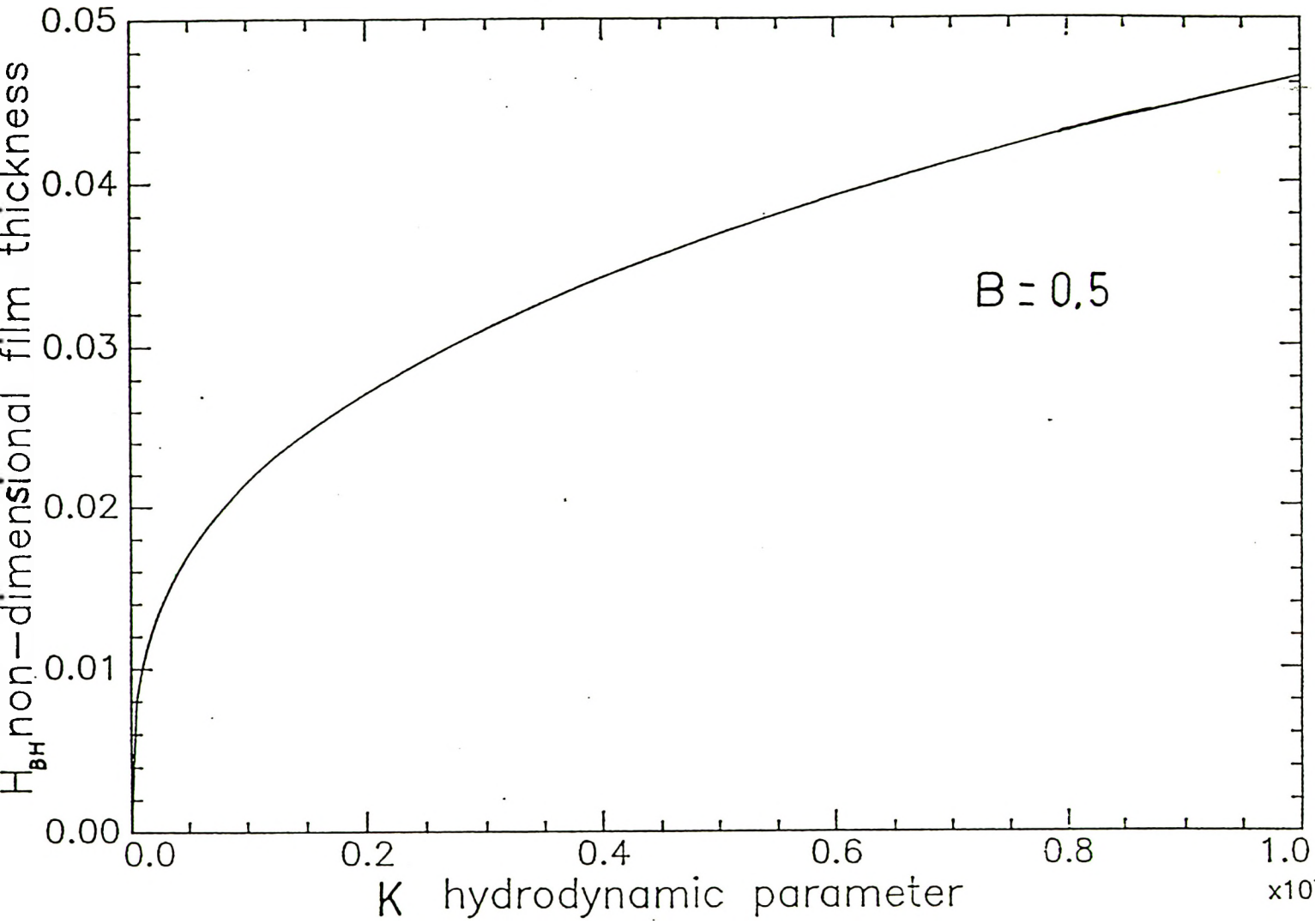

FIG. 7 VARIATION OF NONDIMENSIONAL FILM THICKNESS H_{BH} WITH NONDIMENSIONAL HYDRODYNAMIC FACTOR K

2. The film thickness between the upper surface of the metal sheet blank and the blank holder, and the lower surface of the metal sheet blank and the die converges toward the die shoulder according to the following relationship:

$$h = h_1 + (r-r_1)\tan\theta$$

$$\tan\theta = h_1/r_1 \qquad (32)$$

where h is the local film thickness at radius r of the compression zone. h_1 is the film thickness at radius r_1 of the leading edge of the die zone where the metal sheet blank starts to yield. θ is the converging wedge angle that both blank holder and die surfaces form with the metal sheet blank.

3. The behaviour of metal blank is considered to be rigid-plastic.

4. The thickness t_o of the metal blank remains constant during bending deformation.

Assumptions 1 & 2 are derived from the geometry of the drawing process. Assumptions 3 & 4 are those used in plastic deformation analysis of pure drawing and also to simplify the mathematics.

3.4.2.1 Hydrodynamic Lubrication of Compression Zone

The amount of lubricant carried into the die zone is controlled by the compression zone. From the above assumptions, the pressure is calculated by the Reynolds equation,

$$dp/dr = 6\mu U(h - h_0)/h^3 \qquad (33)$$

where h is the local film thickness, μ is the lubricant viscosity, p is the pressure of local film thickness, r is the local radius, h_0 is the film thickness where pressure gradient is zero, U is the mean velocity of sheet blank surface, and

$$h_0 = h_1 \tag{34}$$

$$U = -V \tag{35}$$

where h_1 is the film thickness at the boundary between die and compression zones, and V is the punch velocity.

Substituting in equation (33) for film thickness h from equation (32) and for h_0 from equation (34) and for U from equation (35), and then integrate over the compression zone, yields

$$p = - 6\mu V r_1[(h_1/2h^2 - 1/h)/h_1] + c \tag{36}$$

The boundary condition of the lower edge of the die or blank holder is $h = \infty$, $p = 0$, is used to calculate constants of integration.

$$p = - 6\mu V r_1[(h_1/2h^2 - 1/h)/h_1] \tag{37}$$

The film thickness h1 is calculated from the equation (37) by substituting the upper boundary condition $h = h_1$, $p = \sigma_y(t_o/r_2)$, where the pressure is related to the yield strength of the blank metal. This equation is derived in the deformation analysis of lubricated die zone and given by equation (68).

Thus, the film thickness h_1 is

$$h_1 = [3\mu V r_1 r_2/(\sigma_y t_0)]^{1/2} \tag{38}$$

In order to facilitate the plotting of inlet film thickness h_1 with different parameters, equation (38) is rearranged in a nondimensional form as,

$$h_1/r_2 = (r_1/r_2)^{1/2}[3\mu V/(\sigma_y t_o)]^{1/2} \qquad (39)$$

The graphs for the nondimensional inlet film thickness $H_1 = h_1/r_2$ with respect to hydrodynamic parameter $G = 3\mu V/(\sigma_y t_o)$ and for various values of $R_d = r_1/r_2$ is shown in Fig.<8>. The nondimensional film thickness H_1 increases nonlinearly with both parameters G and R_d.

The pressure distribution given in equation (37) is simplified if the value of h1 is substituted from equation (38) and it becomes

$$p = t_o\sigma_y[2h_1/h - (h_1/h)^2]/r_2 \qquad (40)$$

The variation of nondimensional pressure $P = p/\sigma_y$ with respect to nondimensional film thickness $H = (h/h_1)$ for various values of (t_o/r_2) is shown in Fig.<9>. The lubricant pressure decreases from leading edge to the trailing edge. The establishment of film thickness h1 which in turn depends on the lubricant viscosity, yield strength and velocity of the blank has an important effect on pressure distribution.

3.4.2.2 Hydrodynamic Lubrication of Die Zone

In the die zone the blank bends plastically and moves with the punch into the die cavity. This zone extends from the leading edge of compression zone to the exit of the curved section of the die. The pressure gradient is small in this zone (assumption <15>), and hence from the continuity of the lubricant flow in this zone,

$$q = Vh_1/2 = Vh/2 \qquad (41)$$

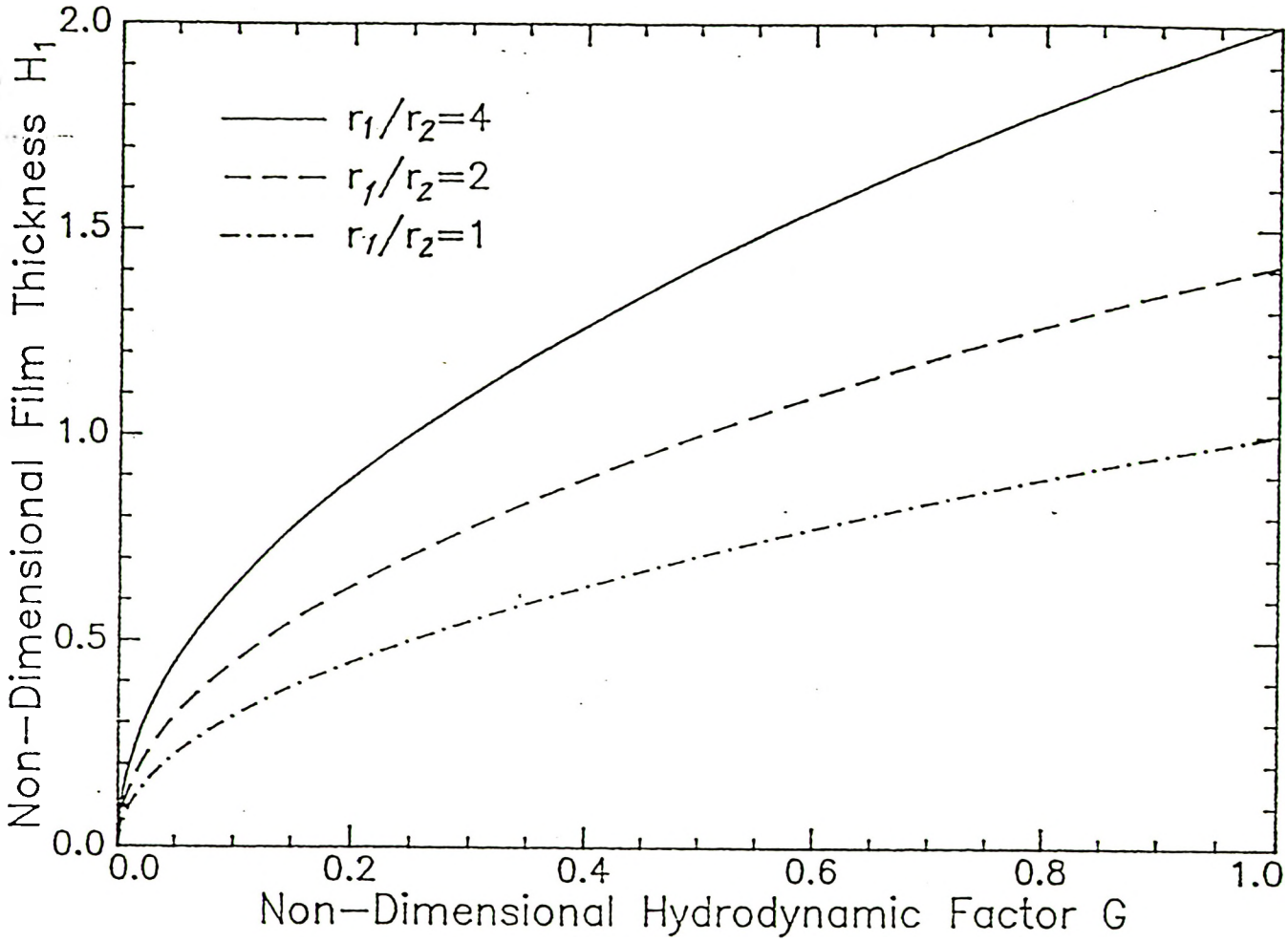

FIG. 8 VARIATION OF NONDIMENSIONAL INLET FILM THICKNESS H_1 WITH HYDRODYNAMIC LUBRICATION FACTOR G

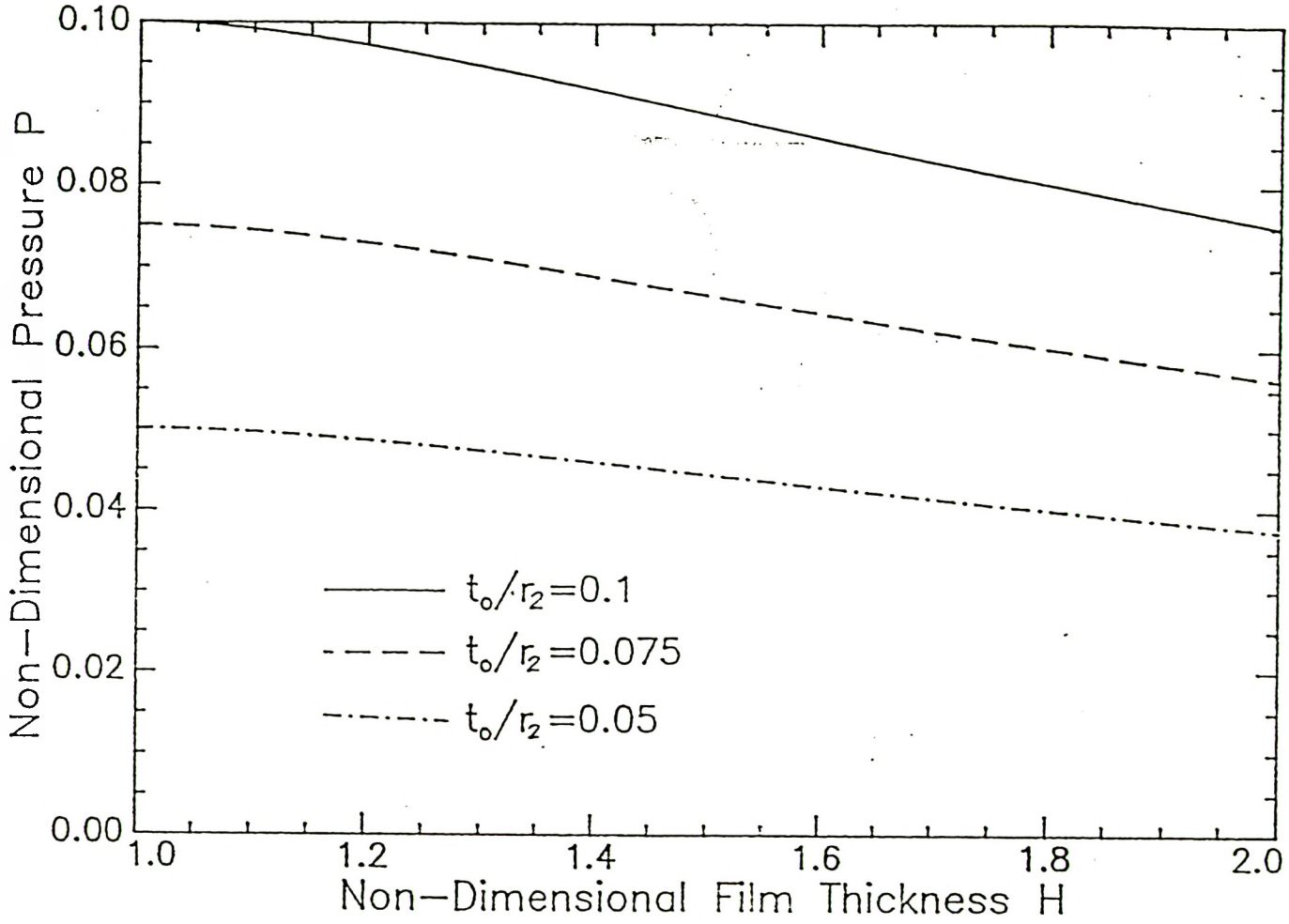

FIG. 9 VARIATION OF NONDIMENSIONAL PRESSURE P WITH NONDIMENSIONAL FILM THICKNESS H

Therefore, $h=h_1$ and the shear stress on the surface of blank is obtained from the equation

$$\tau_d = \mu V/h_1 \qquad (42)$$

substituting for h_1 this equation becomes

$$\tau_d = [\mu V \sigma_y t_o/(3r_1r_2)]^{1/2} \qquad (43)$$

This equation is used in plastic deformation analysis of the die zone.

3.4.2.3 Deformation Analysis of Lubricated Compression Zone

The radial stress of the metal blank in compression zone is needed for calculating the drawing force in the deformation of die zone. The equilibrium condition of the element dr, dΘ, in the radial direction can be written as

$$(\sigma_r + d\sigma_r)(r + dr)d\Theta t_o - \sigma_r r d\Theta t_o + 2\sigma_t dr t_o \sin(d\Theta/2) + 2\tau_0 d\Theta dr = 0 \qquad (44)$$

Replacing $\sin(d\Theta/2)$ by $d\Theta/2$ and neglecting high order products of differential terms and simplifying,

$$d\sigma r/dr + (\sigma_r+\sigma_t)/r + 2\tau_0/t_o = 0 \qquad (45)$$

where τ_0 is the shear stress acting on the surface of the element, σ_r and σ_t are radial and tangential stresses acting on the element as shown in Fig. <10>. The Tresca yield criterion states that

$$\sigma_r - \sigma_t = \sigma_y \qquad (46)$$

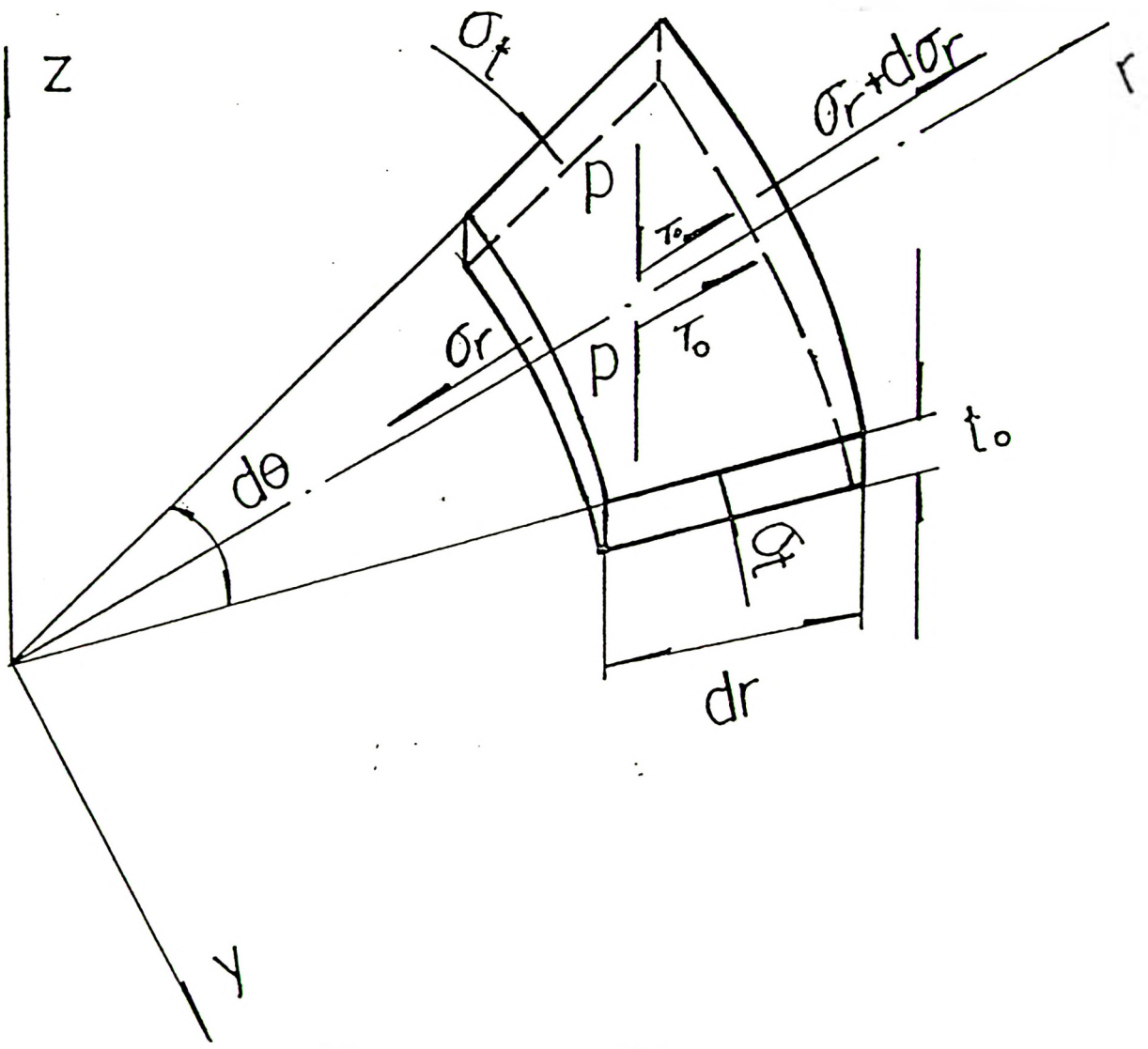

FIG. 10 FREE BODY DIAGRAM FORAN ELEMENT dr OF THE COMPRESSION ZONE

Substituting for σ_t from equation (46) in equation (45) , it becomes

$$d\sigma_r/dr = -\sigma_y/r - 2\tau_0/t_o \quad (47)$$

The shear stress $\tau 0$ on the surface of the blank metal is given by

$$\tau_0 = \mu(du/dz)_{y=0} \quad (48)$$

Considering the equation governing the viscous flow in the lubricant film thickness, the velocity across the film thickness as shown in FIG.<11>. And can be expressed as

$$u = (z^2 - zh)dp/(dr\ 2\mu) + Vz/h + V \quad (49)$$

According to equation (49), the flow rate across the film thickness is given by

$$du/dz = (2z - h)dp/(dr\ 2\mu) + V/h \quad (50)$$

And

$$[du/dz]_{y=0} = (-h)dp/(dr\ 2\mu) + V/h \quad (51)$$

Substituting for [du/dz]y=0 from equation (51) into equation (48), the shear stress acting on the surface of the blank can be written as

$$\tau_0 = -hdp/(2dr) + \mu V/h \quad (52)$$

From assumption (14), in region of the compression zone the pressure gradient may be neglected. Thus,

$$\tau_0 = V\mu/h \quad (53)$$

Substituting for τ_0 from equation (53) in equation (47) yields

$$d\sigma_r/dr = -\sigma_y/r - 2\mu V/\{[h_1+\tan\theta(r-r_1)]t_0\} \quad (54)$$

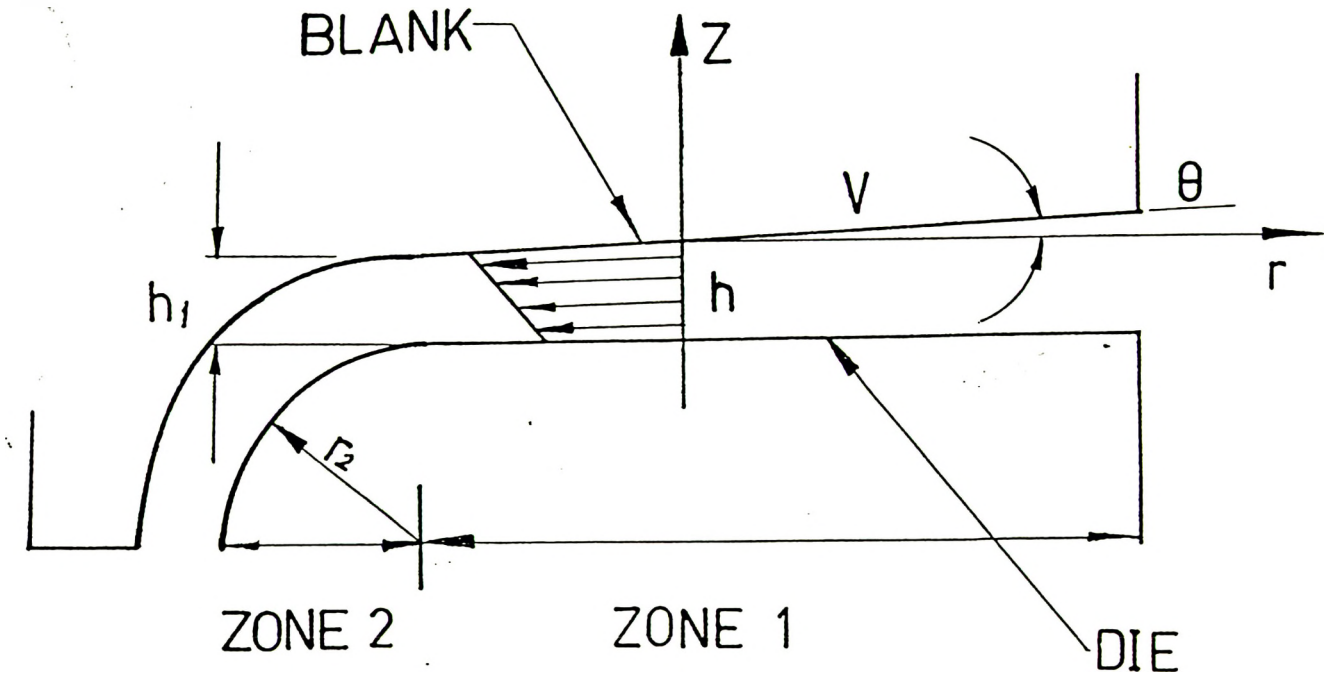

FIG. 11 VELOCITY V ACROSS FILM THICKNESS h

The radial stress obtained by integration of equation (54) from the outside to the inside radii of blank holder,

$$\sigma_r = \sigma_y \ln r_0/r + [2\mu V r_1/(h_1 t_0)] \ln\{[6\mu V r_2 + (r_0-r_1)\,\sigma_y\, t_0 \tan 2\theta]/[6\mu V r_2 + (r-r_1)\,\sigma_y\, t_0 \tan 2\theta]\} \quad (55)$$

Introducing the nondimensional parameters

$$A = 2[\mu V r_1/(3 t_0 \sigma_y\, r_2)]^{1/2} \quad (56)$$

$$B = 2\, r_1/r_0 \quad (57)$$

$$R = r/r_0 \quad (58)$$

$$\sigma_R = \sigma_r/\sigma_y \quad (59)$$

the equation (55) becomes

$$\sigma_R = -\ln R + A \ln [B+2/(B+2R)] \quad (60)$$

The variation of nondimensional stress with respect to nondimensional radius R for nondimensional parameters A and B is shown in Figs. <12> & <13>.

The nondimensional radial stress is zero at the trailing edge of the compression zone and increases towards the leading edge of the compression zone. In case of B = 0.75 as the hydrodynamic effect A increases, the radial stress σR is increased. This increase in σ_R is less significant for changes in value of B where A = 0.19 as shown in Fig. <14>.

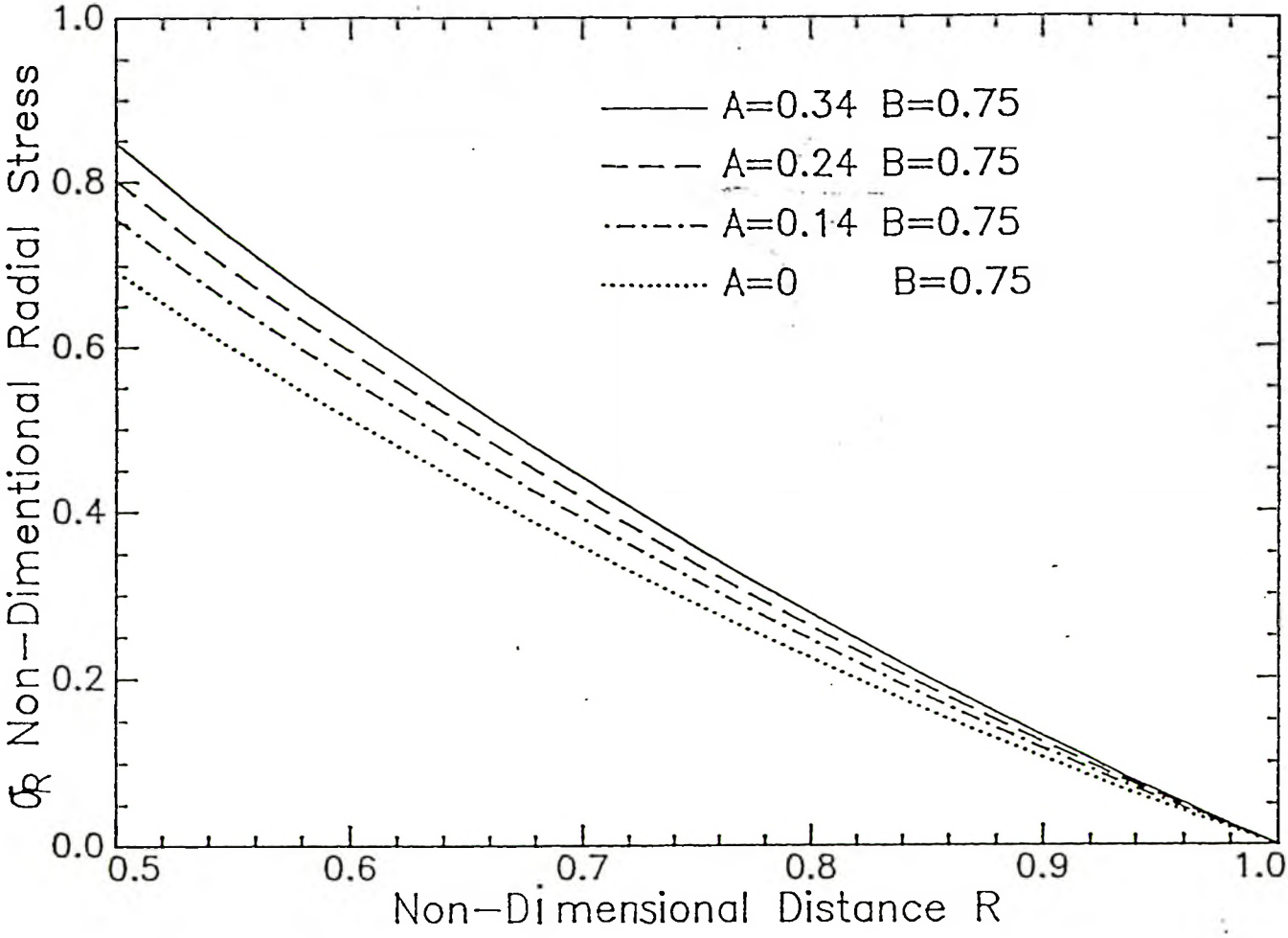

FIG. 12 VARIATION OF NONDIMENSIONAL RADIAL STRESS σ_R WITH NONDIMENSIONAL RADIUS R FOR NONDIMENSIONAL PARAMETERS A & B

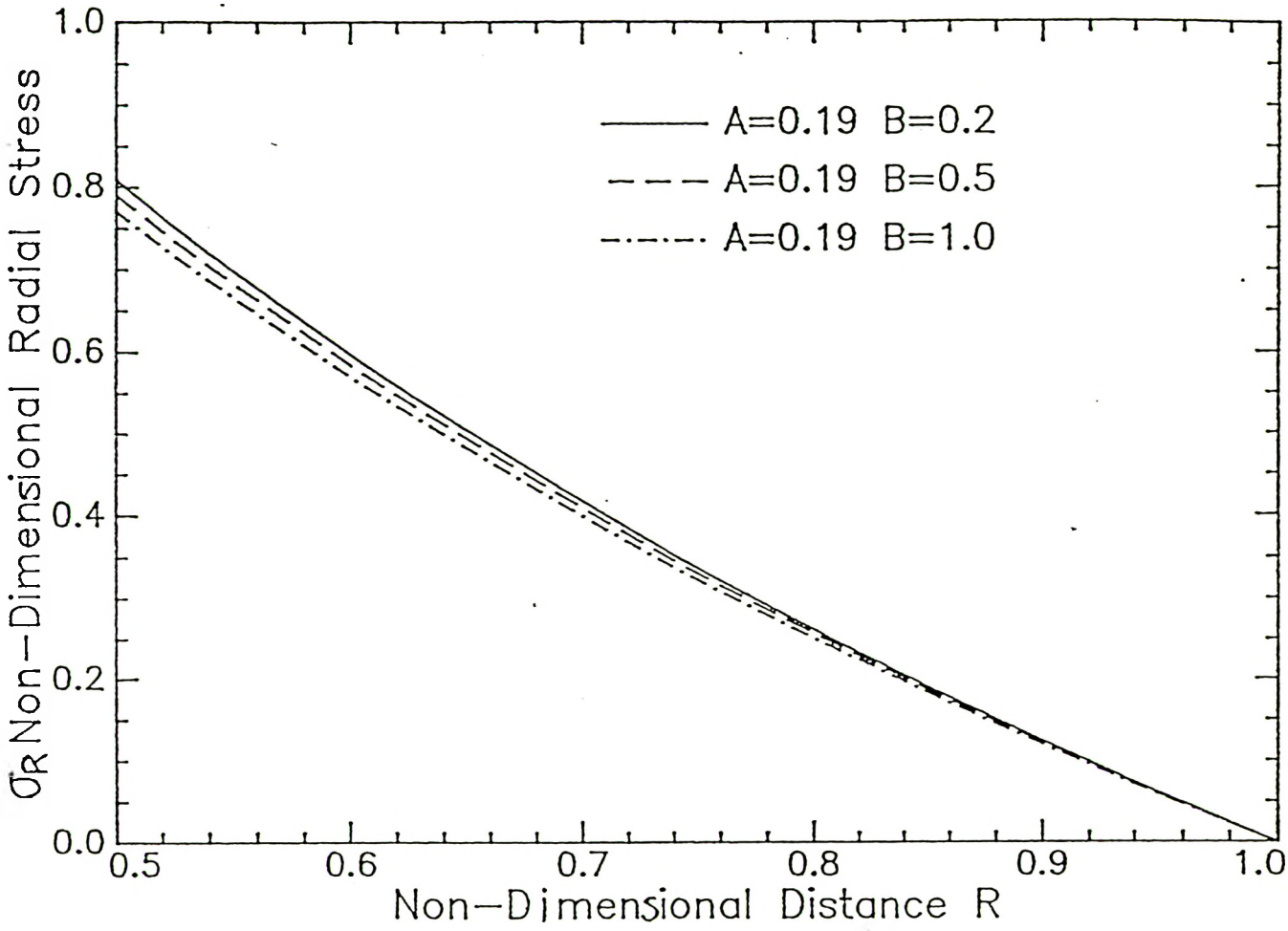

FIG. 13 VARIATION OF NONDIMENSIONAL RADIAL STRESS σ_R WITH NONDIMENSIONAL RADIUS R FOR NONDIMENSIONAL PARAMETER B

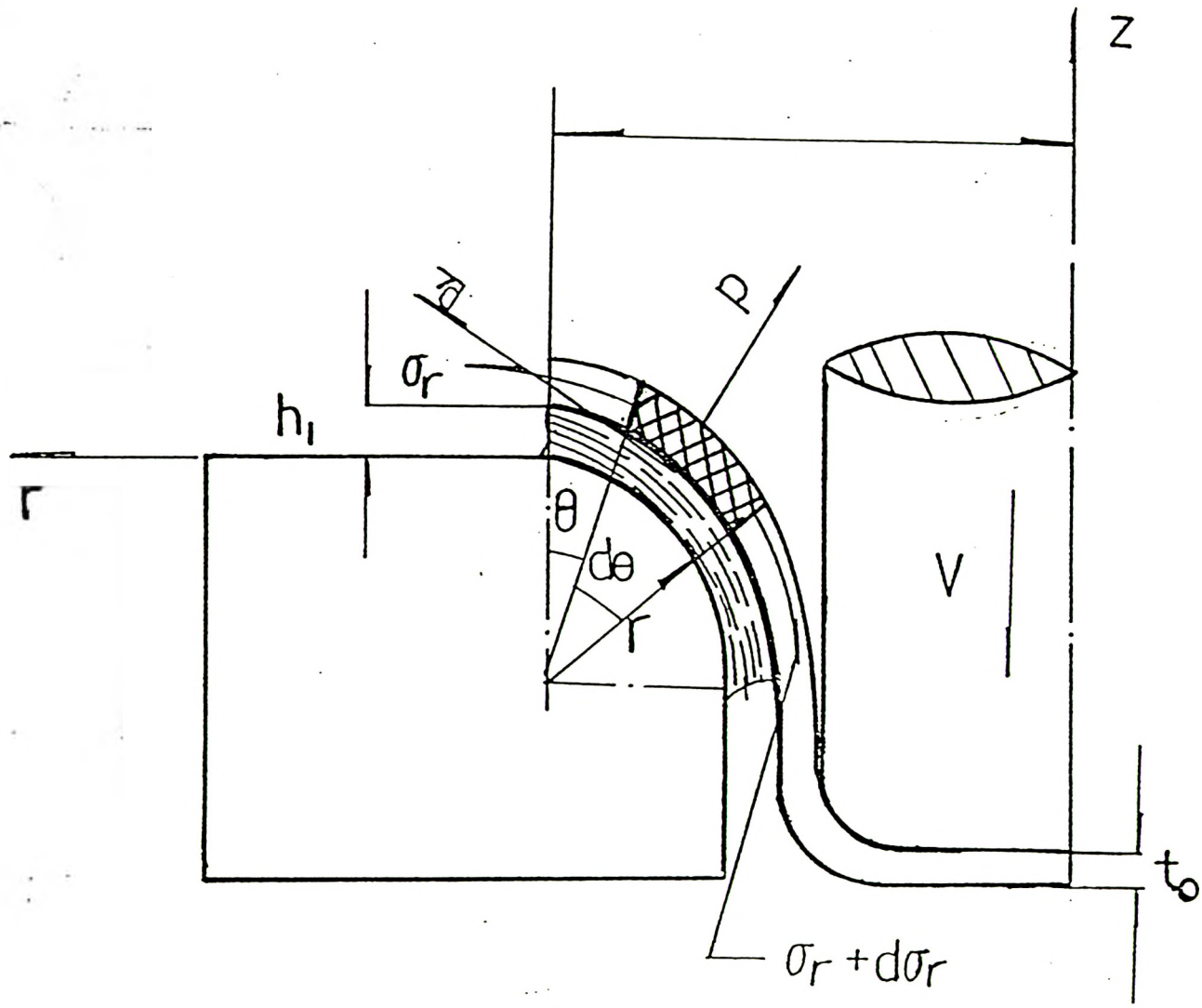

FIG. 14 FREE BODY DIAGRAM FOR ELEMENT dθ OF DIE ZONE

3.4.2.4 Deformation Analysis of Lubricated Die Zone

Considering only the friction at die zone (neglecting bending moment), the radial equilibrium of forces from the free body of the element shown in Fig. <14> is

$$dN - F\sin(d\Theta/2) - (F + dF)\sin(d\Theta/2) = 0 \qquad (61)$$

where dN is the resultant normal force towards on the $d\Theta$ element, and F is the radial tension force in the blank.

Approximating $\sin(d\Theta/2)$ by $d\Theta/2$, equation (30) can be written as

$$dN - Fd\Theta = 0 \qquad (62)$$

Since,

$$dN = pr_2 d\Theta \qquad (63)$$

$$F = \sigma_r t_0 \qquad (64)$$

where p is the pressure in the film thickness of the die zone, σ_r is the radial stress in the element of blank of the die zone.

Thus, substituting for dN and F from equations (63) and (64) into equation (62) yield,

$$p = \sigma_r t_0 / r_2 \qquad (65)$$

From the Tresca yield criterion

$$\sigma_r = \sigma_y - p \qquad (66)$$

where σ_y is the yield strength of the blank, σ_r is then substituted in equation (65) that result

$$p = \sigma_y (t_o/r_2)/(1 + t_o/r_2) \quad (67)$$

The approximated form of this equation is

$$p = \sigma_y (t_o/r_2) \quad (68)$$

The value of p was used in hydrodynamic lubrication analysis of compression zone to calculate h1.

The equilibrium of forces in tangential direction is

$$dF = df \quad (69)$$

where df is the frictional force on the surface of the element of the blank.

From dividing by both equation (62) and (69), yield

$$dF/F = df d\theta/dN \quad (70)$$

According to assumption (21), differentiating equation (64),

$$dF = d\sigma_r t_o \quad (71)$$

And,

$$df = \tau_d r_2 d\theta \quad (72)$$

where τ_d is the frictional stress on the surface of the element of the blank in die zone. That remaines constant and is proportional to the constant inlet film thickness h_1.

Substituting for dF, F, dN and df from equations (71), (64), (63) and (72) into equation (70), then it became

$$d\sigma_r/\sigma_r = \tau_d/p \, d\theta \quad (73)$$

Substituting for τ_d from equation (43) and for p from equation (68) into this equation and then integrate with the boundary conditions of $\Theta=0$, $\sigma_r=\sigma_r$, and $\Theta=\pi/2$, $\sigma_r=\sigma_z$ it yields

$$\sigma_z = \sigma_r \, e^{[V\mu/(2h_1\sigma_y)]r_2\pi/t_o} \qquad (74)$$

where σ_z is the drawing stress.

Introducing nondimensional parameters

$$\sigma Z = \sigma_z/\sigma_y \qquad (75)$$

$$C = r_2/r_1 \qquad (76)$$

in equation (74) and substituting for σ_R from equation (60) it gives

$$\sigma Z = \{A \ln [B+2/(B+2R)] - \ln R\} \, e^{\pi AC/4} \qquad (77)$$

3.4.2.5 Discussion of Results

The equation (77) calculates the nondimensional drawing stress in the presence of the hydrodynamic lubrication regime. The drawing stress varies with lubricant viscosity, drawing reduction and speed of drawing. The variation of nondimensional drawing stress σZ with R for cases where B=0.75 and parameters A and B are both either constant or variable are shown in Figs. <15> & <16>. The nondimensional drawing stress σZ increases as the nondimensional hydrodynamic lubrication parameter A is increased. The hydrodynamic lubrication parameter A has a more pronounced effect on the drawing stress value than parameters C and B. Any increase in value of A directly related to viscosity increase that results a higher lubricant shear stress to the surface of the blank that consequentially associate with a higher drawing stress.

In order to visualize the significance of the present theoretical analysis, the variation of nondimensional drawing stress σ_Z with respect to nondimensional radius R for the cases of frictionless, dry friction, and lubricated are plotted in Fig.<17>. This indicates that the estimate of drawing stress is more realistic by the present model. The formation of a hydrodynamic lubrication regime modifies the drawing stress value in comparison with dry friction considerably.

Neglecting the less significant parameter B in equation (77) by results of discussion above, it may be written in simplified form as

$$\sigma_Z = [(-\ln R)(A+1)]e^{\pi AC/4} \qquad (78)$$

3.4.3 Steady Deformation Phase [2]

The second approach for steady deformation phase analysis is conducted with the assumption that the converged wedge shape for hydrodynamic lubrication film is obtained from

$$\tan\Theta = (h_{BH} - h_1)/(r_0 - r_1) \qquad (79)$$

The above assumption based on the fact that the pressure difference at locations of E and C causing the blank to tilt at a angle Θ. The value of the Θ is dictated by difference in the boundaries film thickness. Furthermore, it indicates that the wedge angle Θ is not only created by tooling geometry, but also influenced by normal blank-holder pressure.

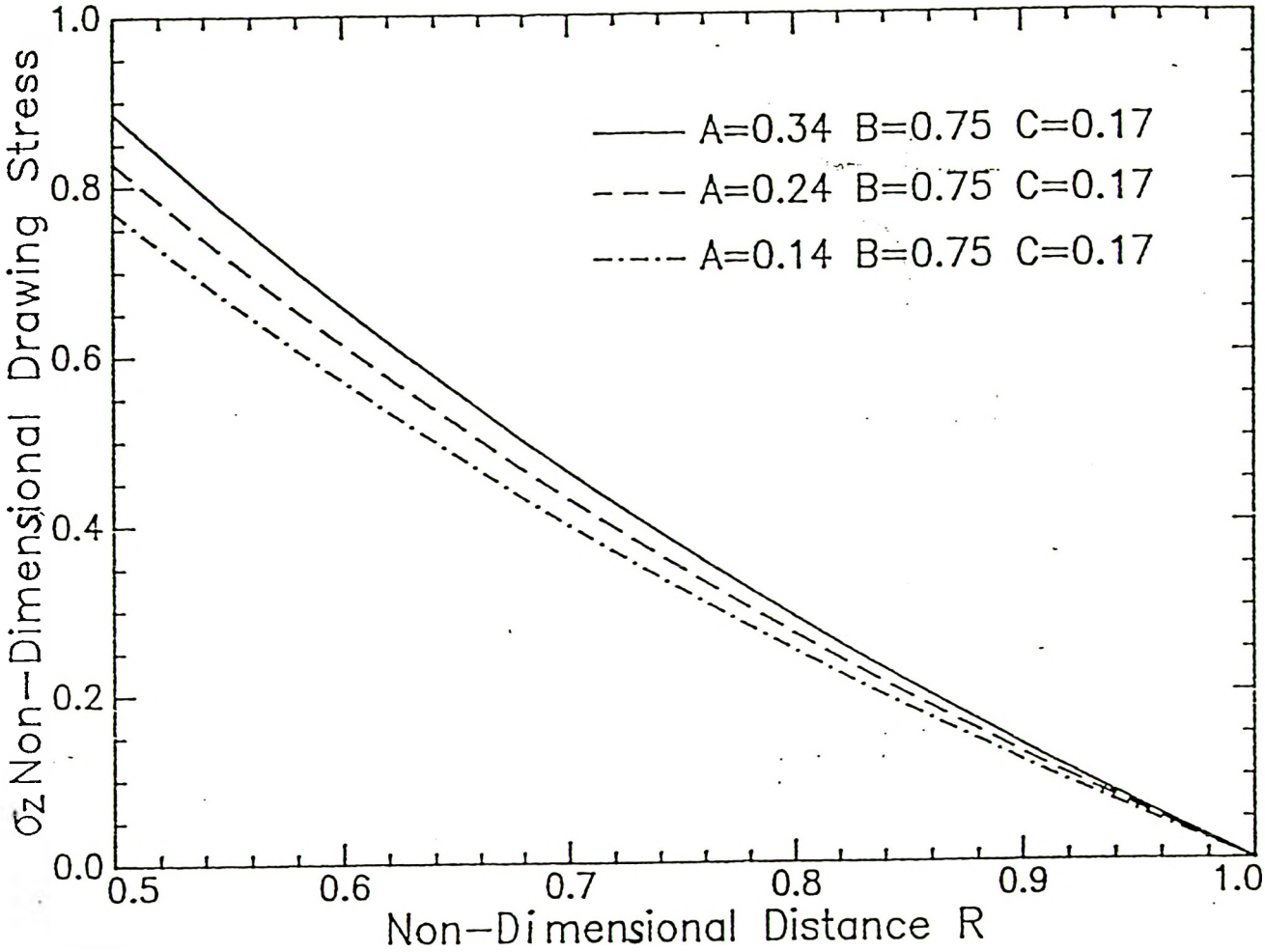

FIG. 15 VARIATION OF NONDIMENSIONAL DRAWING STRESS σ_Z WITH NONDIMENSIONAL RADIUS R FOR NONDIMENSIONAL PARAMETER A

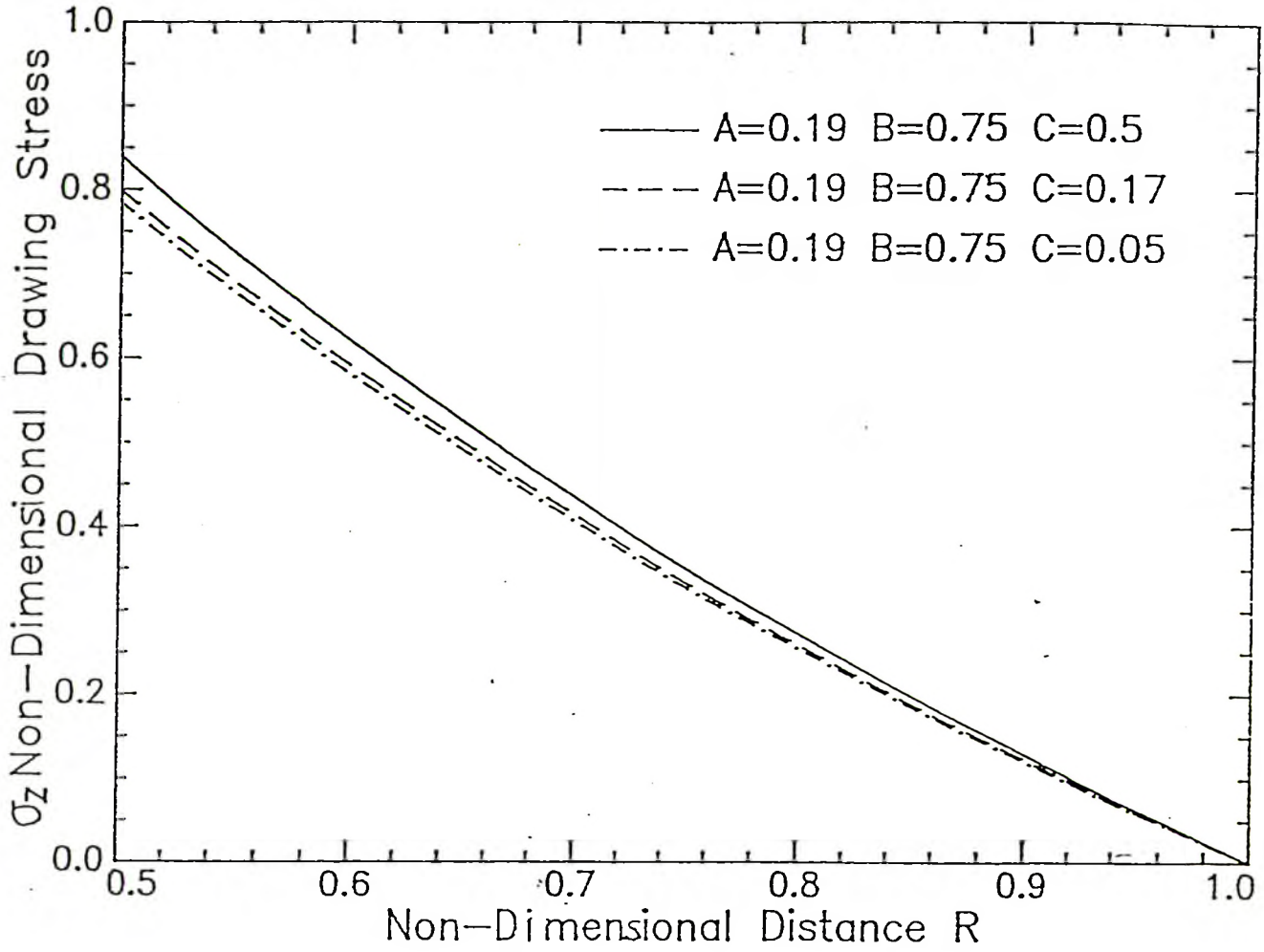

FIG. 16 VARIATION OF NONDIMENSIONAL DRAWING STRESS σ_Z WITH NONDIMENSIONAL RADIUS R FOR NONDIMENSIONAL C

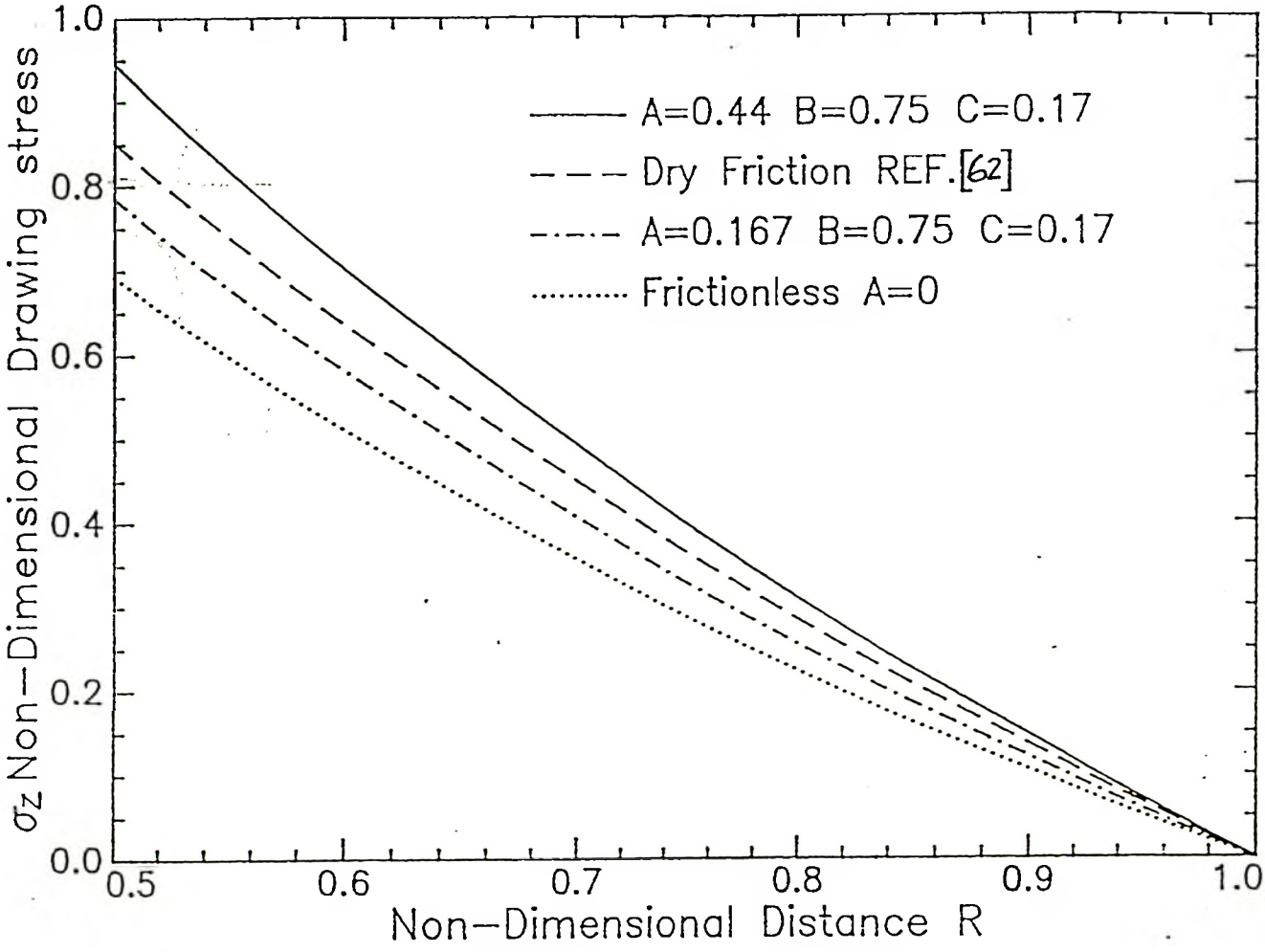

FIG. 17 VARIATION OF NONDIMENSIONAL DRAWING STRESS σ_Z WITH NONDIMENSIONAL R FOR COMPARISON WITH FRICTION AND FRICTIONLESS ANALYSES

3.4.3.1 Hydrodynamic Lubrication of Compression Zone

Differentiating equation (32), gives

$$dh = \tan\theta \, dr \qquad (80)$$

Substituting for h, dh, h0, and U from equations (32), (80), (34), and (35) into equation (33) gives

$$dp = 6\mu V/\tan\theta[(h_1 - h)/h^3]dh \qquad (81)$$

Integrating over compression zone, it yields

$$p = 6\mu V/\tan\theta[1/h - h_1/(2h^2)] + c \qquad (82)$$

Using same boundary condition as it has been used in previous section, h1 may be expressed as

$$h1 = 3\mu V r_2/(\sigma_y t_0 \tan\theta) \qquad (83)$$

Substituting for h_{BH} and h_1 from equations (20) and (83) into equation (79) yields

$$\tan 2\theta(r_0 - r_1) - \tan\theta[3\mu V(r_0 - r_1)^2/(2p_{BH})]^{1/3} + 3\mu V r_1/(\sigma_y t_0) = 0 \qquad (84)$$

Simplifing this equation by neglecting $3\mu V r_1/(\sigma_y t_0)$, which is in order of 10-6 ~ 10-7, then equation (84) becomes

$$\tan\theta = \{3\mu V/[2p_{BH}(r_0 - r_1)]\}^{1/3} \qquad (85)$$

Substituting for tanΘ from equation (85) into equation (83) yields

$$h1 = [3\mu V/(\sigma_y t_0)]^{2/3}[2(p_{BH}/\sigma_y]^{1/3}[(r_0-r_1)/to]^{1/3} r_2 \qquad (86)$$

In order to facilitate the plotting of the inlet film thickness h1 with different parameters, equation above is rearranged in nondimensional form as,

$$H_1 = (2G^2\delta L)^{1/3} \qquad (87)$$

The graphs for the nondimensional inlet film thickness $H_1 = h_1/r_2$ with respect to hydrodynamic parameter G for various of geometry parameter L and pressure ratio δ are shown in FIG.(18).

The nondimensional film thickness H_1 increases nonlinearly with increasing parameter G. The film thickness H_1 for a constant value of G varies significantly if both δ and L are increased.

However, this increment is more enhanced where the parameter δ increased. This shows that selecting and controlling appropriate values of blank holder pressure during the deep drawing process in presence of lubricant is important in maintaining a thick lubricant film in practice.

3.4.3.2 Hydrodynamic Lubrication of Die Zone

The analysis is continued in a similer style to hydrodynamic lubrication of die zone in previous approach [1]. The shear stress on the surface of blank is obtained from the equation (42) by substituting for h1 from equation (86)

$$\tau_d = (\sigma_y t_o/r_2)\{\mu V/[18p_{BH}(r_o-r_1)]\}^{1/3} \qquad (88)$$

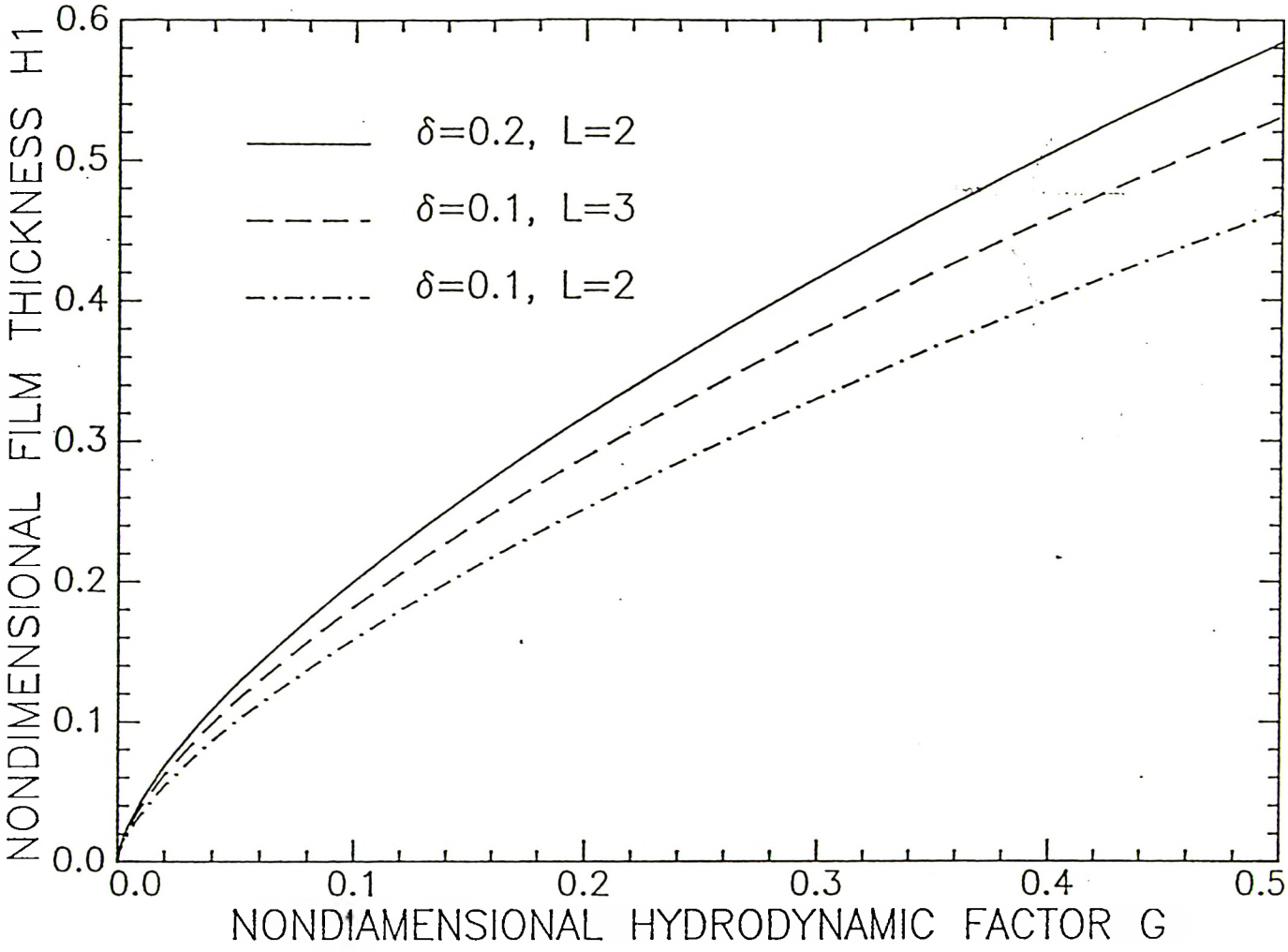

FIG. 18 VARIATION OF NONDIMENSIONAL INLET FILM THICKNESS H_1 WITH NONDIMENSIONAL HYDRODYNAMIC PARAMETER G FOR VARIOUS OF GEOMETRY PARAMETER L AND RATIO OF PRESSURE δ

3.4.3.3 Deformation Analysis of Lubricated Compression Zone

The radial stress obtained by integration of equation (54) from the outside to inside radii of blank holder,

$$\sigma_r = \sigma_y \ln r_0/r + [2\mu V/(\tan\theta t_0)] \ln\{[h_1+\tan\theta(r_0-r_1)]/[h_1+\tan\theta(r-r_1)] \quad (89)$$

Substituting for h_1 and $\tan\theta$ from equations (86) and (85) into equation (89) and introducing the nondimensional parameters

$$G = 3\mu V/(\sigma_y t_0) \quad (90)$$

$$\delta = p_{BH}/\sigma_y \quad (91)$$

$$L = (r_0 - r_1)/t_0 \quad (92)$$

$$I = r_2/r_0 \quad (93)$$

the equation (89) becomes nondimensional form as

$$\sigma_R = -\ln R + (16/27)^{1/3}(G^2L\delta)^{1/3} \ln\{[2I(4GL^2\delta^2)^{1/3} - B + 2]/[2I(4GL^2\delta^2)^{1/3} - B + 2R]\} \quad (94)$$

The variation of nondimensional radial stress σ_R with respect to nondimensional radius R for nondimensional parameters I and B is shown in FIG.<19>.

The nondimensional radial stress σ_R is zero at the lower edge of the compression zone and increases towards the upper edge of the die zone. In case of G = 0.3, L = 2.1, δ = 0.2 as the geometry parameter I decreases, the radial stress σ_R is increased. It is indicated that making large die radius r_2 can results lower level of drawing load.

3.4.3.4 Deformation Analysis of Lubricated Die Zone

The drawing stress in the deformation of die zone is integrated from equation (73) by substituting for τ_d and p from equation (88) and (68), then writing nondimentional form

$$\sigma_Z = \{(16/27)^{1/3}(G^2L\delta)^{1/3} \ln\{[I(4GL^2\delta^2)^{1/3} - B + 2]/[I(4GL^2\delta^2)^{1/3} - B + 2R]\} - \ln R\}\, e[G/2\delta L]^{1/3}\pi/6 \qquad (95)$$

3.4.3.5 Discussion of Results

The equation (95) also calculates the nondimensional drawing stress in presence of the hydrodynamic lubrication regime. The drawing stress varies with lubricant viscosity, drawing speed, blank holder pressure, tooling geometry and strength of the material.

The variation of the nondimensional drawing stress σ_Z with R for the case where I = 0.25, B = 0.45 and various parameters G, L, and δ are shown in FIG.<20>. It shows the difference between the variation of drawing stress with respect to blank holder pressure by using different theories (dry friction and presence of lubrication). In Ref.[62], the drawing stress is slightly increased by a friction term which is proportional to the blank holder pressure and the coefficient of friction under a practical maximum value of p_{BH} = 10 N/mm^2. In present analysis, while increasing p_{BH} may cause a slight reduction in drawing stress where the parameter G is kept constant.

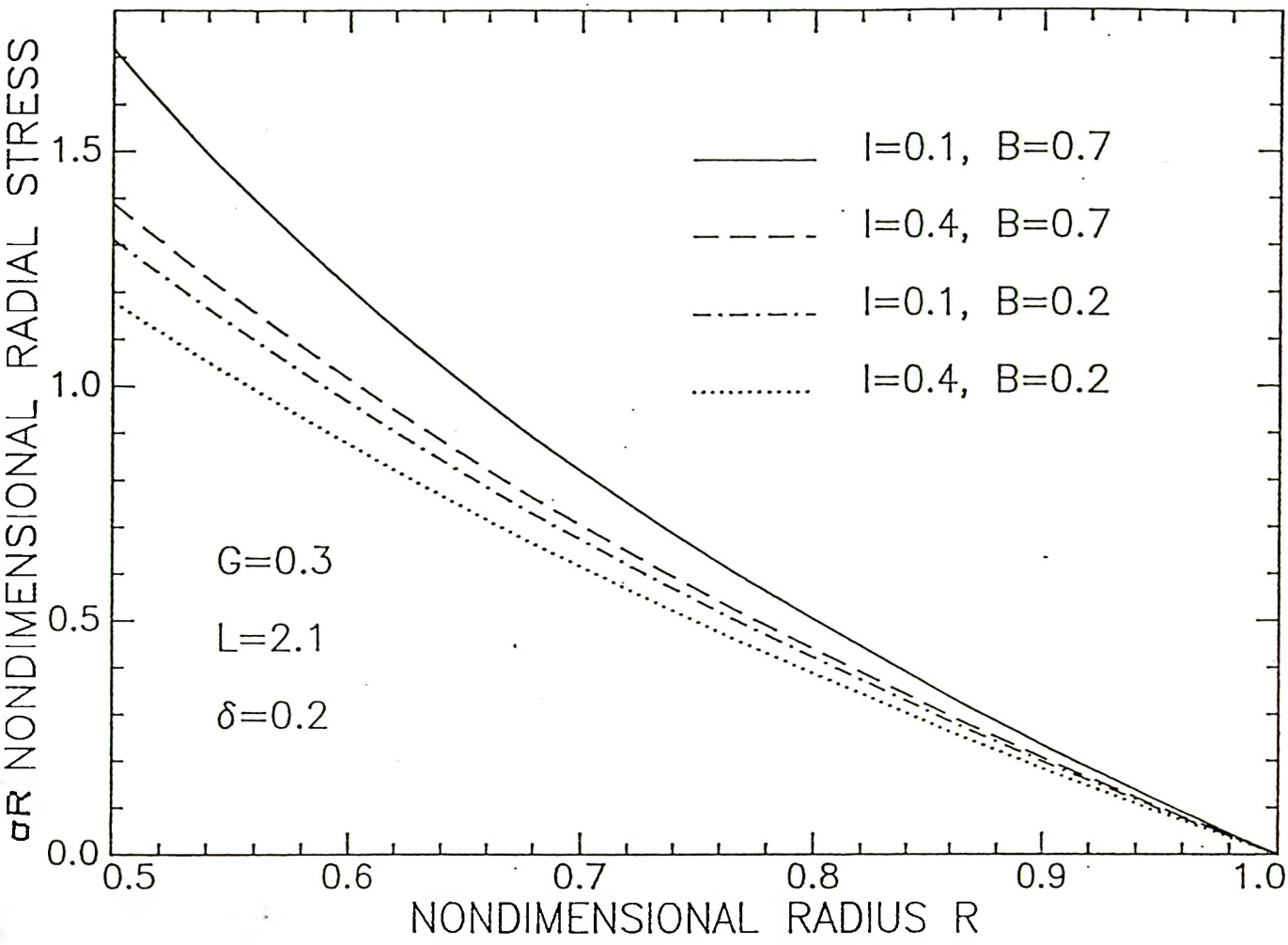

FIG. 19 VARIATION OF NONDIMENSIONAL RADIAL STRESS σ_R WITH NONDIMENSIONAL RADIUS R FOR NONDIMENSIONAL PARAMETERS I AND B

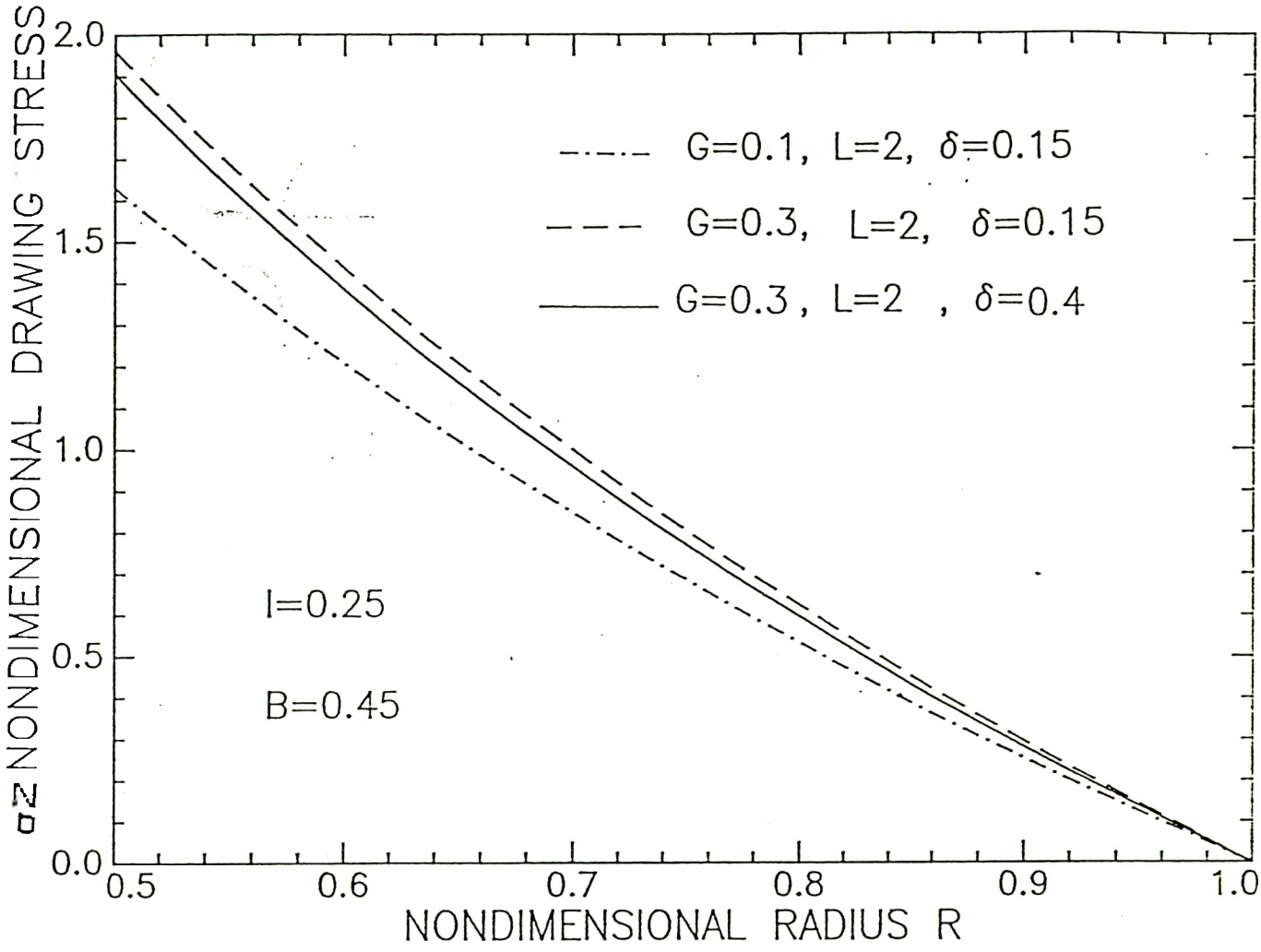

FIG. 20 VARIATION OF NONDIMENSIONAL DRAWING STRESS σ_Z WITH R FOR CASE WHERE I = 0.25, B = 0.45 AND VARIOUS PARAMETERS G, L AND δ

3.4.4 Comparison of Two Approaches

In order to compare these two analyses, equation (78) can be rewritten to the following form

$$\sigma_Z = \{(-\ln R)[3/2(G/C)^{1/2} + 1]\}_e (GC)^{1/2}\pi/6 \qquad (96)$$

by using

$$A = 2/3(G/C)^{1/2} \qquad (97)$$

Introducing drawing stress of dry friction from Ref.[62], and defining reduction of drawing stress as

$$\phi = \sigma_{Z,L}/\sigma_{Z,F} \qquad (98)$$

where $\sigma_{Z,L1}$ and $\sigma_{Z,L2}$ are drawing stress in presence of lubrication for both analyses [1] and [2], [equations (96) and (95)] respectively. $\sigma_{Z,F}$ is the drawing stress of dry friction in the process, as shown in Ref.[62].

The variation of the reduction of drawing stress ϕ with respect to nondimensional hydrodynamic parameter G for ϕ_1 and ϕ_2 is shown in FIG. <21>. The curve has been plotted for the following data:

$$r_0/t_0 = 60$$

$$B = 0.5$$

$$C = 0.833$$

$$I = 0.417$$

$$L = 30.28$$

$$R = 0.5$$

$$\delta = 0.1$$

ß = 0.1

The plots of ϕ_2 and ϕ_1 indicates The values of drawing stresses obtained under identical conditions are different. The maximum reduction of drawing stress is at G=0 for the case of the ratio of frictionless and dry friction forces. This is only available to ideal working condition.

The reduction of drawing force is slightly decreased by increasing hydrodynamic parameter G. It means that drawing force is depended on different hydrodynamic conditions and the presence of lubricant film. The equation (98) is used to compare with experimental results.

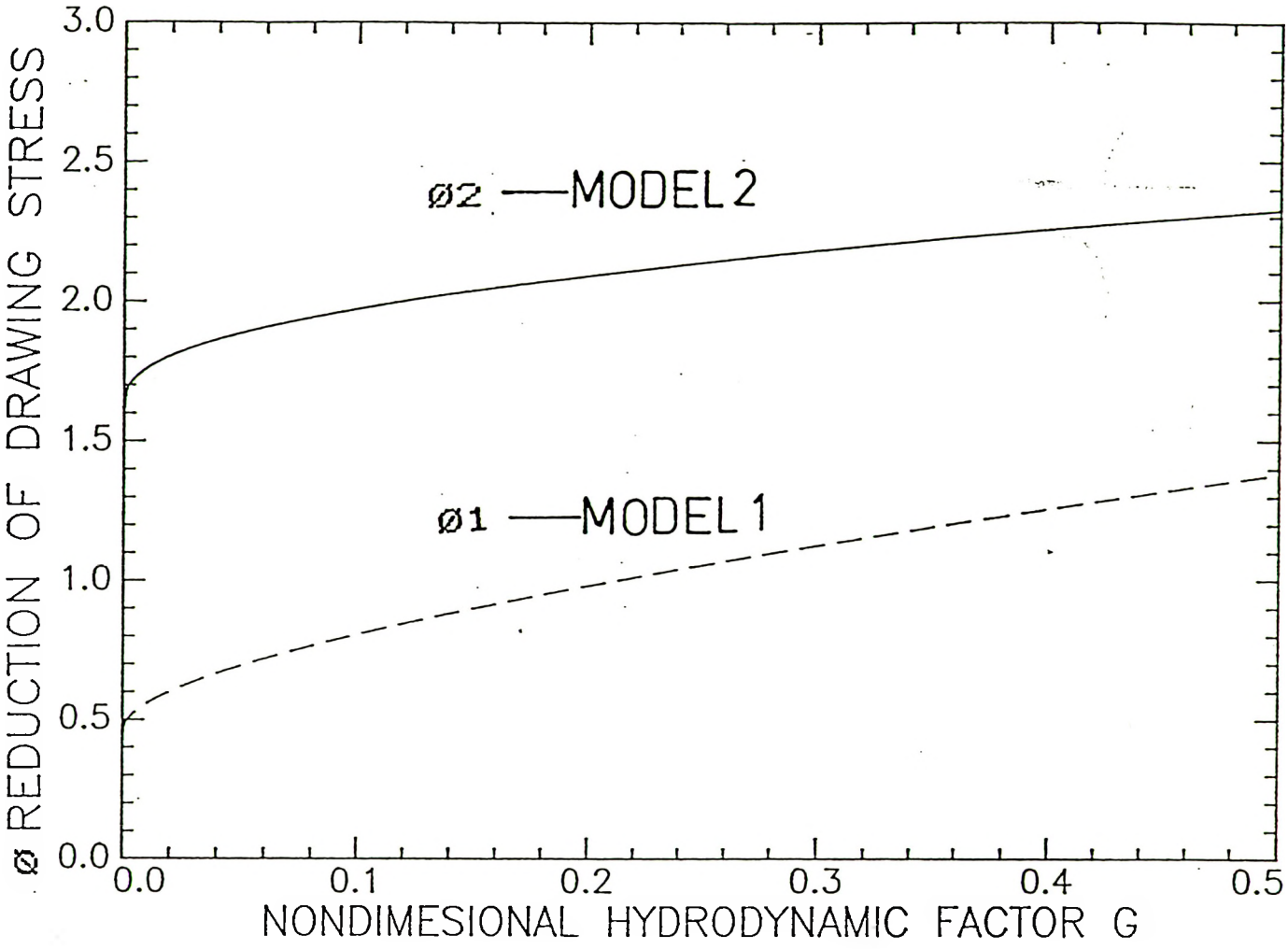

FIG. 21 VARIATION OF REDUCTION OF DRAWING STRESS ϕ WITH NONDIMENSIONAL HYDRODYNAMIC PARAMETER G FOR ϕ_1 AND ϕ_2

CHAPTER IV

EXPERIMENTAL INVESTIGATION

4.1 Overview

An experimental apparatus was designed and built to conduct experiments in a cup drawing process. A series of experiments with various lubricant viscosity were conducted to investigate the formation of a hydrodynamic lubricant film. Various physical quantities before and after drawing experiments were measured to investigate the establishment of a hydrodynamic lubricant film and to estimate the lubricant film thickness.

The results indicate that the formation of a thick hydrodynamic lubricant film cause a cup to be drawn at smaller diameter than the unlubricated drawn cup. The difference is used as a mean to estimate the lubricant film thickness in the drawing process.

4.2 Details of Experimental Apparatus

A cup drawing die and punch with a blank-holder were designed, manufactured, and fitted in two guide posts die set device.

A 300 mm length punch as shown in FIG. <22> were made of two sections. The 280 mm long part is screwed to the top moving plate of the die holding device. This part made of carbon steel. The 20 mm long part is an interchangeable part and made of alloy steel AISI D2 (VEW K105 SPECIAL KNL) and hardened to RC 60. The diameter of the pouch is 62 mm and the shoulder radius is 5 mm.

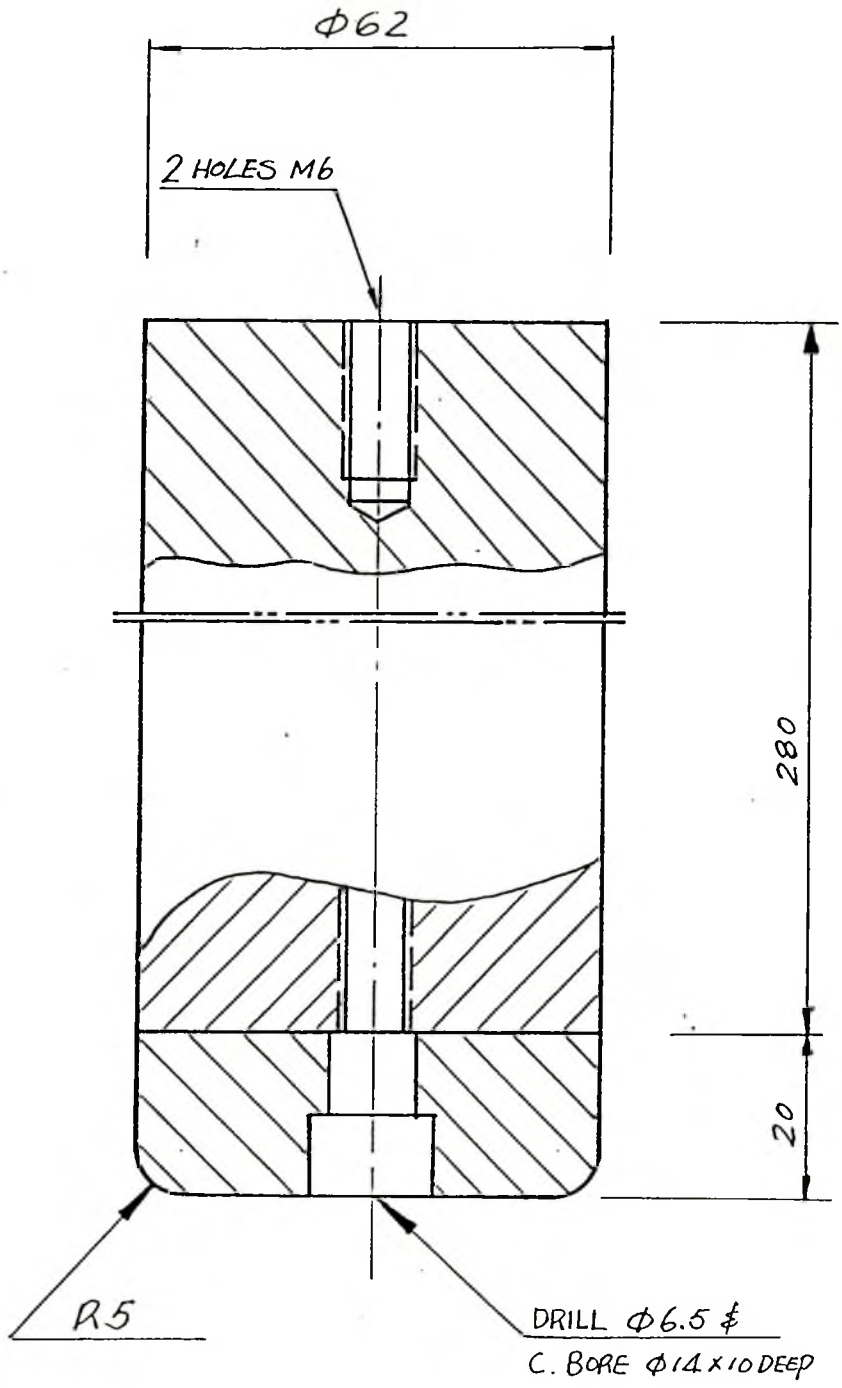

FIG. 22 PUNCH

The die with bore of 65 mm and 8 mm thickness, as shown in FIG.<23> made of VEW K105 SPECIAL KNL alloy steel and heat treated to 60 RC hardness. The die is placed in the die holding device precisely to maintain a uniform clearance and precise alignment with the punch. The die can be interchanged with other die in order to modify the die and punch clearance.

The drawing tooling used for experiments is capable of making a flat end cup shape product with 64 mm diameter and 1.5 mm thickness from 120 mm diameter sheet metal blank.

The blank-holder plate was made of mild steel and mounted on rams of pneumatic cylinders. Four pneumatic cylinders which were mounted in position of 90 degree from each other on the circumference of the blank-holder exert blank-holder force for initial clamping. Some difficulties were faced during the drawing process with increasing the blank-holder force.

In addition to forces from pneumatic cylinders, a set of four coil springs were used to increase the clamping force when the drawing is proceeded. However with the addition of auxiliary forces by springs still it is possible to modify or control the blank-holder force during the drawing process by controlling air inlet to pneumatic cylinders.

The hydraulic press was originally built with solid platen for a special process other than drawing. The use of two frames made of structure steel both for the ram and platen of the press were needed to utilize the press. The tooling was secured to the press platen by means of a structure steel beams frame. A space in the frame has been provided to withdrawn the drawn cup. The details of the tooling and its attachments are shown in Figs.<24> and <25>.

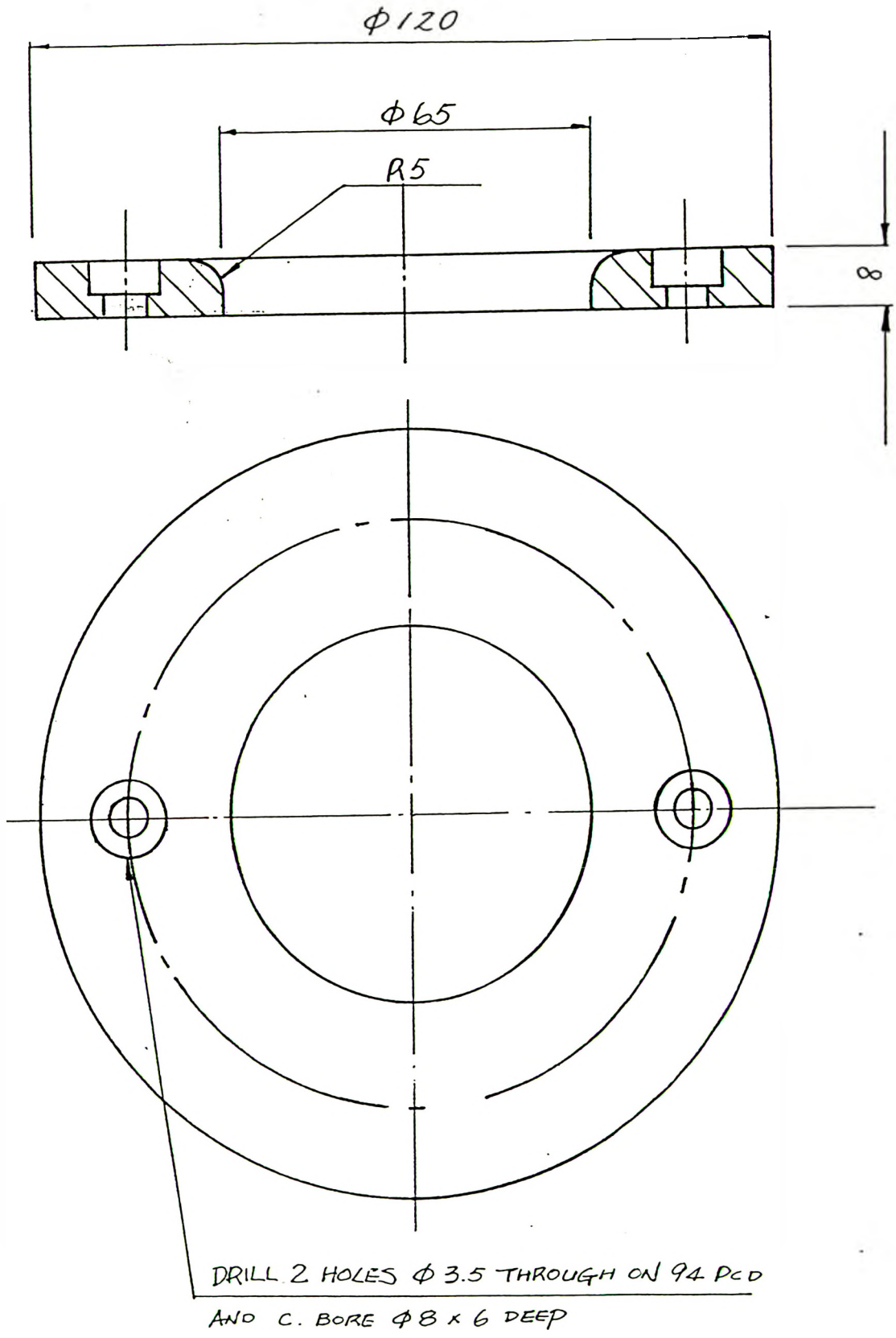
Φ120
Φ65
R5
8
DRILL 2 HOLES Φ 3.5 THROUGH ON 94 PCD
AND C. BORE Φ 8 x 6 DEEP

FIG. 23 DIE

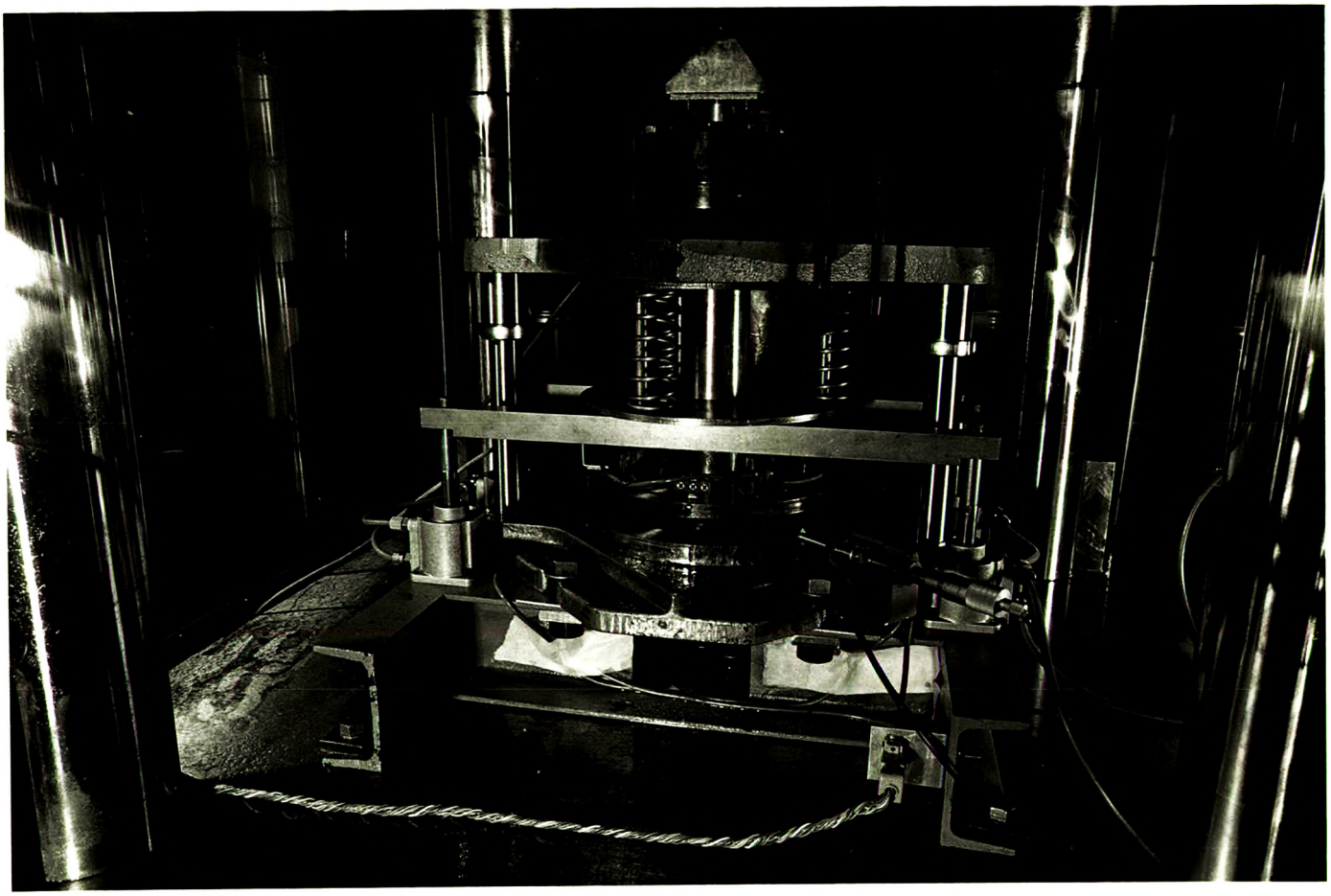

FIG. 24 EXPERIMENTAL SYSTEM -- DRAWING TOOLING AND ITS ATTACHMENTS

FIG. 25 EXPERIMENTAL SYSTEM --DATA ACQUISITION AND CONTROL

4.3 Instrumentation

In the drawing rig, several physical quantities are measured by various sensors. The data received from sensors are recorded and analyzed through a computer linked with data acquisition system. A program to perform those work was written and listed in APPENDIX A.

The relative displacement between the punch and die is measured by a linear-displacement transducer (LVDT). The transducer has been mounted to the press frame and the moving core of the transducer was secured to the press ram.

The punch force is measured by a load cell. A 25 tons strain-gauged type load cell has been placed between the punch and the press ram. The blank-holder force is measured by means of four small proving rings with cemented strain gauges that are mounted between the pneumatic driving shafts and blank-holder plate.

The drawing force applied to the die is estimated from the applied force to the structure of the frame between the tooling end-face and the press platen. Four strain gauges have been mounted to the frame to measure the strain of the frame and consequently the load of the die.

It was attempted to measure the lubricant film thickness through a fotonic sensor device. The sensor measures the local distance between the probe and the target located against the probe. The measurement based on the difference between incident and reflected light from the target. The probe of the sensor was placed and sealed inside, a 3 mm diameter drilled hole from outside to inside diameter of the die, far from the moving deformed blank.

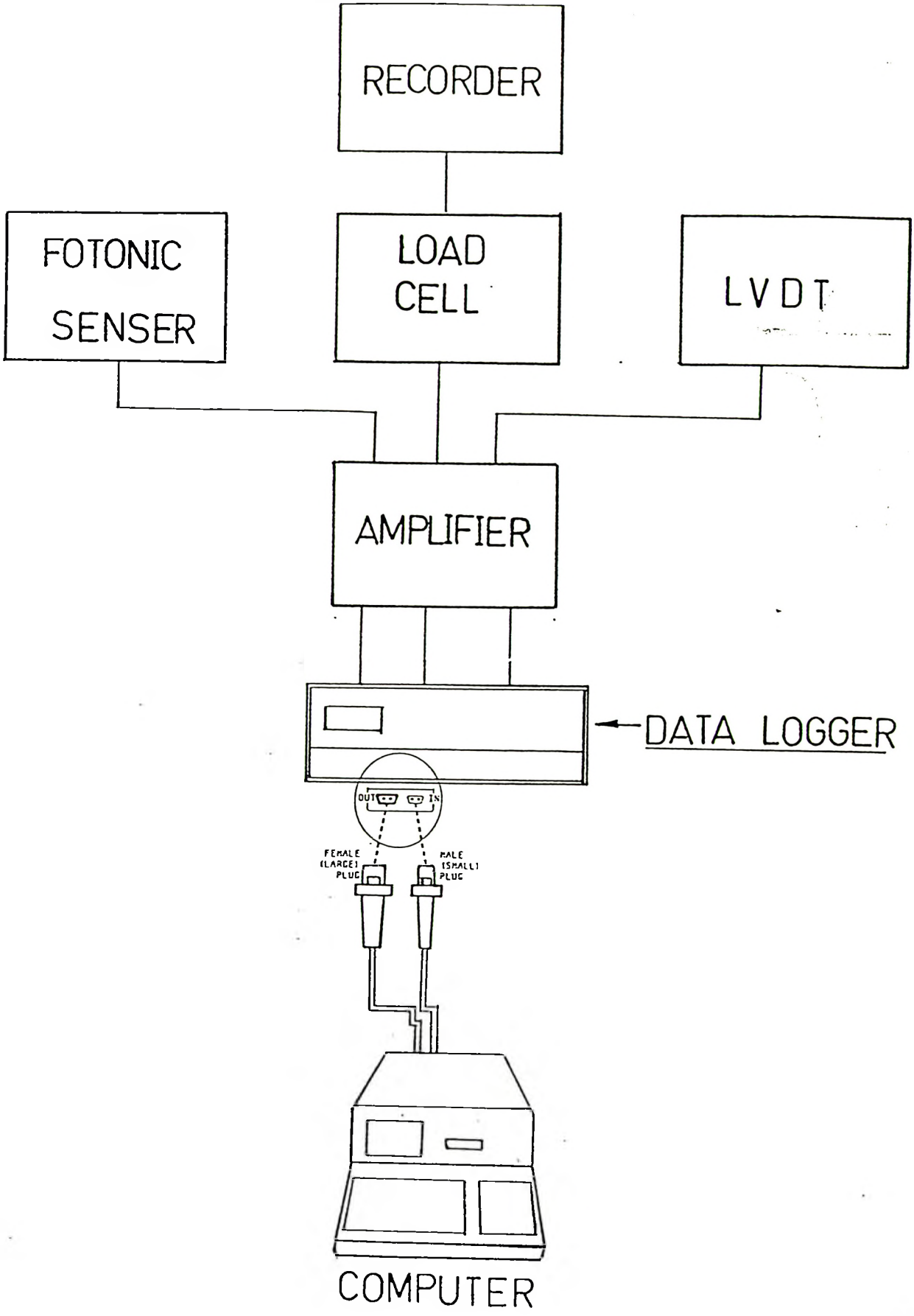

FIG. 26 CONFIGURATION OF MEASUREMENT SYSTEM

As shown in FIG. <26> a 3 channels chart recorder was linked to the outputs of load cells. The variation of the load cell outputs with time were plotted. These results were used to compare with the data taken by data logger for load cells in order to ensure the samples are correctly.

4.4 Experimental Procedure

A series of experiments to draw low carbon steel (CA4SNE) blank were conducted with various lubricants. Samples of 120 mm diameter were cut from sheet of 1 mm thickness. The yield strength of the material is 140-190 Mpa. All blanks were drawn into cup shape products with overall dimensions shown in FIG. <27>.

Numerous lubricants, as given in table <1>, were tested in drawing process. A coat of lubricant was applied to both surfaces of a blank by a brush and then placed and aligned on the surface of the die for drawing operation. For each lubricant a batch of 5 blanks were drawn. For each experiment dimensions of sample before and after drawing, and related blank-holder and drawing forces were recorded. In order to detect the formation of a thick lubricant film, both surfaces of each blank was painted and dried before the application of lubricant. FIG. <28> shows a painted blank before drawing.

The establishment of a thick hydrodynamic lubricant film during the drawing process left the outside painted surface of the blank intact or partially scratch.

The surface of a cup with remained paint layer on its surface is as the result of formation of a thick hydrodynamic lubricant film during the drawing process is shown in FIG. <29>. The removal of the painted layer from the well lubricated cup shows the surface of the cup is matt. This is another indication of establishment of a

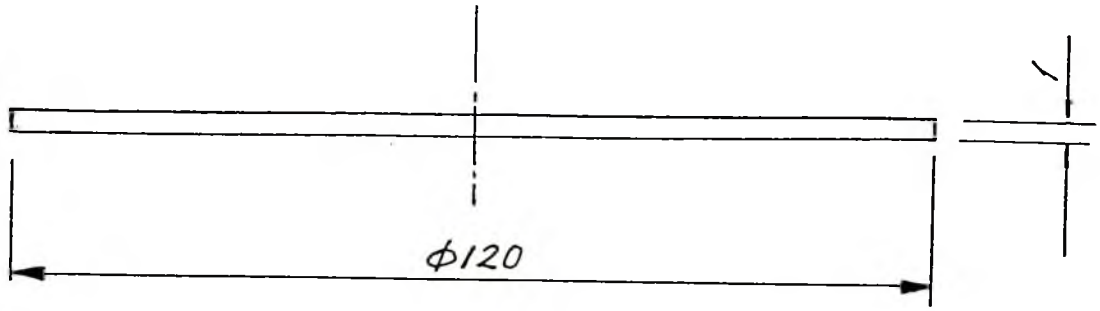

BLANK

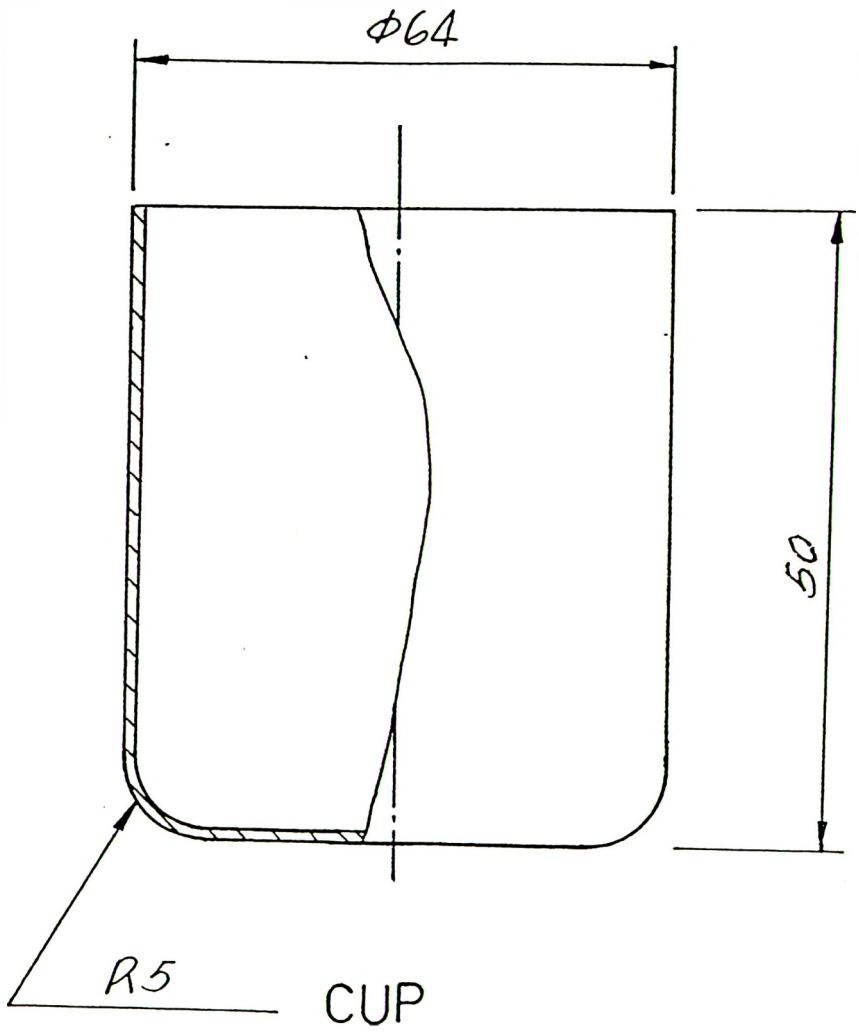

CUP

FIG. 27 BLANK AND CUP

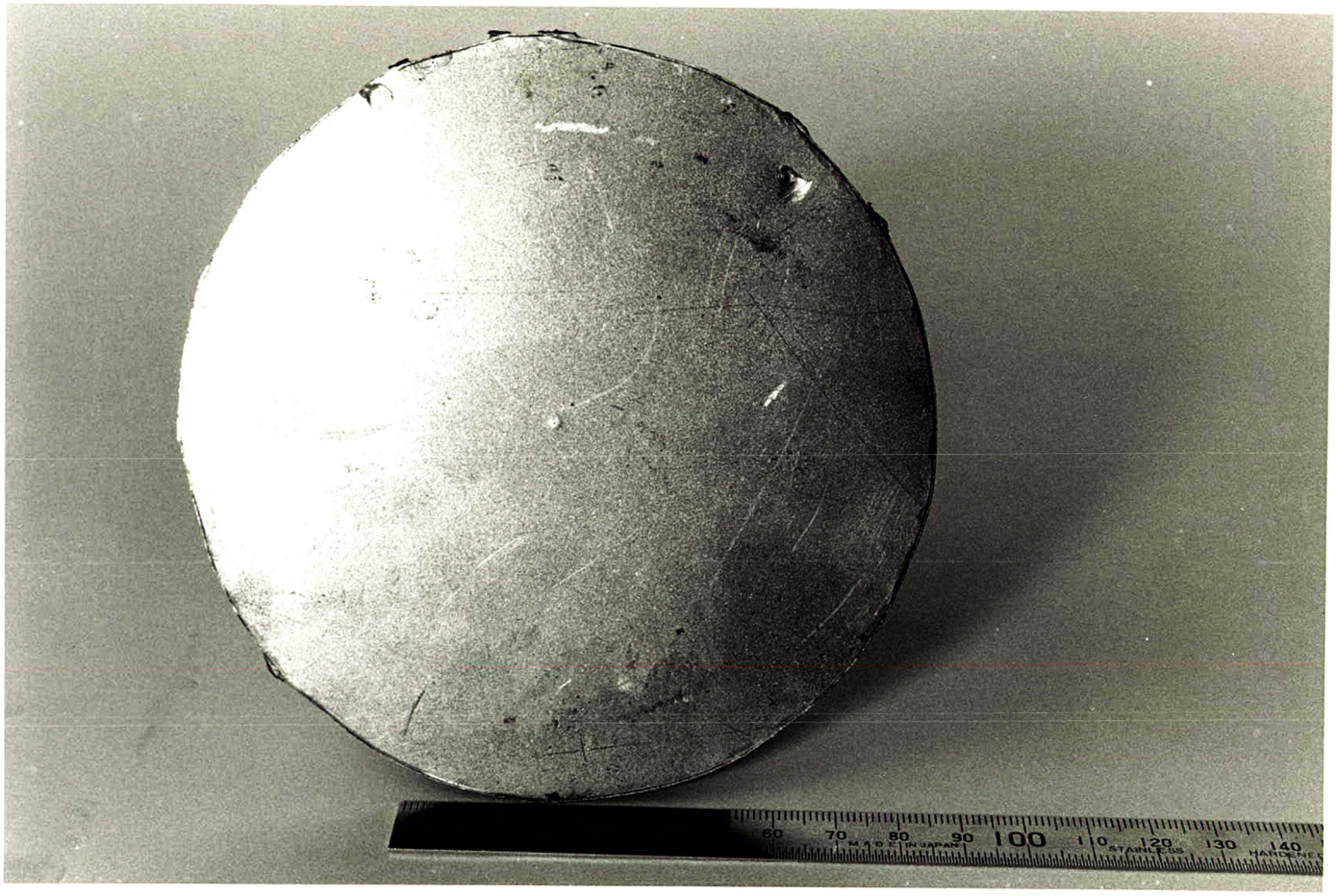

FIG. 28 AN OPTICAL MICROGRAPH SHOWING A PAINTED BLANK BEFORE DRAWING

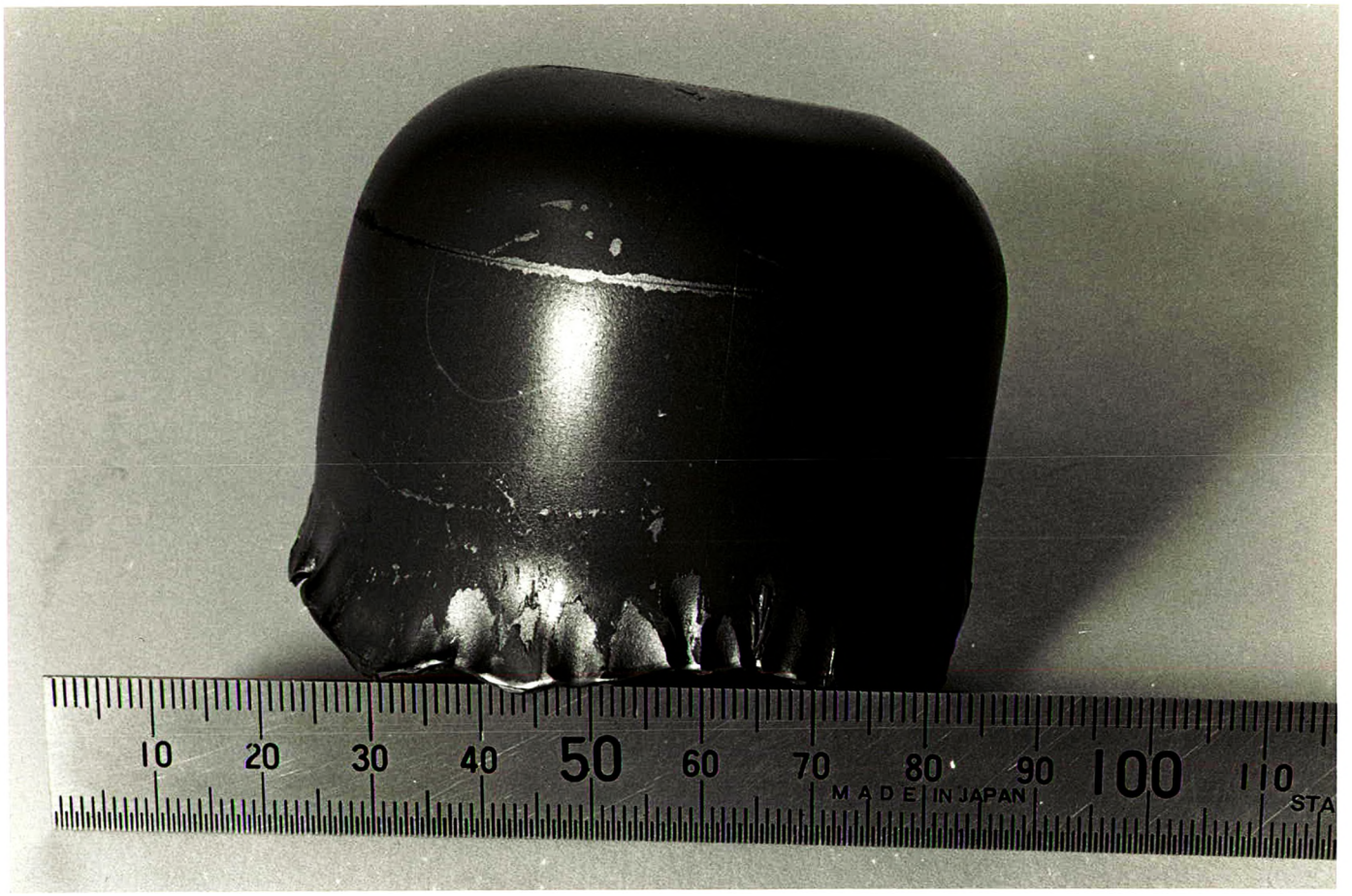

FIG. 29 AN OPTICAL MICROGRAPH SHOWING A PAINT LAYER REMAINED ON DRAWN CUP SURFACE

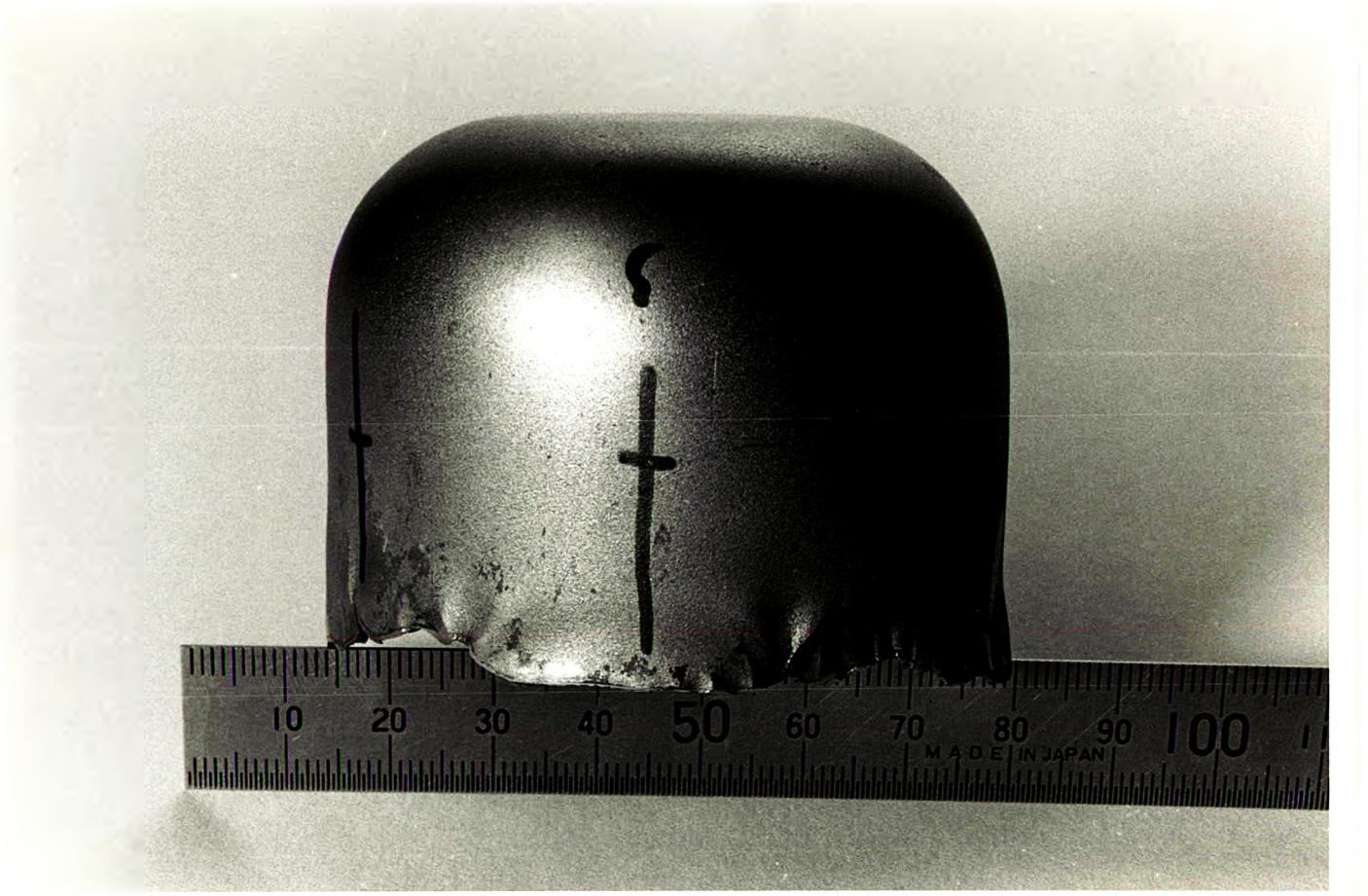

FIG. 30 AN OPTICAL MICROGRAPH SHOWING THE MATT SURFACE AFTER REMOVING THE PAINT LAYER FROM DRAWN CUP SURFACE

hydrodynamic regime in the deep drawing process. FIG.<30> reveals the matt surface of a typical well lubricated cup.

The severity of scratch on the surface of a cup depended on the lubricant viscosity applied to the painted blank surface. In case of unlubricated blank, the paint layer was vanished from the outside surface of the cup and the surface appeared to be burnished. FIG.<31> shows the scratched surface of an unlubricated drawn cup. The difference between the surface textures of blank, lubricated without removal of paint, lubricated with removal of paint and unlubricated cups are clearly may be seen in FIG.<32>.

The paint layer on the inside surface of the cup remained unscratched in both lubricated and unlubricated blank. This shows that the blank is only wrapped over the surface of the punch and there is not any relative movement between the punch and blank surfaces to assist the formation of a hydrodynamic lubricant film.

TABLE 1 Viscosity of Lubricant Used

GROUP NO.	VISCOSITY	NAME OF LUBRICANTS
1	100 cSt.	PROCESS OIL P100
2		CASTOR OIL SAE 30/40
3	220 cSt.	IMPREGNO DRAWING OIL WS
4	240 cSt.	IMPREGNO DRAWING OIL NO.2
5	640 cSt.	MA 42
6	680 cSt.	MONOLUBE 680
7		PTFE NULON L90

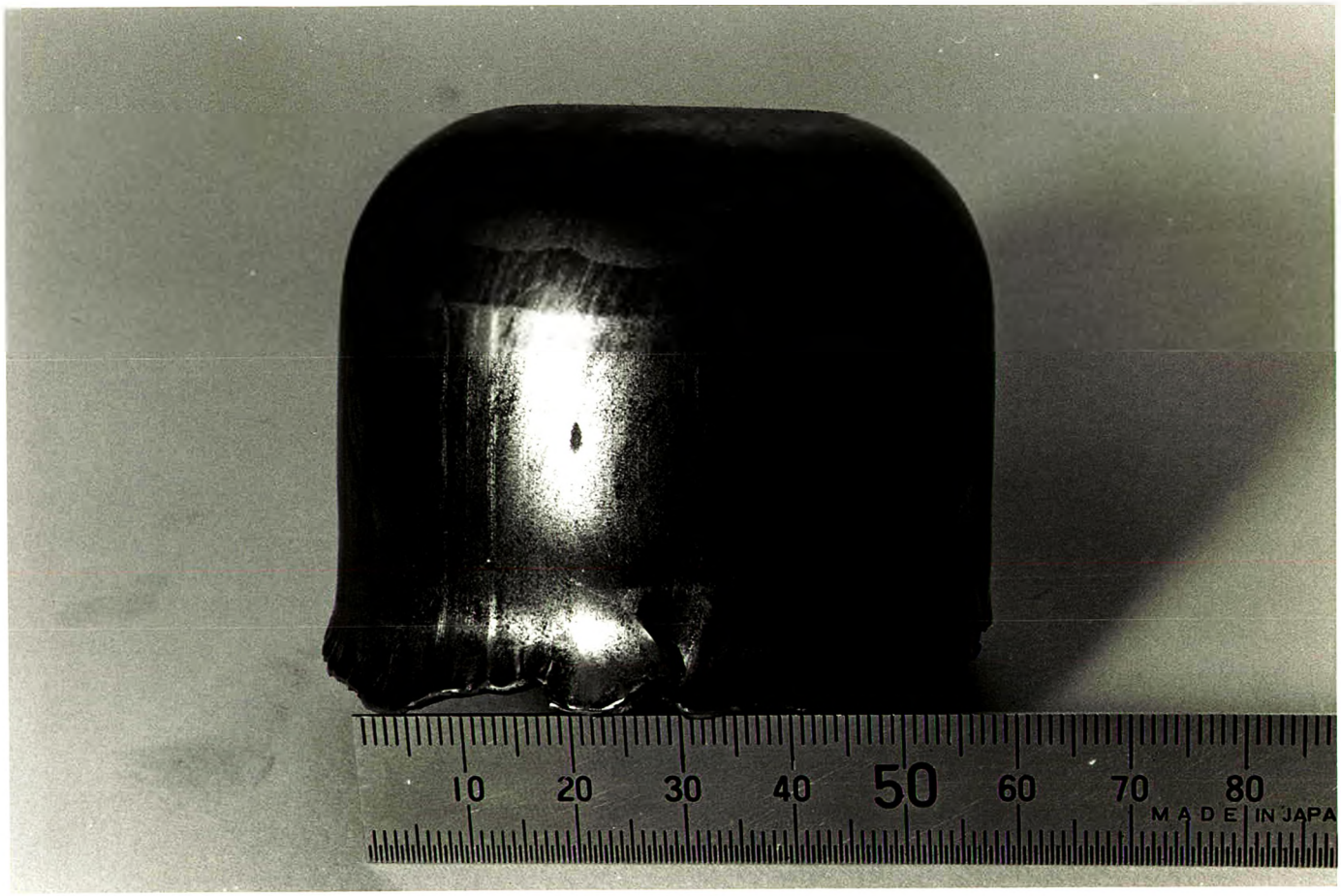

FIG. 31 AN OPTICAL MICROGRAPH SHOWING THE SCRATCHED SURFACE OF AN UNLUBRICATED DRAWN CUP

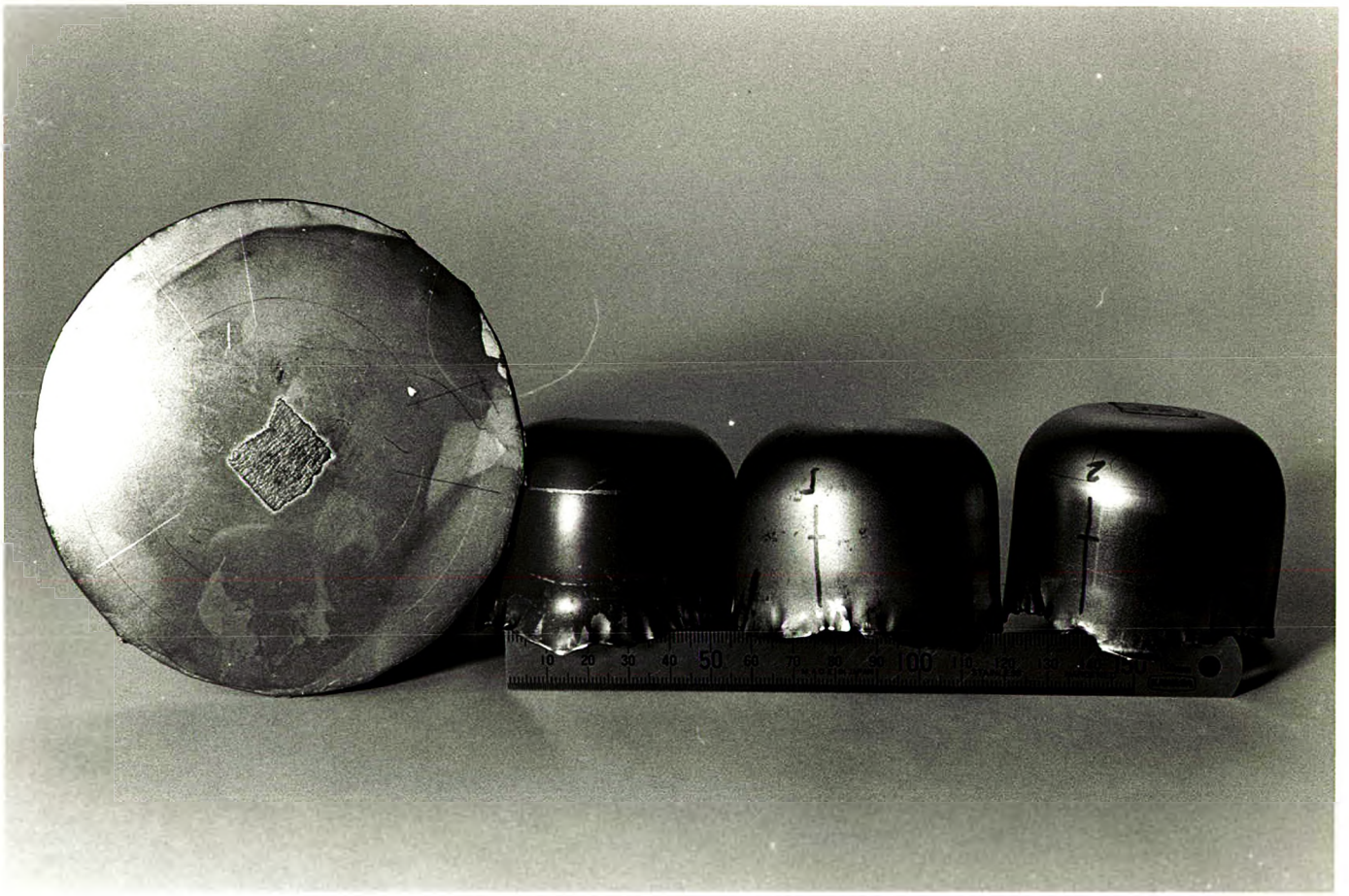

FIG. 32 AN OPTICAL MICROGRAPH SHOWING DIFFERENT SURFACE TEXTURES OF DRAWN CUP

8	1600 cSt.	DK 1172

4.5 Experimental Results

The effect of lubricants viscosity on drawing and blank holder forces were investigated. The sample of chart recorder and computer printouts are given in APPENDIX B.

The outputs of the fotonic sensor was not consistent and because lake of required sensitivity and resolution, it was practically impossible to measure the lubricant film thickness directly. However, the film thickness may be estimated by dimensional measurement of lubricated and unlubricated cups.

4.5.1 Effect of Lubricant Viscosity on Drawing Forces ratio

The effect of lubricants viscosity on drawing force may be visualized better if it is compared with the unlubricated (dry friction drawing force. The variation of ratio of lubricated to unlubricated drawing forces for each batch of experiments is plotted in FIG.<33>. It indicates that the drawing forces ratio is increased slightly with the increase in lubricant viscosity. The process oil P100 has the lowest value of forces ratio of 0.85. The maximum value for forces ratio of 0.92 is for DK1172 lubricant.

4.5.2 Effect of Viscosity on Lubricant Film Thickness (Estimate of Film Thickness)

The outside diameter of each cup were measured at several points on the circumference of the cup. The measurement points were 60 degree apart from each other in the plan

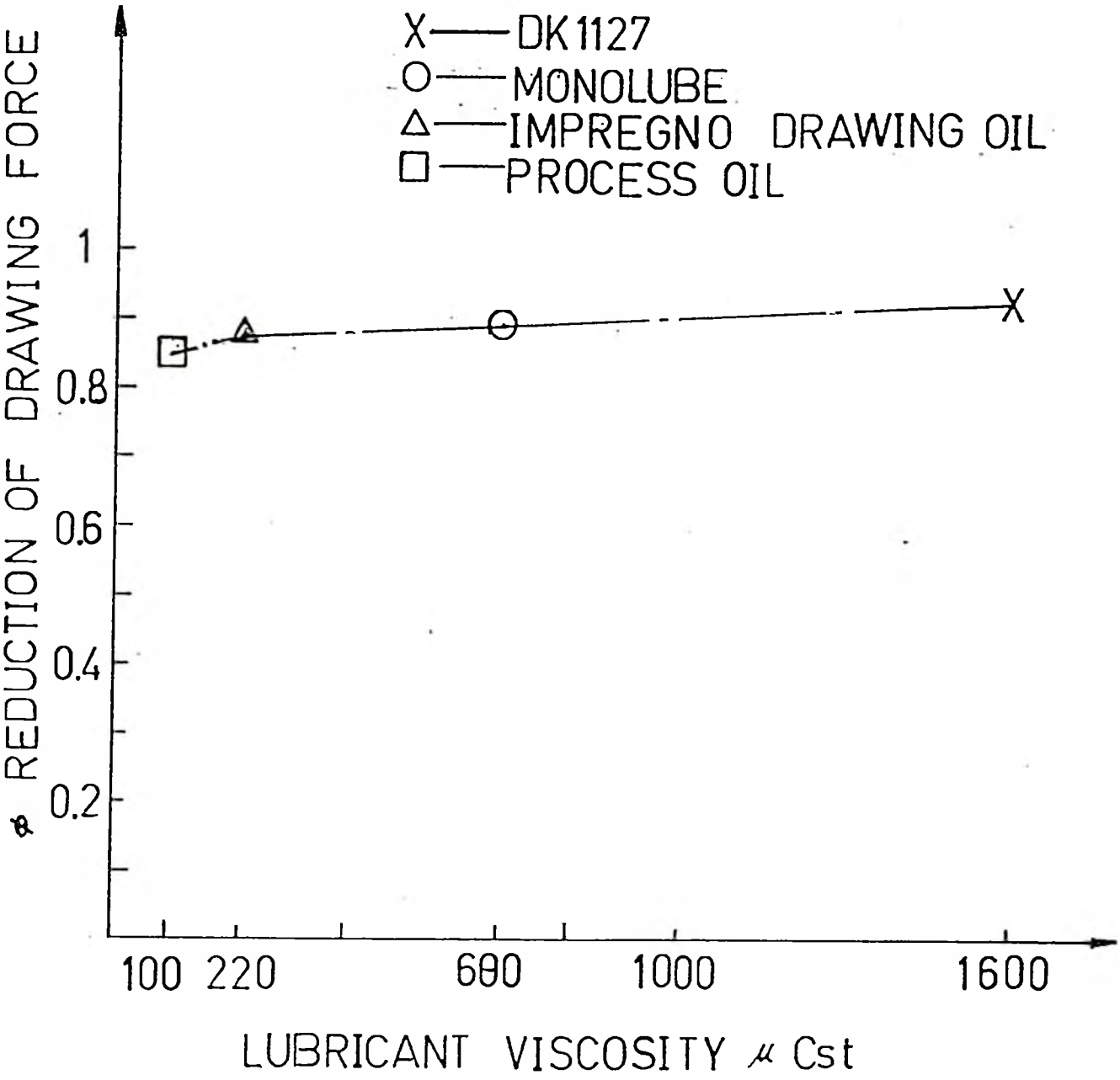

FIG. 33 VARIATION OF REDUCTION OF THE DRAWING FORCE δ WITH LUBRICANT VISCOSITY μ

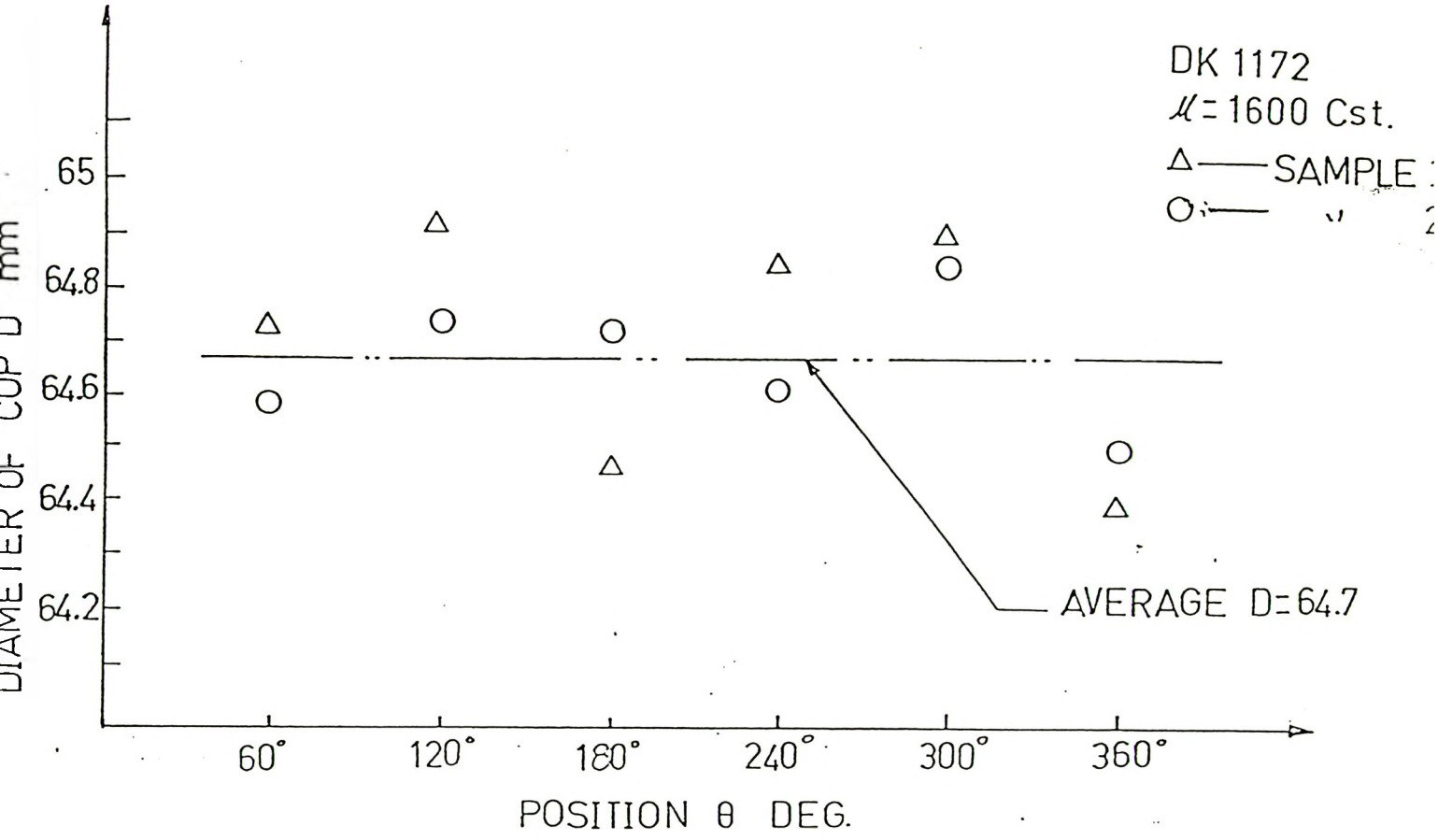

FIG. 34 SAMPLING CUP DIAMETER

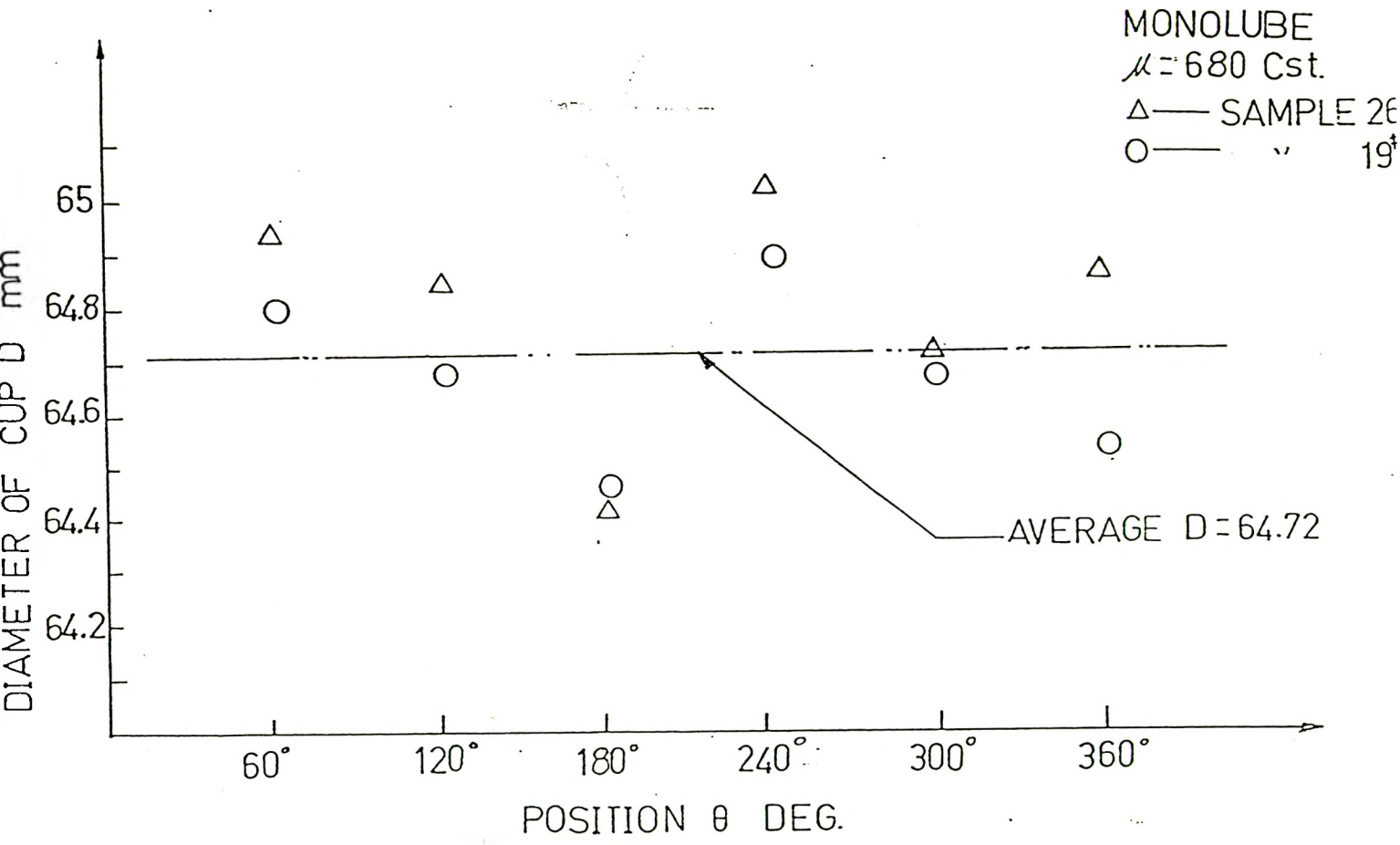

FIG. 35 SAMPLING CUP DIAMETER

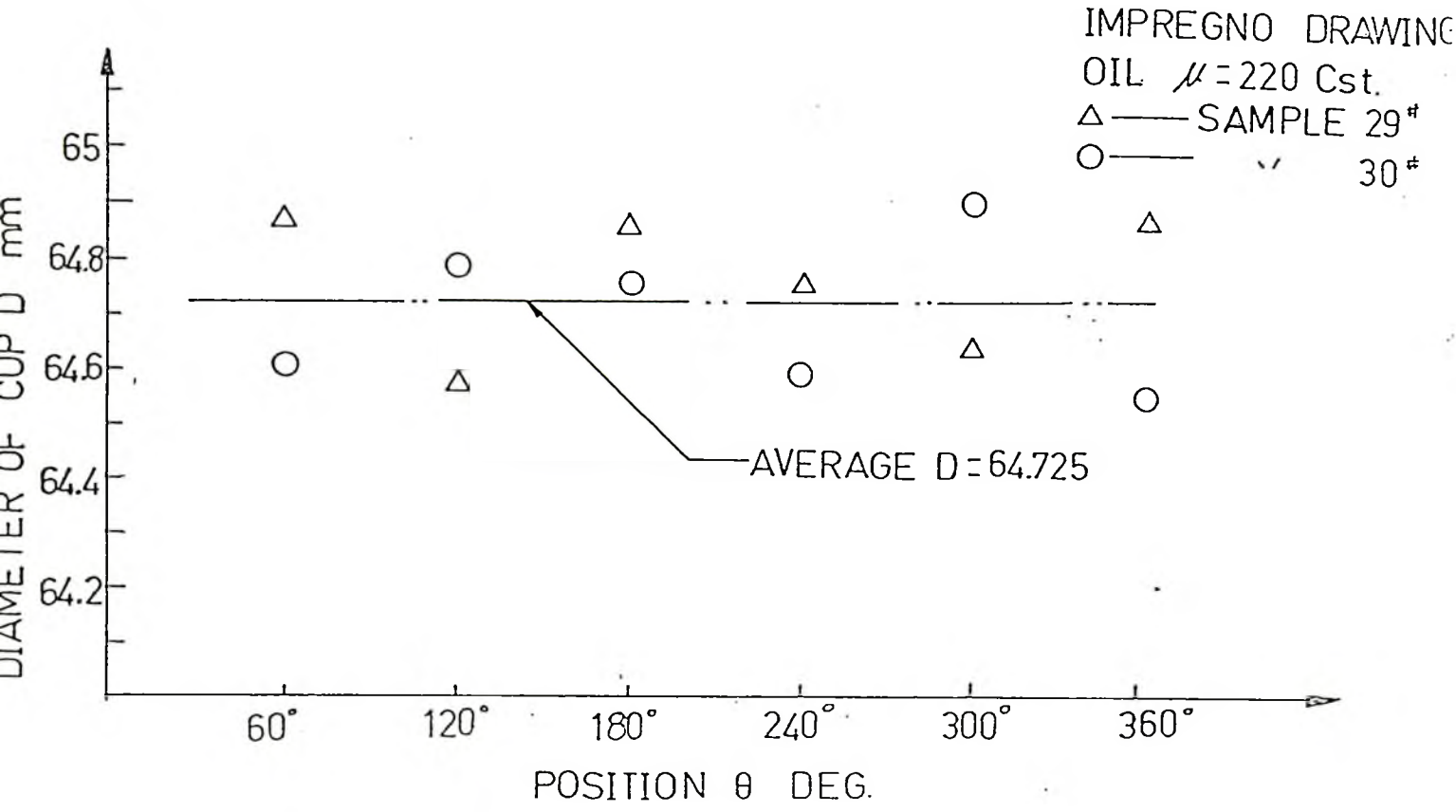

FIG. 36 SAMPLING CUP DIAMETER

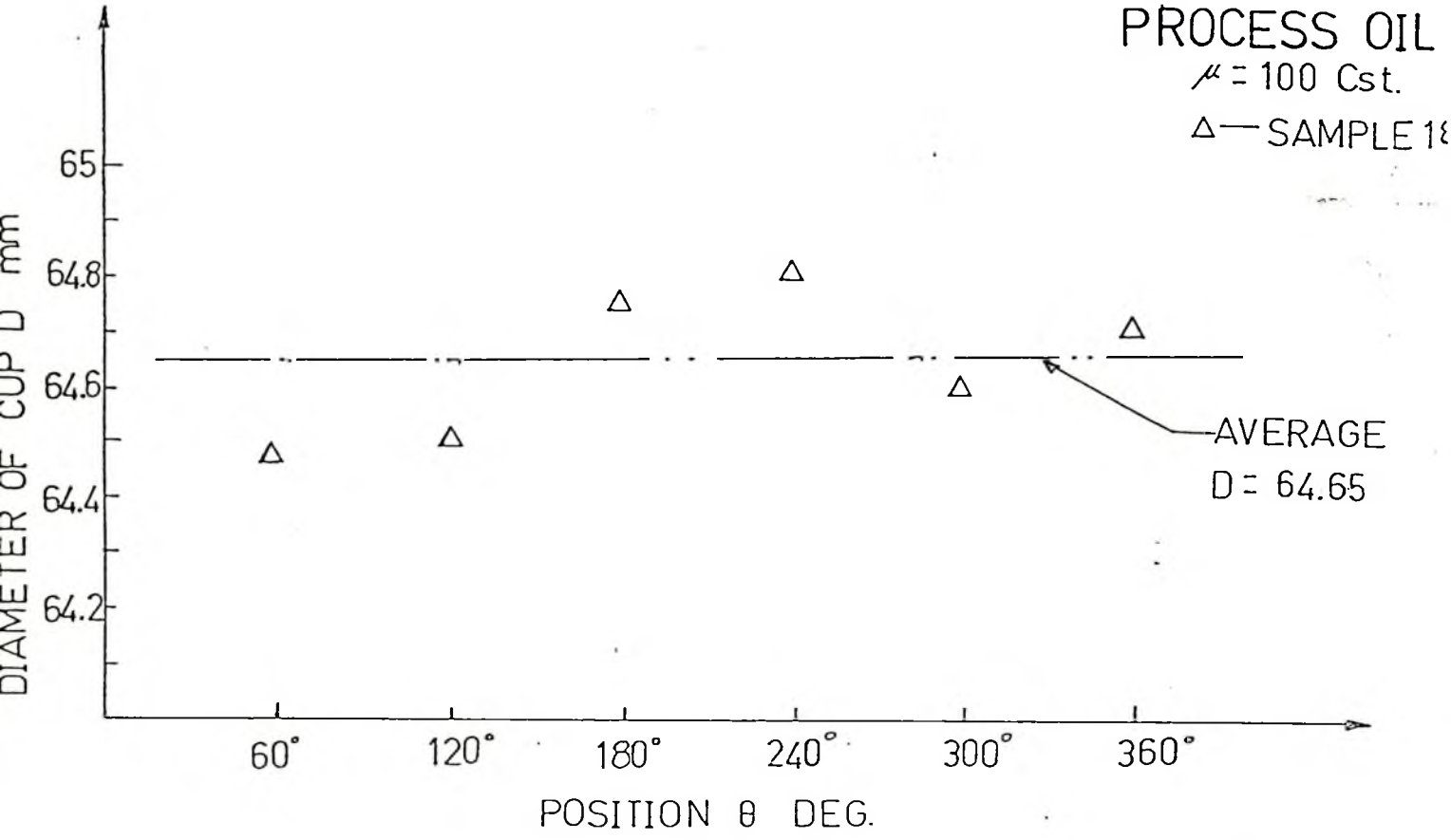

FIG. 37 SAMPLING CUP DIAMETER

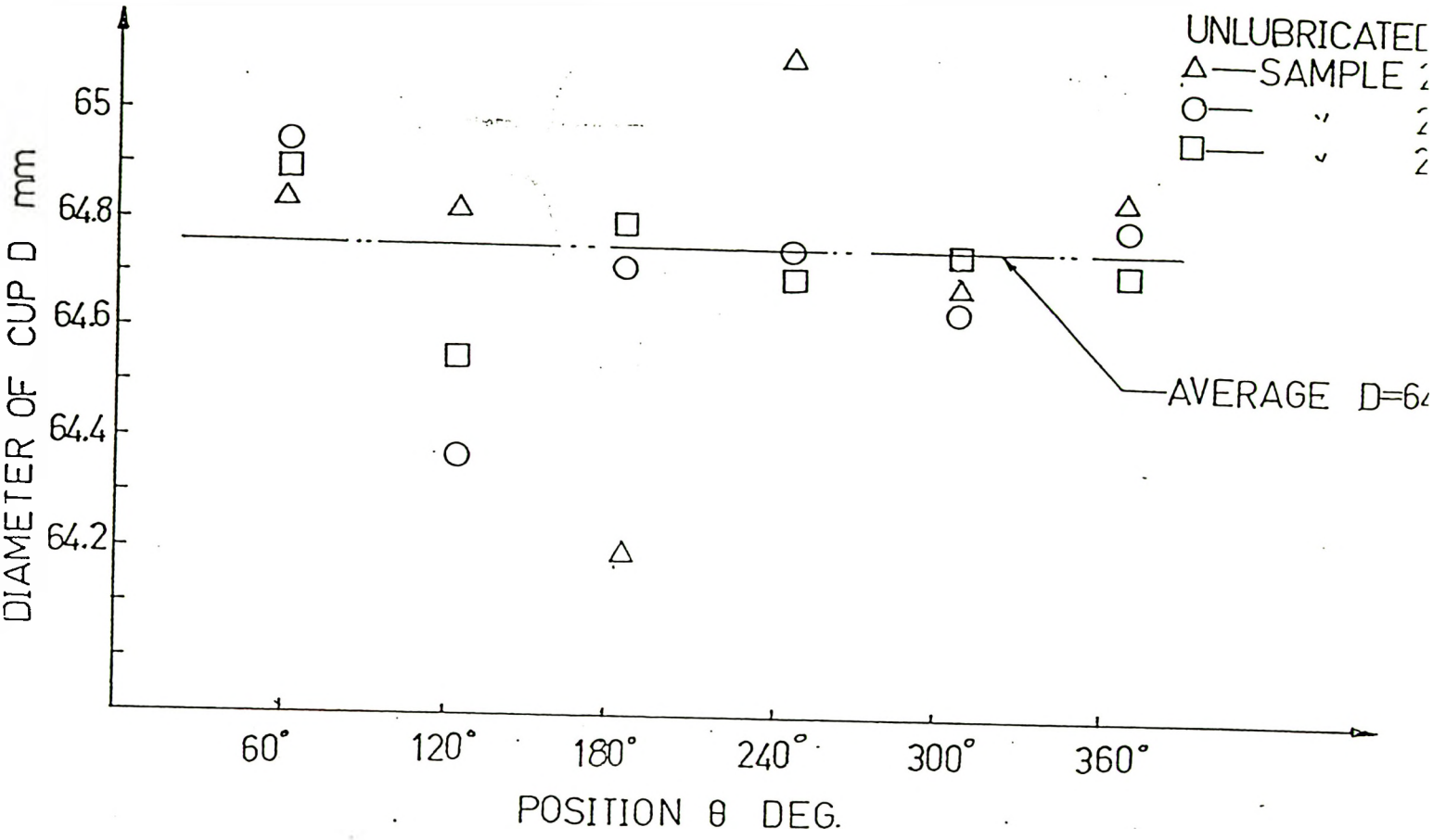

FIG. 38 SAMPLING CUP DIAMETER

perpendicular to the vertical axis and at mid-hight of the cup. It was noticed that cup's diameter varies with the type of lubricant used in drawing process. Figs.<34 - 38> show the measurement of cup diameter for different lubricants viscosity. The lubricated cups diameter is smaller than the unlubricated cups diameter. The difference in diameters varies from 0.0350 mm to 0.0590 mm which is depended on the viscosity of used lubricant. The difference was caused by formation of a hydrodynamic lubrication regime during the drawing process and is an estimate of lubricant film thickness. The value of lubricant film thickness is estimated half of this diameter difference.

4.5.3 Effect of Lubricant Film on Wall Thickness of the Cup

The wall thickness of each cup was measured on several locations and in the same plane where cup diameter had been measured originally. The changes in wall thickness of numerous cups with angular positions around the circumference of cup is plotted in FIG.<39>. The unlubricated wall thickness of all cups are less than the wall thickness of lubricated cups.

4.5.4 Effect of Hydrodynamic Film on Surface Roughness of the Cup

The measurement of surface roughness for several cups were conducted by Talysurface machine. The surface roughness of each cup was measured in both circumferential and longitudinal directions. The RMS measurement of cups surfaces are given in TABLE <2>. The longitudinal surface roughness for both lubricated and unlubricated cases are less than circumferential roughness. The unlubricated cup surface has a better finish than the lubricated cup surface and blank.

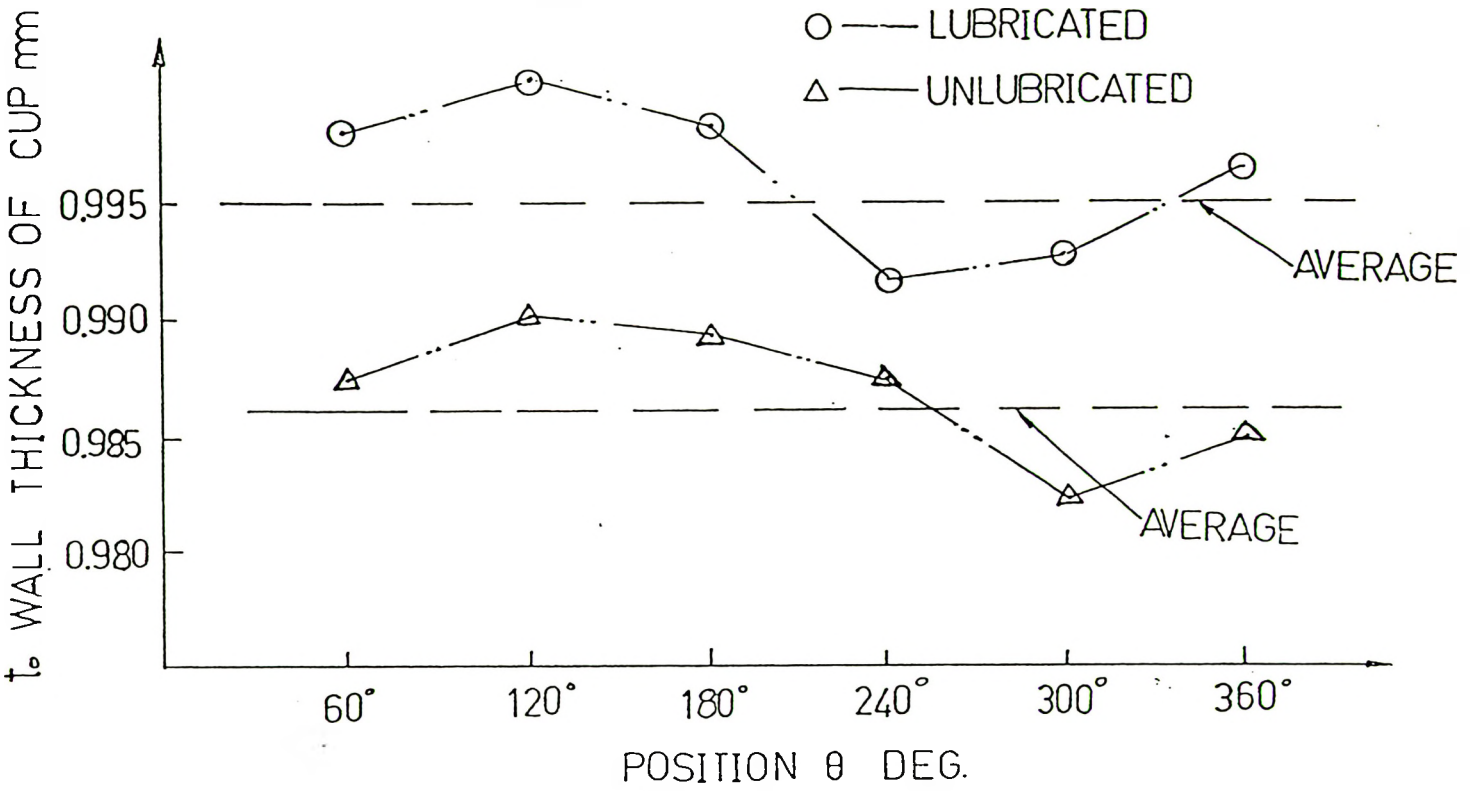

FIG. 39 SAMPLING CUP WALL THICKNESS

TABLE 2 MEASUREMENT OF SURFACE ROUGHNESS

sample no.		SURFACE ROUGHNESS Ra μin	
		IN RADIAL DIRECTION Ra	IN CIRCUMFERENTIAL DIRECTION Ra
LUBRICATED	1	90	90
	2	80	95
	3	70	100
	4	85	88
	5	75	97
UNLUBRICATED	1	32	40
	2	32	45
	3	42	55
	4	45	35
	5	40	45

4.6 Discussion of Experimental Results

The insufficient relative movement or sliding between the punch and blank did not establish a hydrodynamic lubrication regime between interfaces of punch and blank. The trace of unscratched paint layer that remained over inside wall surfaces of both lubricated and unlubricated cups denoted the lack of contact between the blank and punch lateral surfaces.

The generous nominal clearance of 1.5 mm between die and punch for bending 1 mm thick blank over the die shoulder leaves enough space between the cup's wall and punch to keep the blank surface away from the punch surface. All inside surfaces of cups appear to have a surface finish similar to the original blank surface.

The hydrodynamic lubrication regime was established between the blank and die zone for most selected lubricants. The remained paint layer on the outside surface of a cup, as shown in FIG.<29>, was a valid reason to belive the existence of a thick hydrodynamic lubricant film in the drawing process. A further feature of lubrication was that the matt surface finish of lubricated cups in contrast to the burnished surface finish of unlubricated cups.

The effect of lubricant viscosity on the drawing force, as illustrated in FIG.<33>, reveals that the drawing force may exceed the unlubricated drawing force (ratio of greater than one) if a lubricant with viscosity of higher than 1600 Cst. is used in drawing process. The increase in viscosity enhance a thick lubricant film and layer viscous shearing force between the die and blank that consequently required a higher drawing force to push the blank into the die.

Comparisons between the diameters of drawn cups show the lubricated cups formed with smaller diameter than unlubricated cups. The lubricant film pressure established

between the die and the blank pushes the blank towards the punch. The lubricant film eventually becomes part of the die that deformation is performed in a smaller die diameter. Therefore, the difference between diameters of lubricated and unlubricated cups represents twice the thickness of the lubricant film that existed in the lubricated cup. The imperfect roundness of the manufactured tooling, ununiform clearance between the die and punch due to misalignment and variation in the thickness of blank metal are reasons for variation in circumferential measurements of a cup diameter.

The wall thickness of drawn cups are smaller than the original thickness of blanks for both lubricated and unlubricated cases. The blanks were plastically stretched by applied tensile drawing stress that consequently reduced the thickness of the cup. For unlubricated cup the drawing friction between the blank and die and greater drawing force intensify the reduction in wall thickness of the drawn cup.

CHAPTER V

COMPARISON BETWEEN THEORETICAL AND EXPERIMENTAL RESULTS, CONCLUSION AND FUTURE WORK

The drawing speed, lubricant viscosity, and tooling dimensions were used to estimate the hydrodynamic lubricant film thickness and the drawing forces ratio by means of the theoretical model presented in CHAPTER III. The hydrodynamic lubricant film thickness and drawing forces ratio estimated experimentally in CHAPTER IV are compared with the theoretical prediction, the validity of the theory is discussed.

5.1 Drawing Forces Ratio

The variation of drawing forces ratio of lubricated to unlubricated cases with nondimensional hydrodynamic factor G, equation (98) was plotted for two theoretical analyses designated as ϕ_1 and ϕ_2.

The nondimensional parameters of

$$\mathbf{C = 0.142}$$

$$\mathbf{B = 0.583}$$

$$\mathbf{I = 0.0834}$$

$$\mathbf{L = 24.75}$$

$$\mathbf{\delta = 0.9}$$

were substituted in equation (98), to plot ϕ - G variation in FIG.<40>. These parameters were calculated from experimental measurements of die geometry, drawing speed, and blank-holder pressure. These measurements are given by values of

r_0 = 2.362 in.

r_1 = 1.387 in.

r_2 = 0.197 in.

t_0 = 0.0394 in.

p_{BH} = 217.5 psi

V = 0.2 in./sec

σ_y = 2392.5 psi or 16.5 N/mm^2

ß = 0.1

The experimental drawing forces ratio for different types of lubricants are shown in FIG.<40>. The experimental drawing forces ratio follows the same trend as prediction by the theoretical model. For values of G less than 300 the experimental results are closer to ϕ_2 curve. For values of G greater than 1200 the experimental results follows the ϕ_1 curve.

5.2 Film Thickness

The variation of film thickness with lubricant viscosity from equation (38) for experimental conditions as mentioned above, was plotted in FIG.<41>. The experimental estimates of lubricant film thickness values are also presented in FIG.<41>.

The experimental estimate of lubricant film thickness values increases with increasing lubricant viscosity. The experimental results follow the same trend as theoretical results. The experimental value of the film thickness is approximately 10 μm greater than the theoretical estimate.

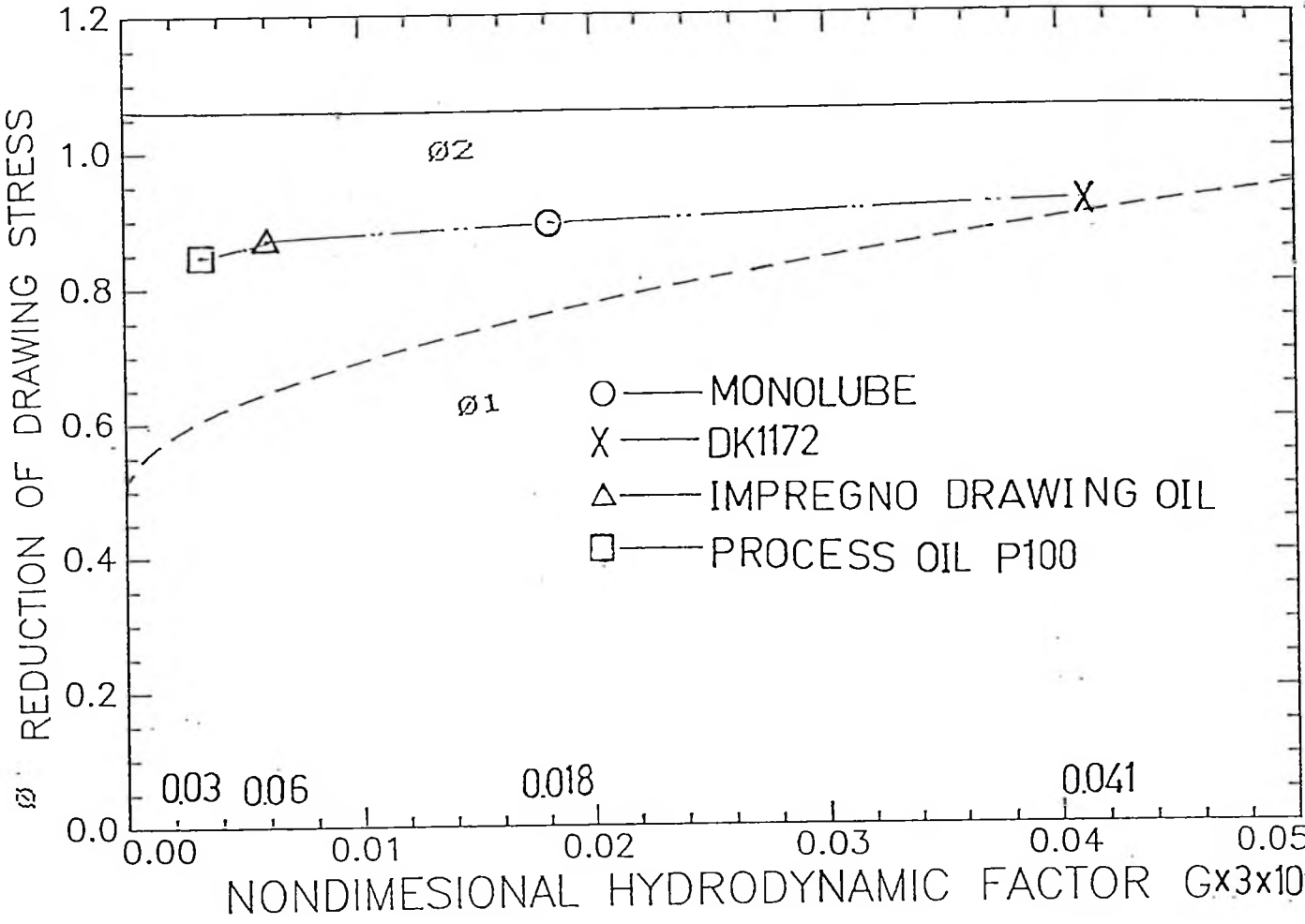

FIG. 40 COMPARISON OF DRAWING FORCE REDUCTION ϕ

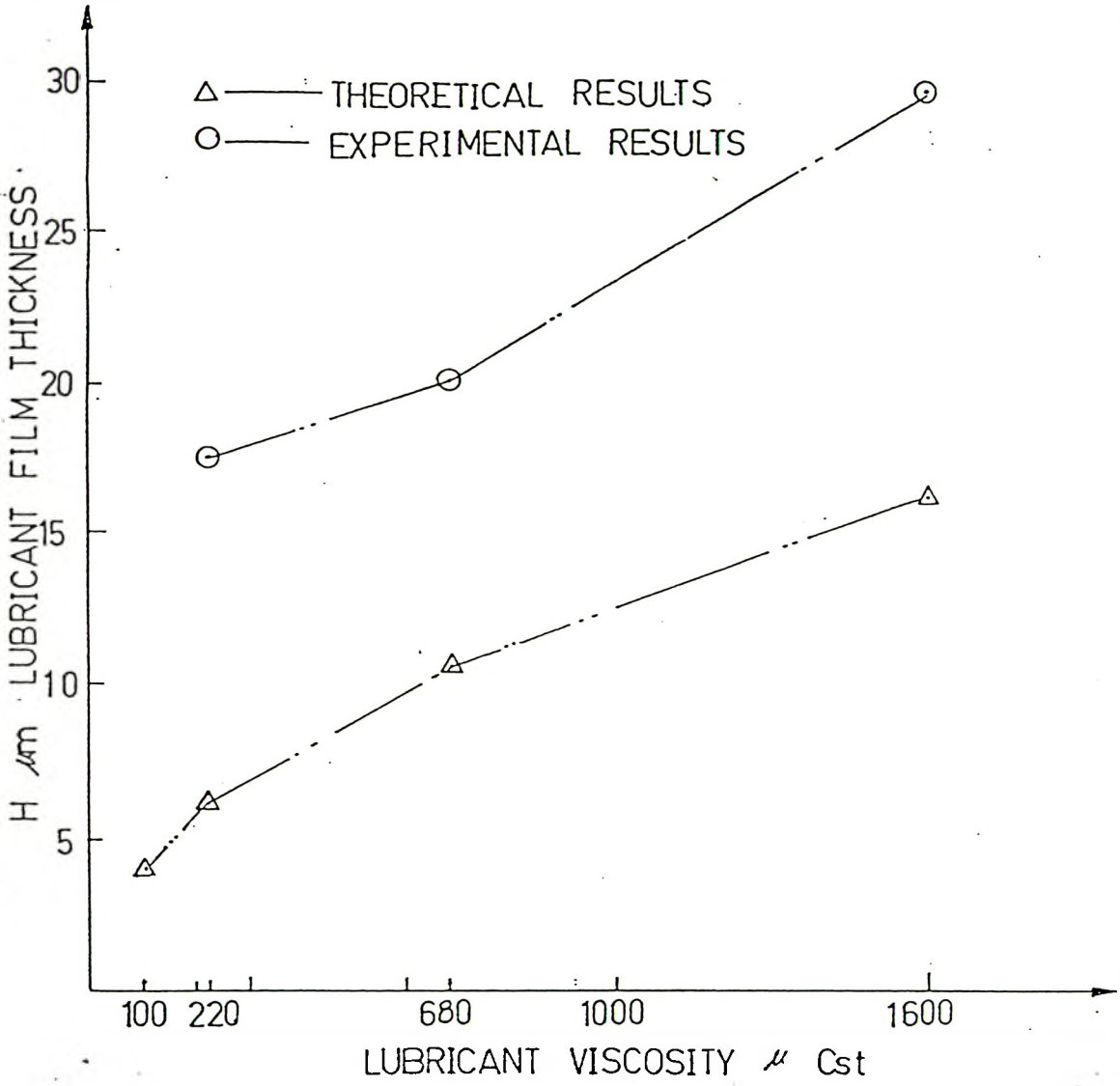

FIG. 41 COMPARISON OF LUBRICANT FILM THICKNESS h_1

5.3 Discussion and Conclusion

An isoviscous steady hydrodynamic lubrication model for a pure deep drawing process has been developed. The theoretical model covers the deformation stages from sheet metal blank to the drawn cup-shaped products. The drawing process has been divided into approaching, yielding, and steady deformation phases. The model has provided equations to calculate lubricant film thickness, lubricant pressure, traction force, and drawing force. The conditions that affect the formation of a thick hydrodynamic lubricant film in the process were studied.

An experimental deep drawing system has been developed. A series of experiments in cup drawing have been carried with different type of lubricant. The effects of lubricant viscosity on drawing force, surface finish, thickness, and diameter of drawn cup were investigated in detail. The lubricant film thickness has been estimated by measurement of differences in diameter of lubricated and unlubricated cups for viscosities in the range 100 - 1600 Cst.. The changes in diameter of the drawn cup and its matt surface finish have been discernible by micrometer measurement or observe with natural eyes.

The comparison of experimental and theoretical results indicates they are following identical trends. The developed theoretical model is in a better agreement with experiments than dry friction models. The validated present theoretical analysis may be applied to improve tool life, better process control of deep or cupping drawing of beverage cans, and automotive parts in metal working industry.

5.4 Future Work

Further work is necessary to improve the present model by including the viscosity dependence on pressure and temperature. The model may be extended beyond the pure bending such as ironing process. The direct measurement of lubricant film thickness in a drawing process will assist a better comparison between theory and experiment.

REFERENCES

1. Hillier, M. J., "A Hydrodynamic Model of Hydrostatic Extrusion", Int. J. of Prod. Res., vol. 5, 1966, pp. 171-181.

2. Wilson, W. R. D., and Walowit, J. A., "An Isothermal Hydrodynamic Lubrication Theory for Hydrostatic Extrusion and Drawing Processes with Conical Die", J. of lubrication Technology, ASME. vol. 93, no. 1, 1971, pp. 69-74.

3. Snidle, R. W., Dowson, D., and Parson, B., "An Elasto-Plastohydrodynamic Lubrication Analysis of the Hydrostatic Extrusion Process", J. of Lubrication Technology, ASME. vol. 95, no. 2, 1973, p. 113.

4. Wilson, W. R. D., and Mahdavian, S. M., "Hydrodynamic Lubrication of Hydrostatic Extrusion", J. of Lubrication Technology, ASME. vol. 98, no. 1, 1976, p. 27.

5. Snidle, R. W., Parsons, B., and Dowson, D., "An Elasto-Plastohydrodynamic Lubrication Analysis of the hydrostatic Extrusion Process Including the Effect of Strain Hardening and Redundant Deformation", SYMP. Elastohydrodynamic Lubrication, Inst. Mech. Engrs., 1972, p. 107

6. Snidle, R. W., Parson, B., and Dowson, D., "A Thermal Hydrodynamic Lubrication Theory for Hydrostatic Extrusion of Low Strength Material", ASME. J. of Lubrication Technology, vol. 98, no. 2, 1976, p. 335.

7. Mahdavian, S. M., "A Thermal Hydrodynamic Lubrication Analysis for Hydrostatic Extrusion of a Work Hardening Metal", ASME. J. of Tribology, vol. 108, July, 1986, p. 368.

8. Wuerscher, A., and Rice, R. B., "An Experimental Investigation of Lubrication in Hydrostatic Extrusion Using Wax as a Model Material", Transaction of the ASME. J. of Engineering for Industry, August, 1972, p. 913.

9. Thompson, P. J., and Symmons, G. R., "A Radial Mechanism for the Trapping of a Viscous Lubricant by a Cylindrical Tool a Plastohydrodynamic Analysis", Proceeding of the 18th International Machine Tool Design and Research Conference, Lodon, Sept. 14-16, 1977, MacMillan Press Ltd.

10. S. M. Madavian, "A Refined Analytical Model for Hydrodynamic Lubrication of Cold Extrusion and Its Comparison with Experiments", ASME. J. of Lubrication Technology, vol. 104, January 1982, p. 46.

11. Kalpakjian, S., "Forging Lubrication in Metal Forming Processes: Friction and Lubrication", ed. J. A. Schey, 1970, Marcel.

12. Oyane, M., and Osakada, K.,"The Mechanism of Lubrication Trapping under Dynamic Compression", Bull. JSME., vol. 12, no. 49, 1969, pp. 149-155.

13. Osakada, K., and Oyane, M., "The Effect of Deformation Speed on Friction and Lubrication in Cold Forging", Bull. JSME., vol. 13, no. 66, 1970, pp. 1504-1512.

14. Wilson, W. R. D., "An Isoviscous Model for the Hydrodynamic Lubrication of Plan Strain Forging Processes with Flat Die", ASME. Paper no. 73-LUB-10 , Presented at ASME/ASJE Joint Lubrication Conference Atlanta, 1973, to be Published in J. of Lubrication Technology.

15. Wilson, W. R. D., and Carpenter, w. b., "A Thermal Hydrodynamic Model for the Lubrication Breakdown in Upsetting Between Overhanding Die", Wear, vol. 24, 1973, pp. 351-360.

16. Wilson, W. R. D., and Delmoliuo, W. D., "The Influence of Surface Roughness on the Lubrication Breakdown in Upsetting Between Overhanding Die", Submitted to wear, 1973.

17. Christopherson, D. C., and Naylor, H., "Promotion of Fluid Lubrication in Wire Drawing", Proc. Inst. of Mech. Engrs., vol. 169, 1955, pp. 643-653.

18. Tattersall, G. H., "Hydrodynamic Lubrication in Wire Drawing", J. of Mech. Eng. Sci., vol. 3, 1961, p. 378.

19. Osterle, J. F., and Dixon, J. R., "Viscous Lubrication in Wire Drawing", ASLE. Trans. ASME., vol. 81, 1962, P. 425.

20. Bedi, D. S., "A Hydrodynamic Model for Wire Drawing" Int. J. of Proc. Res., vol. 6, 1968, pp. 329-343

21. Dowson, D., Parson, B., and Lidgitt, P. J., "An Elastoplastohydrodynamic Lubrication Analysis of the Wire Drawing Process", Elastohydrodynamic Lubrication-Symposium, I. Mech. Engrs., 1972, pp. 97

22. Thompson, P. J., and Symmons, G. R., "A Plastohydrodynamic Analysis of the Lubrication and Coating of Wire Using a Polymer Melt During Drawing", Proc. Inst. of Mech. Engrs., vol. 191, 1977, pp. 115-123.

23. Hashmi, M. S. J., Crampton, R., and Symmons, G. R., "Effects of Strain Hardening and Strain Rate Sensitivity of the Wire Material during Drawing

under Non-Newtonian Plastohydrodynamic Lubrication Conditions", Int. J. Mech. Tool Des. Res. vol. 21, 1988, pp. 71-86.

24. Felder, E.," Experimental and Theoretical Study of Lubrication Film Thickness in Wet Wire Drawing", Proc. 5th Leeds Lyon Symposium, 1978, pp. 365-371.

25. Avitur, B., Metal Forming: Processes and Analyses. McGraw-Hill, N. Y., 1968

26. Schey, J. A., Metal Deformation Processes; Friction and Lubrication. 1970, Marcel Dekker, N. Y..

27. Matsuura, Y., Rep. Casting Res, Lab. Waseda University, Tokyo, no. 13, 1962, pp. 49-58.

28. Nauhria, R. N., and Bedi, D. S., "A Plastohydridynamic Model for Tube Sinking" Proc. 7th Int .Conf. on Prod. Res., vol. 1, 1983, pp. 487-493.

29. Nauhria, R. N., "Plastohydrodynamic Lubrication in the Tube Drawing",Ph.D. Thesis, 1985, Panjab University.

30. Nauhria, R. N., and Bedi, D. S., "Breakdown of Hydrodynamic Lubrication in Tube Sinking", J. of Inst. of Engrs. India, vol. 66, part ME 6, 1985, pp. 173-178.

31. Nauhria, R. N., and Bedi, D. S., "Plastohydrodynamic Lubrication in Plug Drawing", Proc. 12th AIMTDR. Conf., Tata McGraw-Hill, New-Delhi, 1986, pp. 418-422.

32. Dow, T. A., Kannel, J. W., and Bupara, S. S., "A Hydrodynamic Lubrication Theory for Cold Strip Rolling Including Thermal Effects", J. of Lub. Tech. Trans. ASME., vol. 97, 1975, pp. 4-13.

33. Chen, H. S., Friction and Lubrication in Metal Processing, ASME., N. Y. 1966, pp. 69-80.

34. Bedi, D. S., and Hillier, M. J., "Hydrodynamic Model for Cold Strip Rolling", Proc. Inst. of Mech. Engr., vol. 182, 1968, pp. 158-162.

35. Avitzur, B., and Grossman, G., "Hydrodynamic Lubrication in Rolling of Thin Strips", J. of Engng. Ind. ASME., vol. 94, 1972, pp. 317-328.

36. Wilson, W. R. D., and Walowit, J. A., "An Isothermal Hydrodynamic Lubrication Theory for Strip Rolling with Front and Back Tension", Tribology Convention, Inst. of Mech. Engrs., London, 1971, p. 169.

37. Wilson, W. R. D., and Murch, L. E., "A Refined model for the Hydrodynamic Lubrication of Strip Rolling", J. of Lub. Tech. ASME., vol. 98, 1976, p. 426.

38. Tsao, Y. H., and Sargent, T. B., "A mixed Lubrication Model for Cold Rolling of Metals," Trans. ASLE., vol. 20, 1977, p. 55.

39. Tsao, Y. H., and Sargent, L. B., "Friction and Slip in Cold Rolling of Metals", Trans. ASLE., vol. 21, 1978, p. 20.

40. Reid, and Schey, J. A., "Full Fluid Lubrication in Aluminium Strip Rolling", ASLE. Trans. ASME. 1978.

41. Aggarwal, B. B., and Wilson, W. R. D., "Thermal Effects in Hydrodynamically Lubricated Strip Rolling", Proc. 5th Leeds Lyon Symposium, 1978, pp. 351-359.

42. Wilson, W. R. D., "Friction and Lubrication in Sheet Metal Forming"in Mechanics of Sheet Metal Forming, ed Koistenen, D. C., and Wang, N. M., Plenum Press. N. Y., 1978.

43. Wilson, W. R. D., and Wang, J. J., "Hydrodynamic Lubrication in Simple Stretch Forming Process", Trans. ASME., J. of Tribology, vol. 166, January 1984, pp. 70-77.

44. Newnham, J. A., "Sheet Metal Forming Lubrication" in Metal Deformation Processes: Friction and Lubrication, ed. Schey, J. A., Marcel Deker, N. Y. 1970, pp. 703-770.

45. Wilson, D. V., Sheet Metal Ind. 43, 1966, pp. 929-944.

46. Wilson, D. V., Butler, R. D., J. of Inst. Metals, 90, 1961-1962, pp. 473-483.

47. Swift, H. W., Sheet Metal Ind. 31, 1954, pp. 811-828.

48. Loxty, E. M., and Freeman, P., J. of Inst. Petrol., 40, 1954, pp. 299-307.

49. Perace, R., Sheet Metal Ind. 41, 1964, pp. 567-570.

50. Moore, D. F., Principles and Application of Tribology, Pergoemon Oxford, 1975, pp. 115-373.

51. Blok, H., and Rossum, J. J. Van, Lubric. Eng., 1953, p. 316.

52. Hasek, V., and Kramer, G., "Kraftberechene beim Tiefziehen mit Hilfe des oberen Schrankenverfahrens", Industrie-Anzeiger, vol. 97, no. 101, 1975, pp. 2139-2140.

53. Hasek, V., "Aufnahme und Beurteilung des Grenzformanderungss-chaubidel, Industrie-Anzeiger, vol. 97, no. 1, 1975, pp. 12-15.

54. Muschenborn, W., and Sonne, H-M., "Einfluss des formanderungsweges auf die Grenzformanderungen des Feinblechs", Archiv fur des eisenhuttenwesn, vol. 46, no. 9, 1975, pp. 597-602.

55. Mae, Y., "Der Einfluss des R-WERTES auf die Festgkeit und das Um formverhalten von Blechen aus TIA15Sn2.5", Industrie-anzeiger, vol. 96, no. 88, 1974, pp. 1963-1966.

56. Hasek, V., "Einfluss der Plastischen Anisotropie beim Zichen Vongrossen Blechteilen", Industrie-Anzeiger, vol. 95, no. 28, 1973, pp. 545-546.

57 Neubauer, A., Eichhorn, A., and Fisher, U.,"Untersuchung der Zich Verhaltnisse beim Tiefziehen Plastbeschichteter Stahlfeinbleche", Fertig Ungstechnik und Betrieb vol. 25, no.1, 1975, pp. 24-25.

58. Tangermann, D., "Herstellen Nahtloser Dosen Durch Abstreckziehen" Industrie-Anzeiger, vol. 195, no. 38, 1973, pp. 791-793.

59. Osterburg, U., "Zugabstufung beim Tiefziehen-Analyse des Derzeitigen Standes bei der Festlegung der Grenzziehverhaltnisse fur furf Ziehstufen", Fertigungstechnik und Betried, vol. 23, no. 4, 1973, pp. 219-222.

60. Galinowski, J., "Analyse der Formgebung Zylindrischer Napfe aus Quadratischen Zuschnitten aus Blechen mit Anisotropie", Fertigungstechnik und Betrieb, vol. 23, no. 11, 1973, pp. 669-674.

61. Radtke, K., and Dirks, F. J., "Untersuchungen uder des Freie Stulpen von Napfen", Zeitschrift fur Wirtschaftlichen Fertigung, vol. 69, no. 7, 1974, pp.327-329.

62. Lange, K., "Handbook of Metal Forming", McGraw-Hill, 1985.

APPENDIX A

PROGRAM FOR CONTROLLING 3421A DATA ACQUISITION UNIT

```
10    REM *DIGITAL VOLTAGE MEASUREMENT*
20    REM CH2 IS FILM THICKNESS
30    REM CH3 IS DRAWING STROKE
40    REM CH4 IS DRAWING FORCE
50    OPTION BASE 1
60    DIM A(20,3)
70    OUT PUT 709; "T0F1Z0N4LS2-4, 2-4, 2-4, 2-4, 2-4, 2-4, 2-4, 2-4, 2-4, 2-4"
80    BEEP
90    DISP "ARE YOU READY ? Y/N";
100   INPUT A$
110   IF A$="N" THEN 1040
120   OUT PUT 709; "T3"
130   FOR Y=1 TO 10
140   FOR X=1 TO 3
150   ENTER 709; A(Y,X)
160   NEXT X
170   NEXT Y
180   TRIGGER 709
190   FOR Y=11 TO 20
200   FOR X=1 TO 3
210   ENTER 709; A(Y,X)
220   NEXT X
230   NEXT Y
240   IMAGE "CH2", 10X, "CH3", 10X, "CH4"
```

```
250   PRINT USING 240
260   FOR Y=1 TO 20
270   PRINT USING 290; A(Y,1); A(Y,2); A(Y,3)
280   NEXT Y
290   IMAGE D.DDDD, 7X, D.DDDD, 7X, D.DDDD
300   BEEP
310   DISP "ARE YOU GOING TO";
320   DISP "DRAW A CURVE ? Y/N";
330   INPUT B$
340   IF B$="N" THEN 1040
350   GCLEAR
360    SCALE -2, 4, -0.2, 0.6
370   XAXIS -0.2 @ XAXIS 0.6
380   YAXIS -2 @ YAXIS 4
390   XAXIS 0, 0.1, -1, 3.8
400   YAXIS -1, 0.05, 0, 0.5
410   LDIR 90
420   FOR X=-1 TO 3.8 STEP 0.5
430   MOVE X+0.1, -0.15
440   LABEL VAL$(X)
450   NEXT X
460   LDIR 0
470   MOVE -2, 0.55
480   LABEL "THICKNESS VARY WITH DISPLACEMENT"
490   FOR Y=0 TO 0.5 STEP 0.1
500   MOVE -1.8, Y-0.02
510   LABEL VAL$(Y)
```

```
520   NEXT Y
530   PENUP
540   FOR Y=7 TO 17
550   PLOT A(Y,2), A(Y,1)
560   NEXT Y
570   COPY
580   GCLEAR
590   SCALE -2, 4, -0.1, 0.3
600   XAXIS -0.1 @ XAXIS 0.3
610   YAXIS -2 @ YAXIS 4
620   XAXIS 0, 0.1, -1, 3.8
630   YAXIS -1, 0.05, 0, 0.25
640   LDIR 90
650   FOR X=-1 TO 3.8 STEP 0.5
660   MOVE X=0.1, -0.07
670   LABEL VAL$(X)
680   NEXT X
690   LDIR 0
700   MOVE -1.5, 0.275
710   LABEL "FORCE VARY WITH DISPLACEMENT"
720   FOR Y=0 TO 0.25 STEP 0.1
730   MOVE -1.85, Y-0.01
740   LABEL VAL$(Y)
750   NEXT Y
760   PENUP
770   FOR Y=7 TO 17
780   PLOT A(Y,2), A(Y,3)
```

```
790   NEXT Y
800   COPY
810   GCLEAR
820   SCALE -0.2, 0.6, -0.1, 0.3
830   XAXIS -0.1 @ XAXIS 0.3
840   YAXIS -0.2 @ YAXIS 0.6
850   XAXIS 0, 0.05, 0, 0.25
870   LDIR 90
880   FOR X=0 TO 0.5 STEP 0.1
890   MOVE X+0.01, -0.075
900   LABEL VAL$(X)
910   NEXT X
920   LDIR 0
930   MOVE -0.1, 0.275
940   LABEL "FORCE VARY WITH THICKNESS"
950   FOR Y=0 TO 0.25 STEP 0.1
960   MOVE -0.1, Y-0.01
970   LABEL VAL$(Y)
980   NEXT Y
990   PENUP
1000  FOR Y=7 TO 17
1010  PLOT A(Y,1), A(Y,3)
1020  NEXT Y
1030  COPY
1040  END
```

APPENDIX B Samples of Chart Recorder and Computer Printout

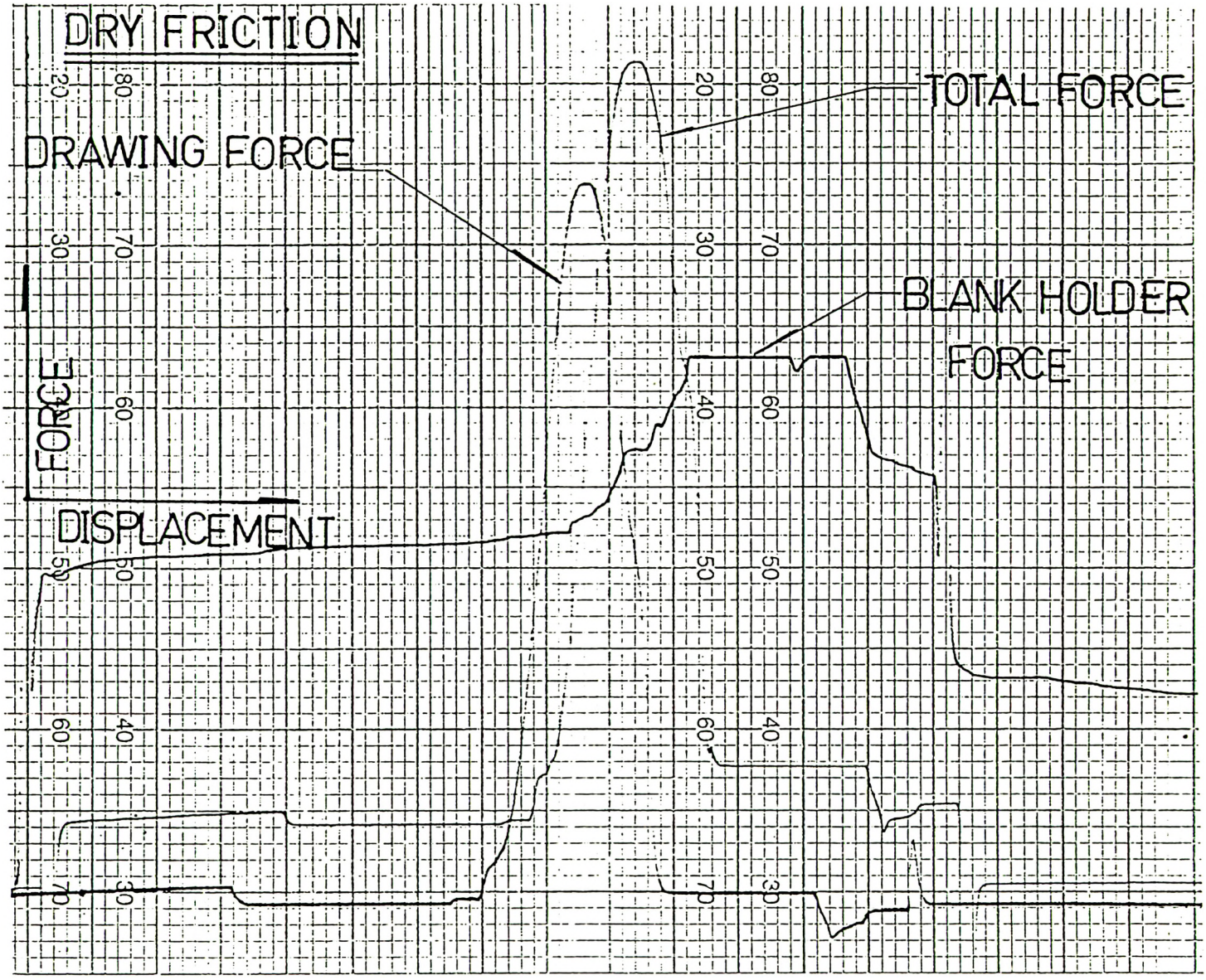

Samples of Chart Recorder

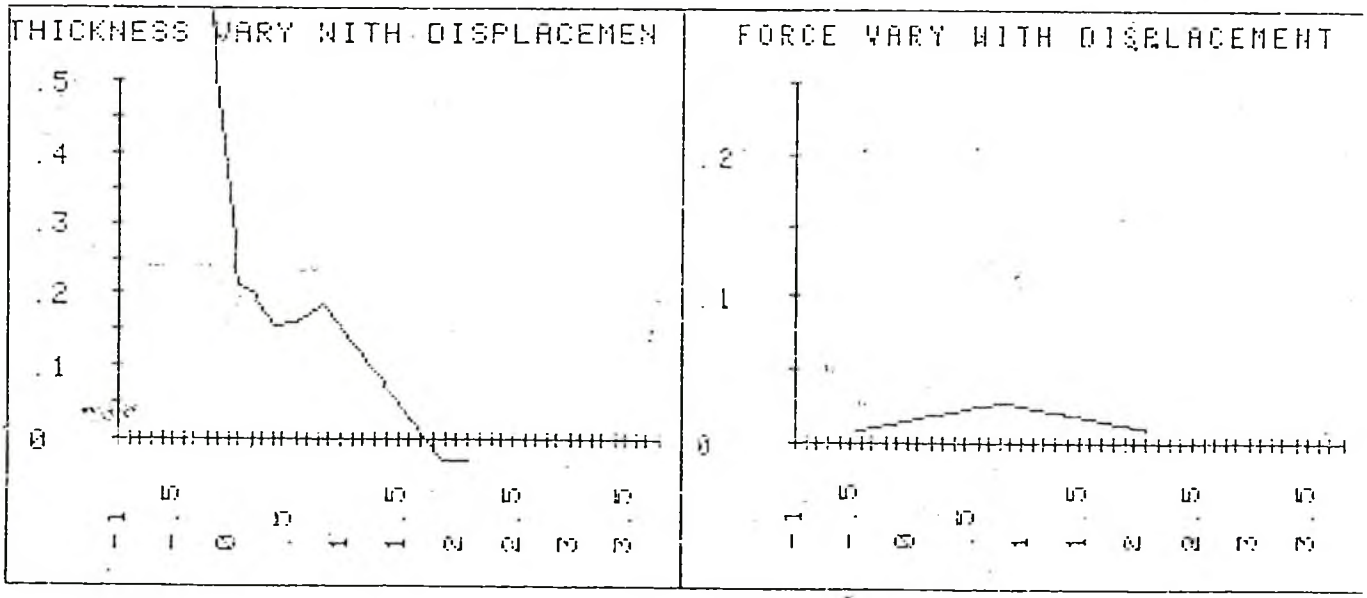

Computer Printout

APPENDIX B Samples of Chart Recorder and Computer Printout

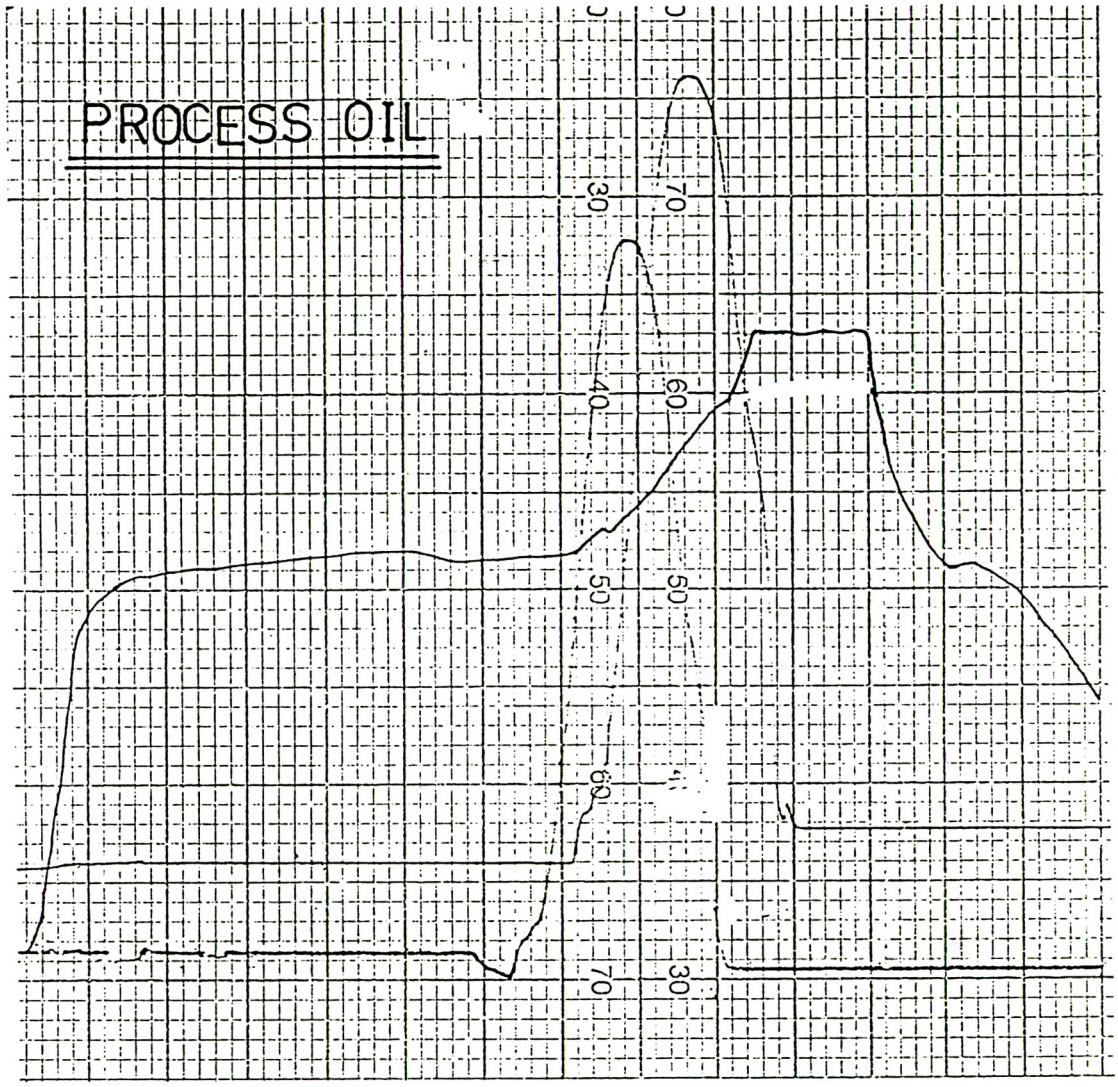

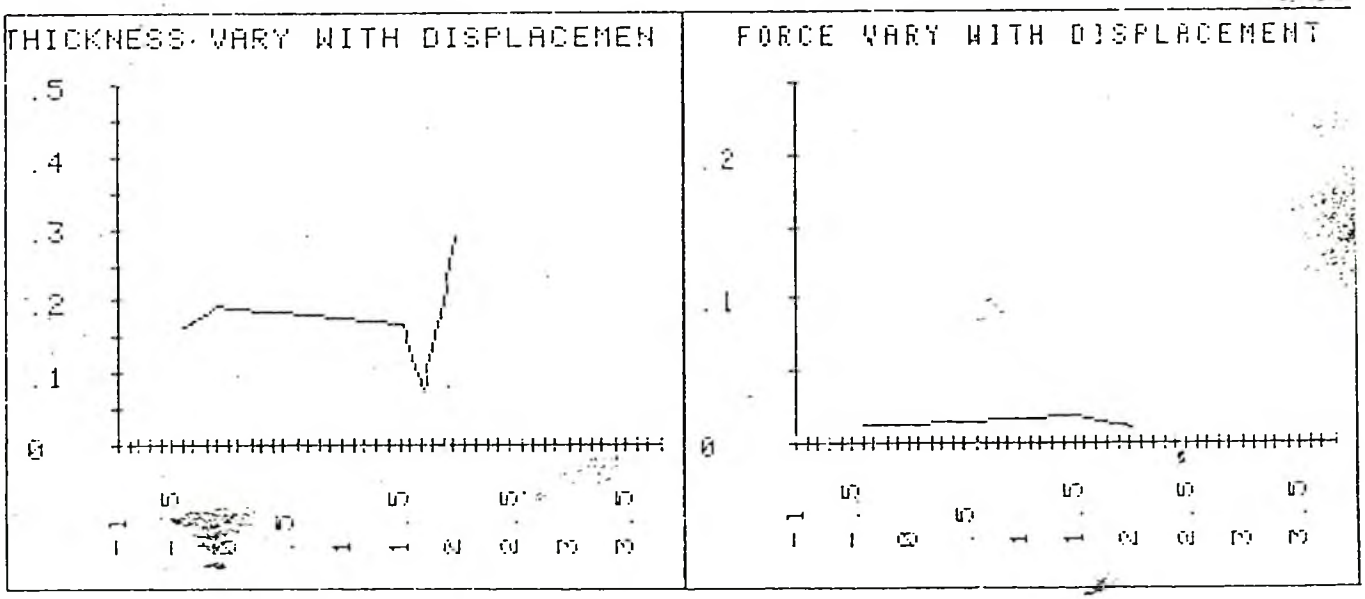

NOTATION RECENT SYMBOLS

$A = 2[\mu V r_1(3t_o\sigma_y r_2)]^{1/2}$, nondimensional hydrodynamic lubrication parameter.

$B = r_1/r_o$, nondimensional geometrical parameter.

$B' = r_3/r_o$, drawing ratio.

$C = r_2/r_1$, nondimensional geometrical parameter.

D = factor of 2-3, as refer to REF. <62>.

$G = 3\mu V/(\sigma_y t_o)$, nondimensional hydrodynamic parameter.

$H = h/h_1$, nondimensional lubricant local film thickness.

$H' = h/r_o$, nondimensional lubricant local squeezing film thickness.

$H_1 = h_1/r_2$, nondimensional lubricant film thickness.

$H_{BH} = h_{BH}/r_o$, nondimensional lubricant squeezing film thickness.

$I = r_2/r_o$, nondimensional geometrical parameter.

$K = \mu V/(2\sigma_y r_o)$, nondimensional hydrodynamic squeezing parameter.

$L = (r_o - r_1)/t_o$, nondimensional geometrical parameter.

$P = p/\sigma_y$, nondimensional pressure of lubricant film.

$P' = pr_o^2/(6\mu v)$, nondimensional pressure of lubricant squeezing film.

$R = r/r_o$, nondimensional local distance.

U = mean surface velocity of blank in r co-ordinate.

V = punch speed.

h = local lubricant film thickness.

h_0 = film thickness corresponding to zero pressure gradient.

h_1 = film thickness at boundary between die and compression zones.

h_{BH} = squeezed film thickness corresponding to blank-holder pressure.

p_{BH} = blank-holder pressure.

p = pressure of the local film thickness.

r = distance along die radius from origin of the Cartesian co-ordinate. (centre line)

r_1 = distance along die radius from oringin of the Cartesian co-ordinate to the point E as shown in FIG.<4>.

r_2 = the radius of die curvature.

r_3 = inter radius of the die.

r_c = distance along die radius from oringin of the Cartesian co-ordinate to the centre of blank-holder pressure.

r_o = initial outer radius of blank.

t_o = thickness of blank.

Θ = angle between blank and die surfaces.

σ_r = local radial stress.

σ_t = local tangential stress.

σ_z = local drawing stress.

σ_z' = local drawing stress of dry friction, as shown in Ref.[62].

σ_y = material yielding stress.

$\sigma_R = \sigma_r/\sigma_y$, nondimensional radial stress.

$\sigma_Z = \sigma_z/\sigma_y$, nondimensional drawing stress.

$\sigma_Z' = \sigma_z'/\sigma_y$, nondimensional drawing stress of dry friction.

$\phi = \sigma_Z/\sigma_Z'$, reduction of the drawing stress.

τ = local shear stress in the film thickness.

τ_0 = local frictional stress on the blank surface of lubricated compression zone.

τ_d = lubricant frictional stress on the blank surface of lubricated die zone.

μ = lubricant viscosity.

ß = coefficient of friction.

$\delta = p_{BH}/\sigma_y$, nondimensional blank-holder pressure.